Peptide-gold nanozymes as catalysts for green chemistry applications ranging from cascade catalysis to carbon capture

Inaugural-Dissertation

to obtain the academic degree

Doctor rerum naturalium (Dr. rer. nat.)

Submitted to the Department of Biology, Chemistry and Pharmacy

of Freie Universität Berlin

by

Dorian Jamal Mikolajczak, M. Sc.

from Berlin, Germany

January 2020

The present research was carried out under the supervision of Prof. Dr. Beate Koksch from December 2016 until January 2020 at the department of Biology, Chemistry and Pharmacy of the Freie Universität Berlin.

1st Reviewer: Prof. Dr. Beate Koksch (Freie Universität Berlin)

2nd Reviewer: Prof. Dr. Rainer Haag (Freie Universität Berlin)

Date of Defense: 04.06.2020

Declaration of authorship

I hereby declare that I have prepared the present dissertation entitled "Peptide-gold nanozymes as catalysts for green chemistry applications ranging from cascade catalysis to carbon capture" on my own and without inadmissible help. All external sources and resources have been specified and properly cited or acknowledged. I further declare that the present thesis has not been submitted, accepted, rated as insufficient or rejected in any other doctorate degree procedure.

Berlin, January 2020   Dorian Jamal Mikolajczak

Publications

Mikolajczak, D. J.; Berger, A. A.; Koksch, B. Catalytically Active Peptide-Gold Nanoparticle Conjugates: Prospecting for Artificial Enzymes. *Angew. Chem. Int. Ed.* (**2020**) Accepted Author Manuscript. doi:10.1002/anie.201908625

Mikolajczak, D. J.; Koksch, B. Peptide-Gold Nanoparticle Conjugates as Artificial Carbonic Anhydrase Mimics. *Catalysts* **2019** *9*(11), 903**.**

Mikolajczak, D. J.; Scholz, J.; Koksch, B. Tuning the Catalytic Activity and Substrate Specificity of Peptide-Nanoparticle Conjugates. *ChemCatChem* **2018**, *10* (24), 5665–5668.

Mikolajczak, D. J.; Koksch, B. Peptide-Gold Nanoparticle Conjugates as Sequential Cascade Catalysts. *ChemCatChem* **2018**, *10* (19), 4324–4328.

Mikolajczak, D. J.; Heier, J. L.; Schade, B.; Koksch, B. Catalytic Activity of Peptide-Nanoparticle Conjugates Regulated by a Conformational Change. *Biomacromolecules* **2017**, *18* (11), 3557–3562..

Heier, J. L.; **Mikolajczak, D. J**.; Böttcher, C.; Koksch, B. Substrate Specificity of an Actively Assembling Amyloid Catalyst. *Pept. Sci.* **2017**, *108* (1), e23003.

Oral presentations

„ *De novo* nanozymes as catalyst for the industrial CO_2-sequestration"; Interdisciplinary DBU-fellow seminar, Lenzen/Germany, 09/05/**2019**.

„Tuning the Catalytic Activity and Substrate Specificity of Peptide-Nanoparticle Conjugates"; 35th European Peptide Symposium, Dublin/Ireland, 29/08/2018.

„*De novo* Nanozyme als Katalysatoren für die industrielle CO_2-Abscheidung und -Speicherung"; Interdisciplinary DBU-fellow seminar, Osnabrück/Germany, 30/11/**2017**.

Posters

„Catalytically Active Peptide-Gold Nanoparticle Conjugates"; 8th Peptide Engineering Meeting (PEM8 - 2018), Berlin/Germany, 08/11 – 10/11/**2018**.

„De novo Nanozyme als Katalysatoren für die industrielle CO2-Abscheidung und -Speicherung"; symposium associated with the "Verleihung des Deutschen Umweltpreises" Erfurt/Germany, 27/10 – 28/10/**2018**.

„Positive Cooperativity and Substrate Specificity of Catalytically Active Peptide-Nanoparticle Conjugates"; Münster Symposium on Cooperative Effects in Chemistry 2018, Münster/Germany, 16/03/**2018**.

„Catalytic Activity of Peptide-Nanoparticle Conjugates Regulated by a Conformational Change"; 4th International Symposium of the Collaborative Research Center SFB 765, Berlin/Germany, 04/10/ - 06/10/**2017**.

Acknowledgements

First and foremost, I would like to thank my supervisor Prof. Beate Koksch for the essential guidance she gave me since my master thesis. She gave me the freedom to pursue new research ideas and interests and provided me with many opportunities to grow as a scientist on paper and in person. Thank you.

I also wish to thank Prof. Rainer Haag for being my second supervisor of this dissertation and for being my second supervisor during my three years in the successful SFB 765.

Moreover, many thanks go to Dr. Allison A. Berger for the fruitful discussions and additional constructive feedback regarding manuscripts and presentations.

In addition, I would like to thank the Research Center of Electron Microscopy under the guidance of PD. Dr. Christoph Böttcher and especially Dr. Boris Schade for his help on operating the TEM and for his useful instructions and knowledge on how to obtain informative TEM-micrographs.

Last but not least, I would like to thank the whole AG Koksch for the relaxed but productive working atmosphere.

Ultimately, I would like to thank the Deutsche Forschungsgemeinschaft in the context of the SFB 765 "Multivalenz als chemisches Organisations- und Wirkprinzip: Neue Architekturen, Funktionen und Anwendungen" as well as the Deutsche Bundesstiftung Umwelt (DBU) for financial support.

Abstract

Protecting the environment and remediating it from the consequences of anthropogenic activities has become an important challenge in today's world. Advancements in the field of catalysis, as an integral part of sustainable and green chemistry, play a major role in the development of new environmentally benign technologies to achieve this. In this regard, the field of nanotechnology opened up new possibilities for the design and synthesis of robust enzyme mimics (nanozymes) that fulfill the criteria of a green catalyst. In particular, gold nanoparticles (Au-NPs) functionalized with catalytically active peptides (Pep-Au-NPs) have proven to be a promising strategy towards the creation of artificial enzymes with remarkable properties in molecular recognition and catalysis. However, the field is still in its infancy.

To extent the contemporary insights into the field of Pep-Au-NPs and establish first design rules, one part of the research conducted in this thesis deals with the systematic study of design principles of Pep-Au-NPs. More specifically, research was focused to systematically elucidate the effect the position of the catalytic center along the peptide sequence has on the catalytic properties of the corresponding Pep-Au-NP assemblies. A correlation was found between the hydrophobic nature of the employed substrate and the region in which catalysis takes place within the generated peptide-monolayer.

The other two studies included in this work were directed to broaden the application scope of these conjugates. First, Pep-Au-NP were studied in their ability to act as a multifunctional cascade catalyst that performs two sequential reactions on a given substrate. By utilizing the hybridity of the system, a peptide-monolayer was established that catalyzed ester hydrolysis, while the Au-NP surface functioned as an efficient hydrogenation catalyst. The reaction was performed as a one-pot reaction in aqueous solution.

Second, a Pep-Au-NP was designed to function as an artificial carbonic anhydrase (CA) mimic for the conversion of CO_2 to HCO_3^- in water. The artificial CA was able to catalyze CO_2-hydration and showed superior catalytic activity over the unconjugated peptide variant. Recycling of the Pep-Au-NP was possible without significant loss in activity even after treatment at elevated temperatures.

The results of this work, on the one hand, contribute to the rational design and synthesis of Pep-Au-NPs as artificial nano-enzymes; on the other hand, provide proof-of-concepts that Pep-Au-NPs are able to perform reactions applied in environmental-friendly processes.

Kurzzusammenfassung

Der Schutz der Umwelt und die Sanierung dieser von den Folgen anthropogener Aktivitäten ist zu einer wichtigen Herausforderung in der heutigen Welt geworden. Fortschritte auf dem Gebiet der Katalyse, als integraler Bestandteil einer nachhaltigen und umweltfreundlichen Chemie, spielen dabei eine wichtige Rolle bei der Entwicklung neuer umweltfreundlicher Technologien. In dieser Hinsicht eröffnete das Gebiet der Nanotechnologie neue Möglichkeiten für das Design und die Synthese von robusten Enzymnachahmungen (Nanozymen), welche die Kriterien eines „grünen" Katalysators erfüllen. Insbesondere Goldnanopartikel (Au-NPs), die mit katalytisch aktiven Peptiden (Pep-Au-NPs) funktionalisiert sind, haben sich als vielversprechende Strategie zur Schaffung künstlicher Enzyme mit bemerkenswerten Eigenschaften hinsichtlich molekularer Erkennung und Katalyse erwiesen. Das Feld steckt jedoch noch in den Anfängen.

Um die aktuellen Erkenntnisse des Gebiets der Pep-Au-NPs zu erweitern und erste Designregeln festzulegen, befasst sich ein Teil der in dieser Arbeit durchgeführten Forschung mit der systematischen Untersuchung der Entwurfsprinzipien von Pep-Au-NPs. Insbesondere konzentrierte sich dieser Teil auf die systematische Aufklärung des Einflusses der Position des katalytischen Zentrums entlang der Peptidsequenz auf die katalytischen Eigenschaften der entsprechenden Pep-Au-NPs. Es wurde eine Korrelation zwischen der hydrophoben Natur des verwendeten Substrats und der Region gefunden, in der die Katalyse innerhalb der erzeugten Peptidmonoschicht stattfindet.

Die beiden anderen in dieser Arbeit enthaltenen Studien zielten darauf ab, den Anwendungsbereich dieser Konjugate zu erweitern. Zunächst wurde untersucht, ob Pep-Au-NPs als multifunktionelle Kaskadenkatalysatoren fungieren können, wobei zwei aufeinanderfolgende Reaktionen an einem Substrat durchgeführt werden. Unter Ausnutzung der Hybridität des Systems wurde eine Peptid-Monoschicht hergestellt, welche die Esterhydrolyse katalysierte, während die Au-NP-Oberfläche als effizienter Hydrierungskatalysator fungierte. Die Reaktion wurde als Eintopfreaktion in wässriger Lösung durchgeführt.

Zweitens wurde ein Pep-Au-NP als künstliche Carboanhydrase (CA) zur Umwandlung von CO_2 in HCO_3^- in Wasser entwickelt. Die künstliche CA war in der Lage, die CO_2-Hydratisierung zu katalysieren und zeigte eine verbesserte katalytische Aktivität gegenüber der nicht konjugierten Peptidvariante. Das Recycling des Pep-Au-NP war auch nach Behandlung bei erhöhten Temperaturen ohne signifikanten Aktivitätsverlust möglich.

Die Ergebnisse dieser Arbeit tragen zum einen zum rationalen Design und zur Synthese von Pep-Au-NPs als künstliche Nanoenzyme bei; Auf der anderen Seite sollten Sie nachweisen und aufzeigen, dass Pep-Au-NPs in der Lage sind, Reaktionen durchzuführen, die in umweltfreundlichen Prozessen angewendet werden.

Table of Contents

Abbreviations

(*S*)/(*R*)-ADH	(*S*)/(*R*)-alcohol dehydrogenase
4-AP	4-aminophenol
4-NP	4-nitrophenol
4-NPA	4-nitrophenyl acetate
Au-MPC	monolayer protected gold cluster
Au-NP	gold nanoparticle
CA	carbonic anhydrase
CTAB	cetyltrimethylammonium bromide
DNPB	dinitrophenylbutyrate
ee	enantiomeric excess
EST	oligomeric esterase
fcc	face center cubic
GHG	green-house gas
hCA II	human carbonic anhydrase II
HSAB	Pearsons acid-base concept (Hard soft acid base)
IPCC	Intergovernmental Panel on Climate Change
IR	infrared
k_0	zero-order rate constant
k_1	first-order rate constant
k_{cat}	turnover number
K_{cat}/K_M	catalytic efficiency
K_M	Michaelis-Menten constant
LSPR	localized surface plasmon resonance
MEA	monoethanolamin

MDEA	methyldiethanolamin
MTA	mesoporous titania supported
NOx	nitrogen oxides
NP	nanoparticle
NR	nitroreductase
PCCC	post-combustion carbon capture
PDB	protein data bank
PEG	polyethyleneglycol
Pep-Au-NP	peptide-gold nanoparticle conjugate
PLE	pig liver esterase
PVA	polyvinylalcohol
PVP	polyvinylpyrrolidone
Sox	sulfur oxides
SPPS	solid-phase-peptide-synthesis
SspCA	thermophilic CA from *Sulfurihydrogenibium yellowstonensis*
TEM	transmission electron microscopy
TMDS	1,1,3,3-tetramethyl disiloxane
TOAB	tetraoctylammonium bromide
tpd	tons per day
Z-L-AA-ONp	*N*-α-Benzyloxycarbonyl protected L-amino acid p-nitrophenyl ester

Abbreviations of the 20 canonical amino acids are consistent with the one- and three-letter code recommended by the IUPAC-IUB Joint Commission on Biochemical Nomenclature (JCBN) [*Eur. J. Biochem.* **1984**, *138*, 9–37].

1 Introduction

The field of catalysis plays an important and indispensable role in today's modern world. Catalysts are involved in 85-90% of all industrial chemical production processes[1] and find frequent application in environmental technologies, including pollution control or water treatment.[2–5] Independent of the field of application, the fundamental goal of a catalyst is the facilitation and acceleration of a chemical transformation with high activity and selectivity. A desired product is thereby accessed in high quantity with minimal energy consumption and limited purification procedures.[1] The development of new catalysts is therefore a continuous process to create innovative technologies that are economical and in the best case also ecological and sustainable. The application of new catalysts enables the improvement of our standards of living and industry and tackles existing or newly emerging challenges.

While decades ago, one of the greatest challenges was the advancement of the industrialization, one of the most urgent challenges today is preserving or remediating the environment from the associated consequences of the industrialization.[6] The extensive and large-scale use of chemical compounds, including fossil fuels, various hydrocarbons (e.g., aliphatic, aromatic, halogenated), nitroaromatic compounds, solvents, and heavy metals as well as the concomitantly produced and (in)correct disposal of chemical waste, significantly contribute to the pollution of the soil or water.[7] Consequently, large parts of natural ecosystems, e.g., the one at the coastal region western of the Urals, are at moderate to high risk of irreversibly perishing.[6,8] Furthermore, anthropogenic activities have caused a rapid rise in the emission of greenhouse gases (GHGs), such as CO_2, into the atmosphere with an ascending trend.[9–12] CO_2, as the most abundant GHG in our atmosphere, plays a central role in irreversible and adverse environmental changes,[13] including global warming,[10,14] and the acidification of the global ocean.[15–17] According to the Intergovernmental Panel on Climate Change (IPCC), human activities led to an increase in global temperature of approximately 1 °C, compared to pre-industrial levels, with a likely increase to 1.5 °C between 2030 and 2050 (Fig. 1.1).[18] In fact, even at temperature increases of 1.5 °C, long-term climate-related consequences are severe and expected to be, e.g., temperature extremes,[19,20] droughts[21,22] and desertification,[23] as well as loss and extinction of certain species on land (specifically, insects, plants and vertebrates) or marine species in aquatic ecosystems.[18] Moreover, increasing losses of ice sheets in Antarctica and Greenland are predicted, which results in a rise in sea level and concomitant flooding of islands and coastal regions. Around 7% of the terrestrial land masses is predicted to undergo a transformation from one ecosystem to another.[18] The IPCC strongly recommends the limitation of CO_2 emission to prevent further warming of the earth to 2 °C by

2100, since the magnitude of the mentioned environmental consequences is predicted to further increase.[18]

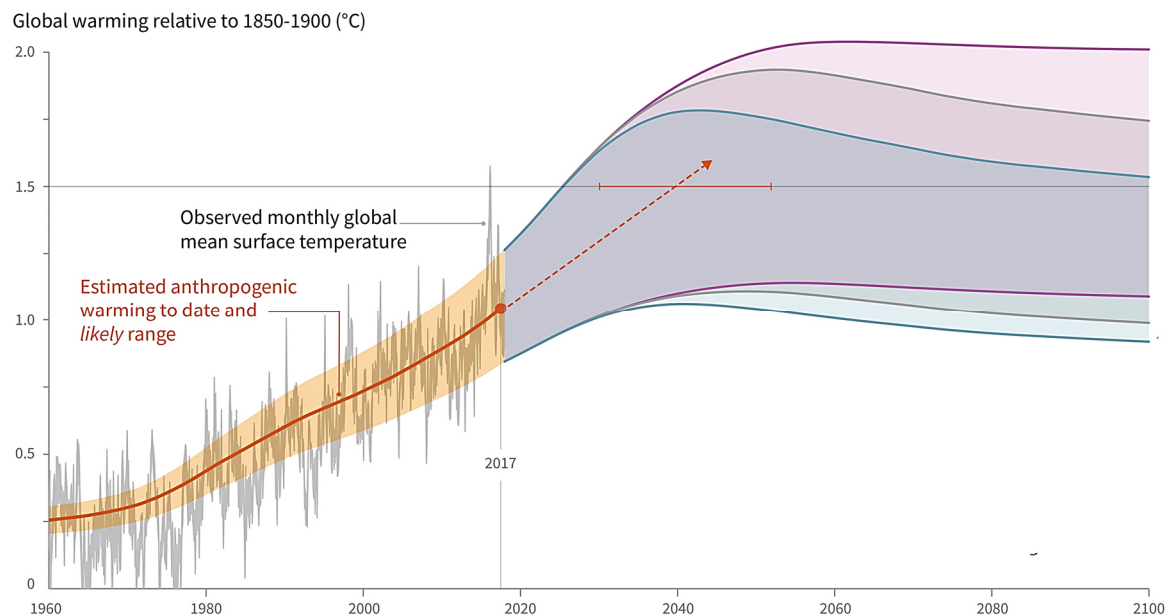Global warming relative to 1850-1900 (°C)

Figure 1.1: Observed monthly global mean surface temperature (grey line) and estimated range of anthropogenic global warming (solid orange line and shading). Future trend of global warming if the current rate of warming continues is shown as orange dashed arrow and horizontal orange error bar. Adapted and modified from IPCC, 2018: Global Warming of 1.5 °C.[18]

To prevent or minimize environmental pollution and CO_2 emission, researchers increasingly adapted the concept of "green chemistry".[24] This term summarizes the development of sustainable and ecofriendly chemical technologies and methodologies. In this regard, the subfield of "green catalysis" emerged as an integral part of green chemistry. Green catalysis is an area of research with major opportunities for the design of new catalysts, or the application of existing catalysts to enable environmentally benign technologies. For instance, natural enzymes are highly efficient and selective catalysts and are considered to be intrinsically green as they are biodegradable and non-hazardous.[25] Although enzymes have been structurally characterized since the early 20th century, only over the last decades, have they been (re)discovered and applied in, e.g., chemoenzymatic cascade reactions or enzymatic CO_2 capture systems. These applications enable the reduction of chemical waste production in organic syntheses and minimize the emission of CO_2 in industrial processes, respectively. However, enzymes are complex biomolecules and as complex is their structure-function-relationship, which strongly responds to changes in their environment.[26] Hence, the application of enzymes in industrial processes or chemical synthesis is considered to be rather limited, as the applied conditions in industry deviate from the natural ones (i.e., high temperatures, extreme pH, organic solvents). To some extent, scientists have developed

techniques to circumvent those limitations, for example, by applying directed evolution the importance of which was acknowledged with a Nobel Prize in chemistry in 2018.[27,28] Another approach is the construction of artificial enzymes. The approach is based on the deciphering of important structural motifs of enzymes that account for the remarkable catalytic properties, and the translation of those into valid synthetic models. The resulting artificial enzymes ideally exhibit rate constants and selectivities similar to their natural analogues, while being more robust towards harsh experimental conditions, recyclable and synthesizable at low-cost on a large scale. Ronald Breslow pioneered and coined the field in the early 1960s by utilizing cyclodextrins as enzyme mimics. Since then, various approaches based on polymers or peptides, as well as supramolecular or organometallic chemistry were used to create artificial enzymes.[29–31] Nowadays, the field of modern nanotechnology and -research further expanded the toolbox for the design of inorganic nanoparticles (NPs) as robust enzyme mimics, referred to as nanozymes. Nanozymes possess unique electronic- and physicochemical properties. They have a size-regime similar to natural enzymes (~2-10 nm), and a high surface-area-to-volume-ratio, thus, a large contact area for substrate conversion. Furthermore, nanozymes are robust solid heterogeneous catalysts, which enable a facile separation from reaction mixtures and recycling. Lastly, their surface can readily be functionalized with a variety of organic ligands.

In this regard, gold nanoparticles (Au-NPs or gold nanozymes) have been intensively studied, due to their unique size-dependent optoelectronic[32,33] and intrinsic catalytic properties,[34,35] their tunable stability,[36] biocompatibility,[36–38] and their straightforward synthesis and surface modification. Au-surfaces are readily functionalized, e.g., by thiolated ligands, which assemble with high affinity at the Au-surface *via* stable S-Au bonds,[39] forming a (functional) ligand-monolayer. The high local ligand density at the Au-NP surface generates new cooperative and synergistic effects between functional groups. Those conjugates have shown remarkable properties in catalysis[40,41] and molecular recognition.[42,43]

In this context, the application of peptides further extended the possibilities to design functional gold nanozymes (peptide-Au-NPs = Pep-Au-NPs). Peptides possess unique sequence dependent specific recognition and catalytic properties and their modular structure combined with the existing toolbox of natural and non-natural amino acids allows to easily diversify and fine-tune catalytic properties of the peptide-monolayer.[44] The confinement of peptides at the Au-NP surface induces close interactions between individual side chain residues, which leads to novel enzyme-like properties, such as the perturbation of pK_a of functional groups, the execution of novel catalytic mechanisms and improved substrate interactions.[45,46]

The development of Pep-Au-NP catalyst is still at an early stage and their potential is largely undiscovered. Therefore, the present work will elaborate on the design and synthesis of novel Pep-Au-NPs as artificial enzymes and on their potential application in green technologies. Specifically, Pep-Au-NPs will be highlighted in their function to act as multifunctional catalysts for chemoenzymatic cascade transformations and catalysts for the conversion of CO_2, respectively. A simplified summary of the applied concept and workflow is shown in Fig. 1.2.
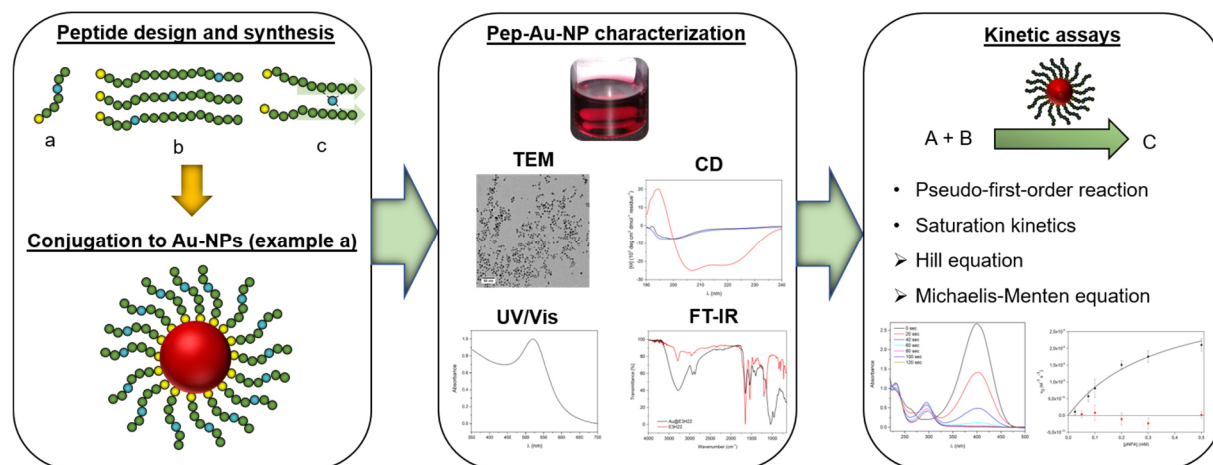

Figure 1.2: Schematic depiction of the concept and workflow applied in the projects of the present work.

2 Green chemistry and catalysis

Green chemistry is a concept first formulated in the 1990s which is defined as the "design of chemical products and processes to reduce or eliminate the use and generation of hazardous substances."[47,48] The application of this concept is an important aspect in modern chemistry and chemical engineering as it is an essential goal to ensure that further generations of materials, chemicals and energy (sources) are more sustainable to previous generations.[49] Therefore, continuous research is required for the discovery and design of new, cost-effective materials and processes to remediate polluted environments, or first and foremost, prevent environmental pollution. The framework of green chemistry is based on twelve principles that were described in 1998 by Paul Anastas and John Warner (Table 2.1).[47] In summary, these principles present a cohesive guideline towards the creation of processes designed across all stages of chemical life-cycle that minimize the use of toxic solvents or avoid the generation of hazardous residues or byproduct.[50] To achieve this, it is vital to use renewable or benign materials together with a good energy and atom economy.

Table 2.1: The twelve principles of green chemistry according to Paul Anastas and John Warner.[47,48]

|	
1. Waste prevention instead of remediation	7. Use of renewable feedstock/materials
2. Atom efficiency	8. Efficient synthesis (avoid derivatization)
3. Less hazardous/toxic chemical synthesis	9. Catalysis
4. Safe and sustainable chemicals by design	10. Degradation of chemical products
5. Use of innocuous solvents and auxiliaries	11. Analytical methods for pollution control
6. Energy efficiency	12. Inherently safer processes (less accidents)

Catalysis as one of the twelve principles presents an important field of research for the development of new methodologies and processes with high efficiency, decreased energy consumption that are atom efficient and produce little waste. Catalysts are also referred to as the solution to pollution.[51] The application of a catalyst greatly reduces the energy input of a reaction by lowering the energy required for the conversion. Moreover, catalysts reduce the produced waste of a reaction by avoiding the usage of stoichiometric amounts of reagents.[48] This also implies an overall lower necessity of feedstock. A negative example that demonstrates the advantages of a catalyst, is the reduction using $NaBH_4$ (Scheme 2.1).[52] $NaBH_4$ is an established reducing agent in organic chemistry that functions as a hydride donor to, e.g., reduce

ketones and aldehydes to the corresponding alcohols. Stoichiometric amounts of $NaBH_4$ are required for a quantitative conversion, which results in additional waste production.[53] By contrast, the catalytic hydrogenation of ketones using a palladium catalyst on active carbon (Pd/C) and H_2-gas proceeds in a non-stochiometric manner and no additional waste is produced. In total, significantly less chemicals, thus feedstock is required, and waste production is minimized.

Stoichiometric reaction
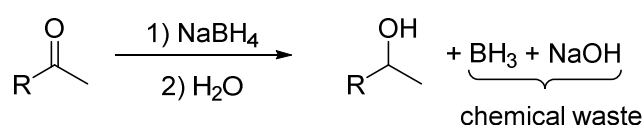
Catalytic reaction
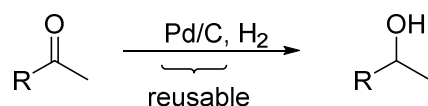
Scheme 2.1: Comparison between stoichiometric and catalytic reduction of ketones to the corresponding alcohols.

Catalysis also opens up new avenues to solve synthetic questions and enable efficient routes towards valuable products that are otherwise not accessible or only accessible by challenging reactions.[48] The development of the Grubbs catalyst presents such an example.[54] The developed ruthenium-complex enabled a facile way of olefin metathesis, a powerful C-C-double-bond forming reactions that is still widely used. The facilitation of metathesis reactions presented an innovative approach towards valuable unsaturated compounds, which was acknowledged with the Nobel Prize in chemistry in 2005. Based on that, a variety of new synthetic routes and strategies were developed and are still under development.[55] In total, the development of the Grubbs catalyst entailed considerable environmental benefits.[48]

Another key aspect in green chemistry and catalysis is the transition to environmentally benign solvents or no-solvent systems. In most chemical synthesis and processes, solvents account for most of the produced waste and recovery of solvents is often linked to energy intensive distillations.[48,56,57] On top of that, the used solvents are often toxic, corrosive, flammable and volatile or water soluble which greatly increases their exposure and danger to natural ecosystems on land, water and air. Thus, various green alternatives are under consideration, including super critical fluids, ionic liquids or simply water.[48,58]

Water is the most abundant solvent on our earth and is considered to be the "universal solvent"[48,59,60] with a lot of advantages. It is non-flammable, non-toxic and non-polluting, thus

does not pose any harm to the environment or contaminates formed products.[58] It is cheap and readily available on a large scale, which makes the use of water as a solvent ecologically and economically attractive.[61] Moreover, organic reactions, such as the Diels-Alder reaction performed in water can even be accelerated by utilizing the hydrophobic effect,[62] which brings suitable substrates into close proximity. Additionally, when the formed product is insoluble in water, purification can readily be performed by filtration. Despite the advantages, applying water as a solvent in organic synthesis also has its drawbacks. For example, many organic compounds are only poorly soluble or insoluble in water, which greatly limits the substrate scope.[63] Besides, undesired side reactions, including hydrolysis, racemization or polymerization are also possible.[64] Another downside resides that mostly extraction-based purification steps are performable, as the evaporation of water is energy intensive.[64] However, solutions to these drawbacks are already addressed at in various research groups.[63,65,66]

Water has great potential to become the staple solvent for green chemistry. As a result, suitable catalysts and catalytic processes functioning in aqueous solutions are increasingly developed. In this context, the application of enzymes or nanocatalysts as artificial enzymes presents a great alternative to conventional chemical catalysts.

3   Enzymes: natures green catalysts

Enzymes are nature's own highly evolved biocatalysts that speed up almost all metabolic processes in living organisms under mild conditions to enable life on the time scale as we know it. They present the best example of a green catalyst, as they are non-toxic, biodegradable and originate from renewable sources (plants, animals, microorganisms).[67] Furthermore, enzyme catalysis functions in aqueous media, at atmospheric pressure and ambient temperatures, while showing exceptional efficiency and high regio-, chemo- and stereoselectivity.[68–70] Hence, enzymatic reactions are considered to be clean with little to no side-reactions or by-products, which in total minimizes energy consumption and waste production. Such advantages are difficult to achieve using conventional chemical catalysts.[69] Moreover, when designed accordingly, enzymes catalyze the synthesis of complex macromolecules, like polysaccharides cellulose[71,72] or hyaluronic acid.[73] Furthermore, immobilization of enzymes also enables their facile recycling, which improves their cost-efficiency and removes a drawback of enzymes being homogenous catalysts.[74] Also, given sufficient robustness and compatibility, enzymes can be used in conjunction with chemocatalysts to enable new green chemoenzymatic cascade processes for multistep syntheses in one-pot (see section 3.2.2).

To date, more than 3000 different enzymes have been discovered and as numerous is their spectrum of catalyzed reactions. Depending on the chemical transformation they accelerate, natural enzymes can be classified into six main categories, i.e., Oxidoreductases, Transferases, Hydrolases, Lyases, Isomerases and Ligases.[75] In addition to these reaction classes, enzymes can also be mutated and engineered, for example, by applying directed evolution, to further diversify the enzymatic toolbox, to also include non-natural reactions like epoxide opening, cyclopropanation, carbene transfer reactions[27] and others. Besides, nowadays most enzymes are readily and widely accessible, and their catalytic mechanisms, which are strongly related to their enzyme structure (see section 3.1), have been increasingly unraveled.[69] Therefore, enzymes - mostly hydrolases and oxidoreductases - find application in their natural or mutated form in current industrial processes, including food, pharmacology, paper, textile industry, and more.

3.1 Structure-function-relationship exemplified by the carbonic anhydrase

Enzymes are generally considered to be proteins, with an exception being RNA-based ribozymes.[75] Enzymes are large biomolecules that consist of one or more linear chains of several tens to several hundred amino acids (primary structure) linked together by peptide bonds that constitute the protein backbone. The primary structure is precisely sequenced, which predetermines the complex and specific intramolecular non-covalent interactions, including ionic- and Van-der-Waals-interactions, or hydrogen-bonding with specific residues or the protein backbone that lead to higher ordered structures. This results in defined, local structural motifs, such as α-helices or β-sheets (secondary structures) that are primarily formed by hydrogen bonding within the protein backbone. In water, these structures spontaneously arrange and fold into an intricate three-dimensional tertiary structure or in case of a multi-subunit enzyme into a quaternary structure. An overview over the protein structures is given in Fig. 3.1. The folding process is primarily driven by the hydrophobic effect, i.e., increasing hydrophobic interactions between non-polar residues, while decreasing the interaction between hydrophobic amino acids and water. This results in the release of solvating water molecules and increases the overall entropy of the system. As a result, a sophisticated protein architecture, where specific regions for protein-protein- or protein-ligand-interactions, cofactor and substrate binding or catalysis are developed.

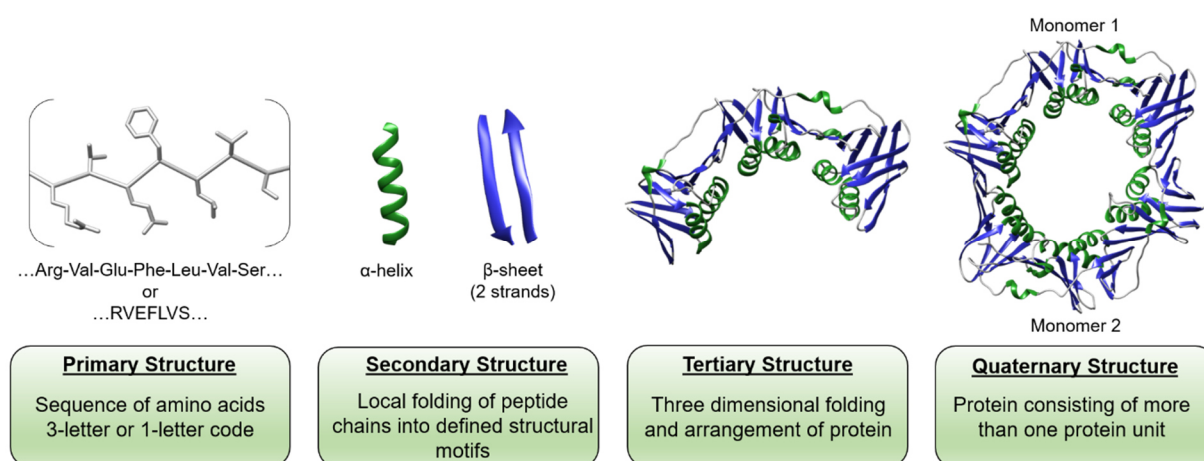| Primary Structure	Secondary Structure	Tertiary Structure	Quaternary Structure
Sequence of amino acids 3-letter or 1-letter code	Local folding of peptide chains into defined structural motifs	Three dimensional folding and arrangement of protein	Protein consisting of more than one protein unit

Figure 3.1: Graphical overview over the four levels of protein structures exemplified by the structure of DNA polymerase III subunit β (PDB code: 4TRT).

Within the folded enzyme structure, a small region is developed, referred to as the active site. The active site is responsible for substrate accommodation, binding, and catalysis. It is usually located in the interior of the folded protein structure in a small pocket or tunnel[76] and contains a conserved arrangement of catalytically relevant amino acids. These residues define the topology of the active site region in terms of solvation of functional groups, presence of

structural water molecules and overall polar/hydrophobic character.[77] Moreover, they are responsible for the substrate-binding interactions and account for the remarkable substrate specificity and stereoselectivity of an enzymatic reaction. Residues present in the active site engage in multiple weak interactions with the substrates (i.e., hydrogen bonds, Van-der-Waals-, electrostatic-, hydrophobic- or π-π-interactions) to form a stable but reversible (non-)covalent enzyme-substrate-complex. The substrate is tightly positioned and oriented and the corresponding orbitals steered to optimally overlap with the corresponding catalytic competent moieties[78,79] to promote transition state interactions and -stabilization. As a result, enzymes greatly decrease the activation energy of a reaction and efficiently convert a substrate with rate increases of 10^6-10^{12},[69,80] compared to the uncatalyzed reaction. Since enzymes reversibly catalyze a certain reaction, they do not affect or alter the thermodynamics of a reaction, e.g., equilibrium constants, even though equilibrium may be attained faster.

The catalytic mechanisms performed by enzymes, such as nucleophilic, covalent, general acid/base or redox catalysis, strongly depend on the nature of the enzyme and its catalytic center. Catalysis can be executed either directly by amino acid side chains, for example, the catalytic Asp-His-Ser triad of serine proteases like chymotrypsin,[81] or can be achieved by coordination of a metal cofactor that acts as the catalytically competent unit. Regarding the latter, several amino acid residues, including the ones of His, Tyr, Cys, Glu or Asp have been identified to coordinate to various metal ions (i.e., Mn, Ni, Co, Fe, Cu or Zn).[82] Those residues (primary coordination sphere) and other residues of the active site (secondary coordination sphere) generate a microenvironment around the metal center, which enables substrate recognition, orientation, fixation and catalytic conversion,[82–85] analogous to non-metal containing enzymes as previously mentioned.

The active site of enzymes and their sophisticated composition of functional groups does not only facilitate substrate binding and conversion, but also the release of product and transfer of, e.g., solvent molecules or protons in and out of the catalytic cavity to revert into the initial state.[86]

An extensively studied enzyme that merges the above-mentioned information into a concrete example, is the human Carbonic anhydrase II (hCA II), whose structure-function-relationship also plays an important role in section 3.2.1 and section 7.4. The hCA II belongs to the overall enzyme class of lyases and is a naturally occurring zinc metalloenzyme that efficiently and reversible catalyzes the hydration of CO_2 into hydrogen carbonate (HCO_3^-) and H^+. The hCA II consist of 260 amino acids that form 9 α-helices and 18 β-strands, which assemble into a complex tertiary structure (Figure 3.2A).[87]
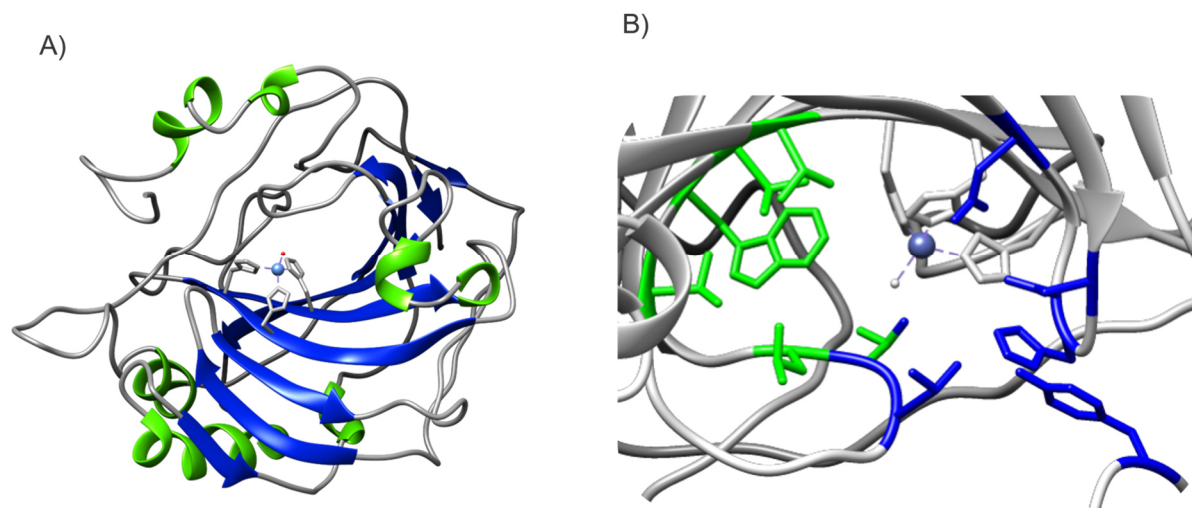
Figure 3.2: (A) Structure of human carbonic anhydrase II (PDB code: 1CA2) showing His64, His96 and His119 coordinating a Zn(II) (grey). α-helices are shown in green and β-strands in blue. (B) Illustration of the active site of hCA II showing amino acid side chains that comprise the hydrophobic region (green) and the hydrophilic region (blue).

The active site of hCA II is located 15 Å deep within a conical groove of the enzyme structure and contains a zinc-ion (Zn(II)) that is coordinated by three His imidazole (His94, His96 and His119), which form the catalytic Zn(II)-center.[88] The bound Zn(II) acts as a Lewis-acid that significantly lowers the pK_a of an associated water molecule, referred to as W_{Zn},[89] down to approx. 7, which enables the conversion of CO_2 by a highly nucleophilic Zn(II)-bound-hydroxide mechanism at neutral pH (Scheme 3.1).[88,90]
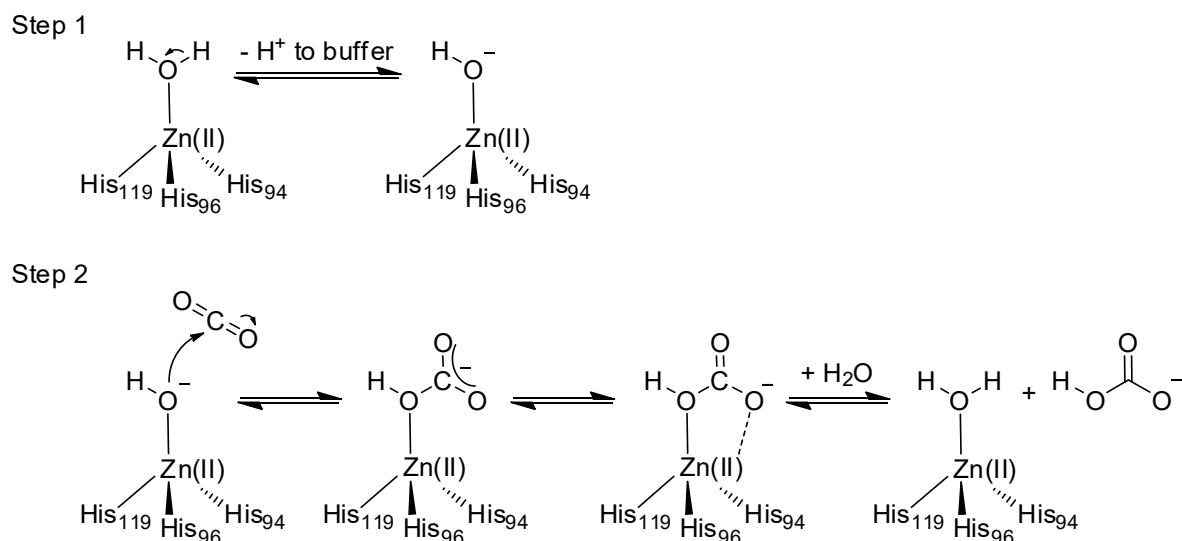
Scheme 3.1. Reaction mechanism of CO_2-hydration executed by the Zn(II)-bound hydroxide of hCA II.

The active site cleft is further divided into a hydrophobic binding site and a hydrophilic region (Fig. 3.2B).[89,91] The hydrophobic binding site contains non-polar amino acids Val121, Val143, Val207, Leu198, Trp209 and Thr199-CH_3 which engage mainly in Van-der-Waals-interactions with the apolar substrate CO_2 to facilitate diffusion into the catalytic cavity and accelerating it

towards the Zn(II)-center.[89,92] After different intermediate states along the binding process, CO_2 is ultimately directed to linearly orient to and interact with the Zn(II)-ion, which maximizes the polarization of the CO_2 carbon, making it more susceptible for the incoming nucleophilic attack.[92] This leads to extraordinarily high first-order rate constants of CO_2-hydration (k_{cat}) of $\sim 10^6\ s^{-1}$ and second-order rate constants (k_{cat}/k_M) approaching the diffusion limit of $\sim 10^8\ mol^{-1}\ s^{-1}$.[93] Fascinatingly, with hCA II nature has evolve a catalyst whose catalytic process is only limited by fundamental physical phenomena, such as diffusion or proton transfer processes. Although these processes being rate determining, they are also optimized and sped up by various sequential processes within the enzyme structure in order to minimize their effect on catalysis. Specifically, the transfer of generated protons out of the active site into the bulk solvent is performed in an elegant fashion by residues of the hydrophilic region.

The hydrophilic region mainly consists of polar amino acids Tyr7, Asn62 and Asn67, His64, and of Thr199-$O_{\gamma 1}$, as well as Thr200-$O_{\gamma 1}$ that elaborately interact with water, to form a dynamic hydrogen-bonded solvent network.[89,94] This intricate network facilitates the release of HCO_3^- and plays a key role in solvent and proton shuttle processes to regenerate the functional catalytic Zn(II)-center.[95,96] It was identified that the imidazole of His64, located approx. 8 Å away from the Zn(II)-center, is a vital residue for the proton transfer process. It extends into the active site cavity and orchestrates the process by concurrently changing its imidazole conformation into two rotameric states: the "His_{in}"-state, that accepts protons and points into the active site; the "His_{out}"-state that donates a proton to the bulk solution and points out of the active site (Fig. 3.3).[89,97]
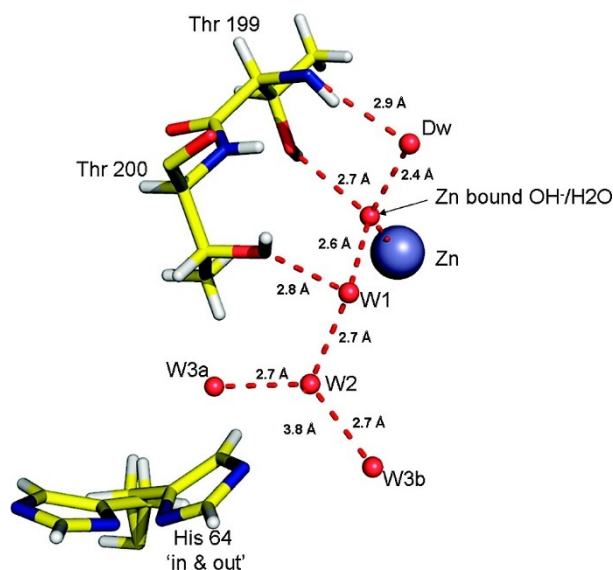

Figure 3.3: Depiction of the ordered hydrogen-bonded water network (red) and the His "in & out" rotation of His64 during the proton shuttle process. Adapted from Ref.[97]. Copyright © 2010, American Chemical Society.

During the initial phase of CO_2-hydration, W_{Zn} is activated by releasing a proton, to generate the Zn(II)-bound-hydroxide. The proton is transferred through two localized water molecules to the N_π of His64 in its His_{in}-state. The resulting protonated imidazole of His64 is said to be electrostatically repelled from the positively charged Zn(II), which leads to the conformational rotation into the His_{out}-state and structural changes in the solvent network.[98] Subsequently, the bound proton is released into the bulk solution and the imidazole flips back into the His_{in}-state. Zn(II) plays an important role in the proton shuttle process as it was shown, that in the absence of Zn(II), His64 resides predominantly in the His_{out}-state and is associated with additional water molecules.[89]

The formed polar product HCO_3^-, is released through the hydrophilic region, while rearrangements of water molecules take place to regenerate the catalytic center.[89,99,100] That is, a water molecule in the vicinity of the metal-center binds to Zn(II), forming the new W_{Zn}. Additional water is recruited from bulk solution and the former well-ordered hydrogen-bonded solvent network rearranges and replaces vacant water positions in the cavity. The active site reverts into the initial state and a new cycle of CO_2-hydration begins.

The structure of hCA II – or of enzymes in general – evolved over billions of years and is still adapting to this day. Each individual amino acid is carefully positioned and has a direct or indirect impact on the structural stability and catalysis. Even single substitutions can be detrimental to the catalytic activity. This was demonstrated by site specific substitutions of amino acids Leu198 and Val143, which are responsible for substrate association and are located at the entrance and base of the hydrophobic cleft of hCA II, respectively. Nair and Christianson substituted Leu198 for polar amino acids Glu, Arg and His or less hydrophobic amino acid Ala.[101] The substitution of Leu198 and its isobutyl group for the smaller methyl group of Ala led to a notable decrease in catalytic efficiency k_{cat}/K_M by 3-fold. The substitution of Leu198 for Glu, Arg and His severely diminished catalytic efficiency k_{cat}/K_M by 19-fold, 17-fold and 10-fold, respectively.

An even greater effect on the catalytic efficiency has the substitution of Val143 for bulky amino acids Phe and Tyr as demonstrated by Fierke *et al*.[102] A substitution of Val143 for Phe or Tyr renders hCA II catalytically inactive. The sterically demanding phenylalanine ring occludes the binding pocket, which leads to a loss of substrate association site. Besides, also moderate substitutions of Val143 for Leu or Ile reduced k_{cat}/K_M by factors of 6 and 8, respectively. Moreover, even small alterations in the structure of amino acids that are only indirectly involved in the catalytic process can significantly reduce the catalytic efficiency. For example, the substitution of Gln92, which is involved in the hydrogen-bonding network of the

active site, for slightly smaller Asn led to a 4-fold decrease in k_{cat}/K_M.[103] Tab. 3.1 summarizes the selected single amino acid substitutions performed in hCA II and their effect on catalysis.

Table 3.1: Summary over selected single amino acid substitutions performed in hCA II and their effect on k_{cat}/K_M.

Wild-type residue	Replaced by…	Effect on k_{cat}/K_M
Leu198[101]	Ala	3-fold decrease
	His	10-fold decrease
	Arg	17-fold decrease
	Glu	19-fold decrease
Val143[102]	Phe	catalytically inactive
	Tyr	catalytically inactive
	Leu	6-fold decrease
	Ile	8-fold decrease
Gln92[103]	Asn	4-fold decrease

The structure-function-relationship of hCA II (and of enzymes in general) is not only susceptible to modifications in the primary structure but is also sensitive to changes in their environment. hCA II exhibits highest k_{cat}/K_M values at approx. pH 8.[104] Small deviations from this pH in both directions (i.e., higher or lower than 8) cause a decrease in catalytic efficiency. While even greater pH alterations cause ionizable groups to considerably change their (de)protonation state, which destabilizes the protein structure and catalytic activity is decreased or obliterated. Furthermore, chemical denaturants like (chaotropic) salts,[105] acids, bases, or organic solvents[106] have a similar effect on the enzyme structure, as important interactions (hydrogen bonds, electrostatic or hydrophobic interactions) between functional groups are either not formed or disrupted.

The enzyme structure is also susceptible to physical influences like temperature changes. It was shown that hCA II is stable up to approximately 40 °C and retains up to 90% of its activity.[107,108] However, further elevation of the temperature to, e.g., 60 °C and higher causes the interactions that keep the enzyme structure together to break. Consequently, hCA II denatures and catalytic activity is lost.[109]

The hCA II is just one example among many natural enzymes that possess a sophisticated structure-function-relationship and concomitantly exceptional catalytic properties. Owing to their high catalytic efficiency, outstanding regio-, chemo-, and stereoselectivity, as well as their intrinsic environmental friendliness, enzymes increasingly find application in industry and organic synthesis. However, due to their frailty in unnatural milieus, reactions and technologies must be designed accordingly.

3.2   Examples of green applications

The following two sections provide an overview over the state of the art of two fields of research in which enzymes play key roles: enzymatic post-combustion CO_2-capture processes and chemoenzymatic cascade reactions. Both approaches were developed and are still pursued with the overall intention of decreasing the release of pollutants or emission of GHGs into the environment.

3.2.1   Post-combustion CO_2-capture

CO_2 as the most abundant green-house gas in our atmosphere, plays a central role in anthropogenic, irreversible and adverse environmental changes,[13] including global warming,[10] and the acidification of global oceans (see section 1). Since industrial combustion processes produce billions of tons of CO_2 annually, widely implementable technologies need to be developed[110] that, in the best case, prevent the formation of CO_2 or capture the produced CO_2 in cost-efficient ways. Several approaches have been developed and investigated in order to capture CO_2 from flue gas mixtures[111] produced by power plants, cement plants, or other industry, after combustion processes. Such technologies are referred to as post-combustion carbon capture (PCCC) methods.[110] The released flu gas composition after combustion process usually consists of only 10–20% CO_2 together with O_2, N_2, H_2O vapor and traces of various nitrogen (NO_x) and sulfur oxides (SO_x).[112,113] Thus, selective PCCC methods are required that exclusively capture CO_2 from flue gas streams in order to isolate it with high purity to enable its use as a valuable feedstock. CO_2 finds application as a shielding gas in welding systems,[114] as a refrigerant in industrial refrigerator systems,[115] or as a C1-building block in chemical synthesis of methanol,[116] formate,[117], cyclic carbonates or urea,[118] to name a few.

One of the most effective approaches towards selectively capturing and isolating CO_2 are scrubbing methods, such as the amine scrubbing. In the amine scrubbing, CO_2 is chemically absorbed by amine solvents in a countercurrent fashion in an absorber column and is subsequently released in a desorption process (Fig. 3.4).[108,119] The absorber column is commonly packed with a porous material, which increases the contact surface between the gas and solvent.[120,121] A frequently used solvent for the removal of CO_2 in such a process is monoethanolamine (MEA).[122] MEA is extremely efficient and selective in removing CO_2 by forming stable carbamates at elevated temperatures (30 – 50 °C), is inexpensive and available on a large scale. However, MEA is corrosive and the regeneration of CO_2 from these carbamates

for subsequent processes is highly energy intensive due to the high temperatures (> 120 °C) needed, and therefore accounts for up to 80% of the operating costs.[119,123]
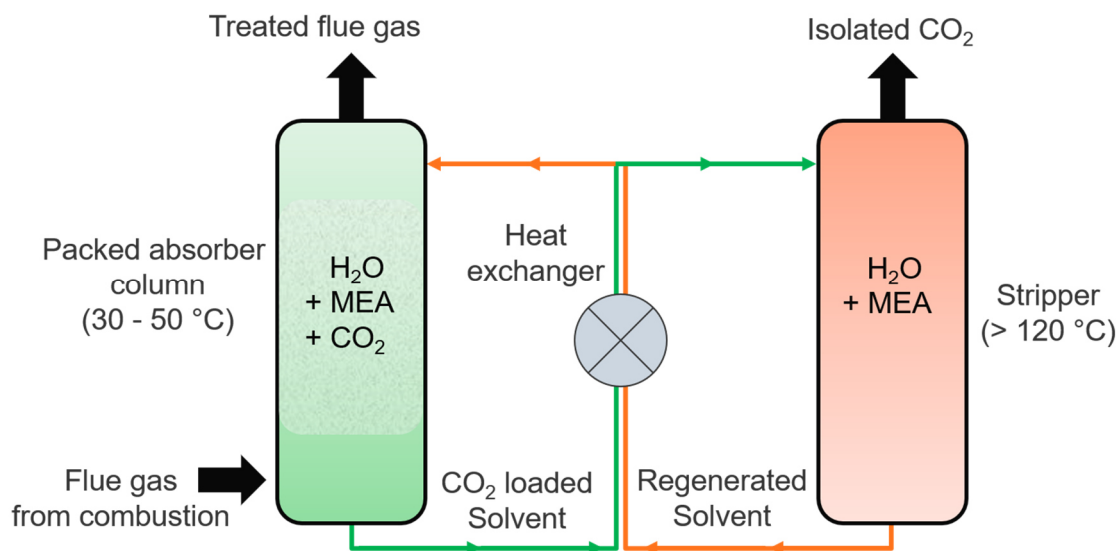

Figure 3.4: Simplified flow sheet for the capture of CO_2 using monoethanolamine in a CO_2-capture plant.

Thus, a multitude of other solvents that lower the stripping costs of CO_2 are under consideration, including sterically hindered[124] and tertiary amines,[125,126] chilled ammonia[127] or aqueous carbonate solutions (K_2CO_3),[128] with the latter being the environmentally most benign. While many of these alternative solvents are able to reduce the energy required for CO_2-stripping, suitable catalysts are required, that promote the absorption rates of CO_2 from running gas streams into the liquid.[108,119] In this context, enzymes, specifically CAs are considered as highly efficient and selective catalysts for the interconversion of CO_2 to HCO_3^- in water as described in detail in section 3.1.

The proof-of-concept that CAs catalyzes the hydration of CO_2 *in vitro* on a laboratory scale was shown by Bond *et al.*[129] However, exposing CA to the harsh, denaturing operation conditions of a CO_2-absorption process, including high temperatures, high ionic strength, high pH and high shear-stress,[130] as well as the presence of potentially inhibiting pollutants from the flue gas mixture, requires comprehensive efforts in reaction and protein engineering and (bio)chemical studies. Bond *et al.* addressed the inhibition of NO_x and SO_x pollutants, by studying the catalytic activity of bovine CA (BCA) in presence of SO_4^{2-} and NO_3^-.[131] CO_2-hydration was monitored using the delta-pH method, which monitors the changes in pH over time upon reaction of CO_2 with H_2O to H^+ and HCO_3^-. Hence, CA-activity can be assessed by following the decrease in pH over time. BCA showed excellent activity in presence of low concentrations (<0.1 M) of NO_3^- and SO_4^{2-} in Tris-buffer pH 7.8, while significant inhibition is observed at higher concentrations of both pollutants. Similar results were obtained by Lu *et*

al.[132] CA kinetics in aqueous 20 wt% $K_2CO_3/KHCO_3$ solutions remained unchanged in presence of SO_4^-, NO_3^- and Cl^- at concentrations of up to 0.9 M, 0.2 M and 0.7 M, respectively. However, the emission of NO_x and SO_x is strictly controlled, and a CO_2 scrubber would be probably be connected in succession to a sulfur scrubber.[131] Thus, high concentrations of these pollutants are unlikely and only low concentrations within the non-inhibiting range are expected. In other words, CA remains intact at relevant concentrations of pollutants present within the capture process.

A much greater challenge for the use of CAs in PCCC processes is their lack of thermostability at elevated temperatures which are applied in scrubbing systems, especially in the CO_2 stripping process. Most CA strains isolated from mammals or prokaryotes are known to lose their catalytic activity at temperatures between 55 – 65 °C[119] which outright prevents their application in industrial scrubbing processes. In order to tackle this problem and successfully implement CAs into valid PCCC processes, the following three approaches are under consideration (Fig. 3.5).
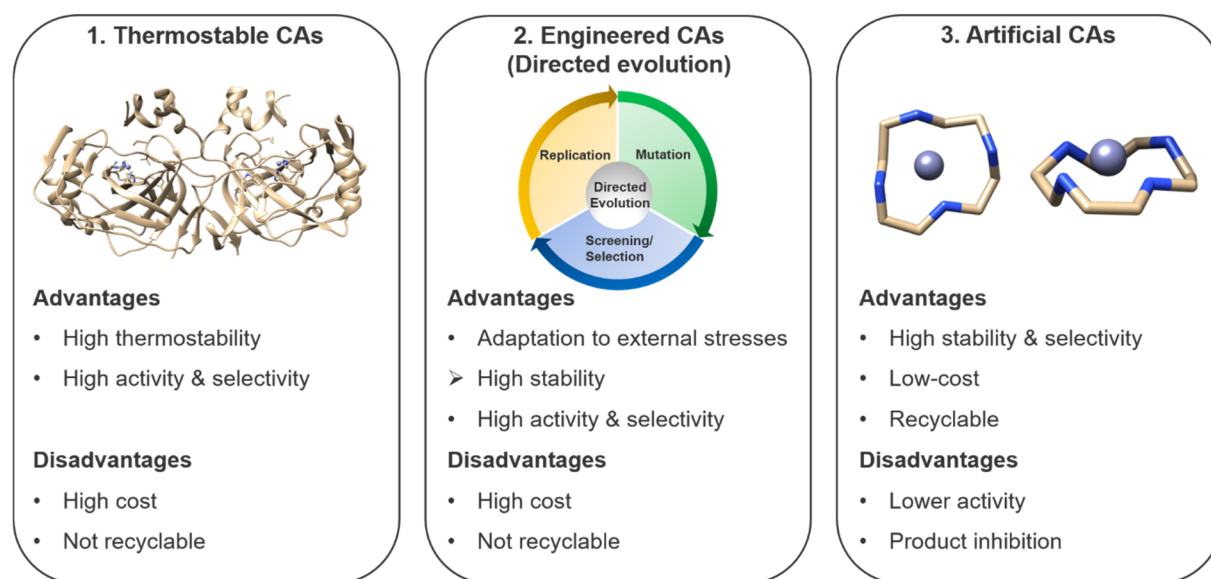
Figure 3.5: Overview over the advantages and disadvantages of the three approaches that are under consideration to implement CAs into CO_2-capture systems. (1) Thermostable CAs (SspCA; PDB code: 4G7A); (2) CAs engineered by directed evolution; (3) enzyme mimcs (Zn(II)-cyclen; PDB code: 3L8Y).

The first approach includes the application of heat stable CAs occurring in thermophilic microorganism. The Capasso group was able to clone and purify a thermostable α-CA, named SspCA, from thermophilic microorganism *Sulfurihydrogenibium yellowstonense* living in hot springs at temperatures of 70-110 °C.[133,134] SspCA showed high degree of thermostability for several hours at 70 °C,[133] and only showed declines in activity after 2 hours at 100 °C, while BCA was unstable above 50 °C (Figure 3.6).
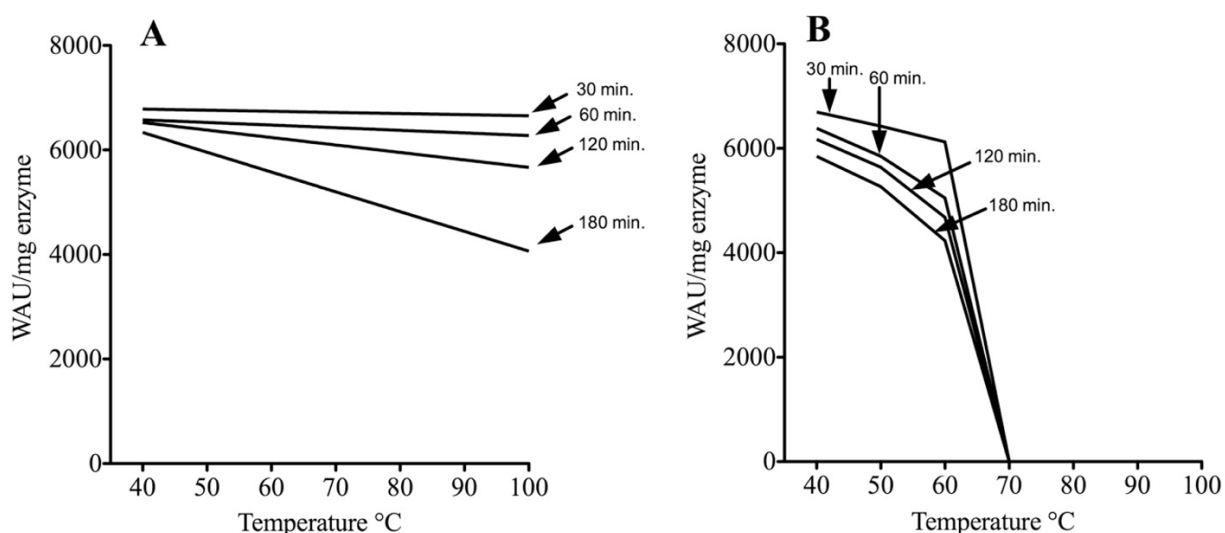
Figure 3.6: Assessment of CO_2-hydration activity of (A) SspCA and (B) BCA II after incubation for a fixed time at the indicated temperatures. Adapted from Ref.[135].

Furthermore, SspCA was immobilized within a polyurethane (PU) foam, which increased its stability as SspCA maintained its activity after incubation at 100 °C for 50 h.[135] Moreover, the immobilization within the PU foam greatly increased the long-term stability of the enzyme. The embedded SspCA was stable up to one month at 25 °C without decreasing its activity.[136] PU-SspCA was then applied for the capture of CO_2 under conditions close to a post-combustion-system by using a three-phase trickle-bed reactor. The system was operated with a countercurrent flow of 20% CO_2 gas in N_2 and H_2O similar to an amine scrubbing set-up. However, only a moderate conversion of CO_2 of approx. 40% was achieved.[136]

In an attempt to facilitate the recovery of SspCA from capture processes, Perfetto *et al.* conjugated the enzyme to magnetic Fe_3O_4-nanoparticles.[134] Compared to the free variant, SspCA did not show decreases in activity after operation at 70 °C for 80 h (Figure 3.7). Regarding long-term stability, Fe_3O_4-SspCA was stable for 30 days at 25 °C, analogous to PU-SspCA. However, by utilizing the ferromagnetic properties of the Fe_3O_4-nanoparticles, recovery of Fe_3O_4-SspCA was possible by simply using a magnet or applying an electromagnetic field.

A patented, more efficient, heat-stable CA strain was obtained from *Bacillus clausii*, which retained 80% of its activity after incubation in bicarbonate solution for 15 mins at 60 °C.[137] At an enzyme loading of 0.6 g/L and gas stream 15% CO_2, this CA was able to extract >99% CO_2, compared to 33% without the enzyme.[137,138] Furthermore, in a 1% MEA solution, CO_2 absorption was also increased by 2-fold.
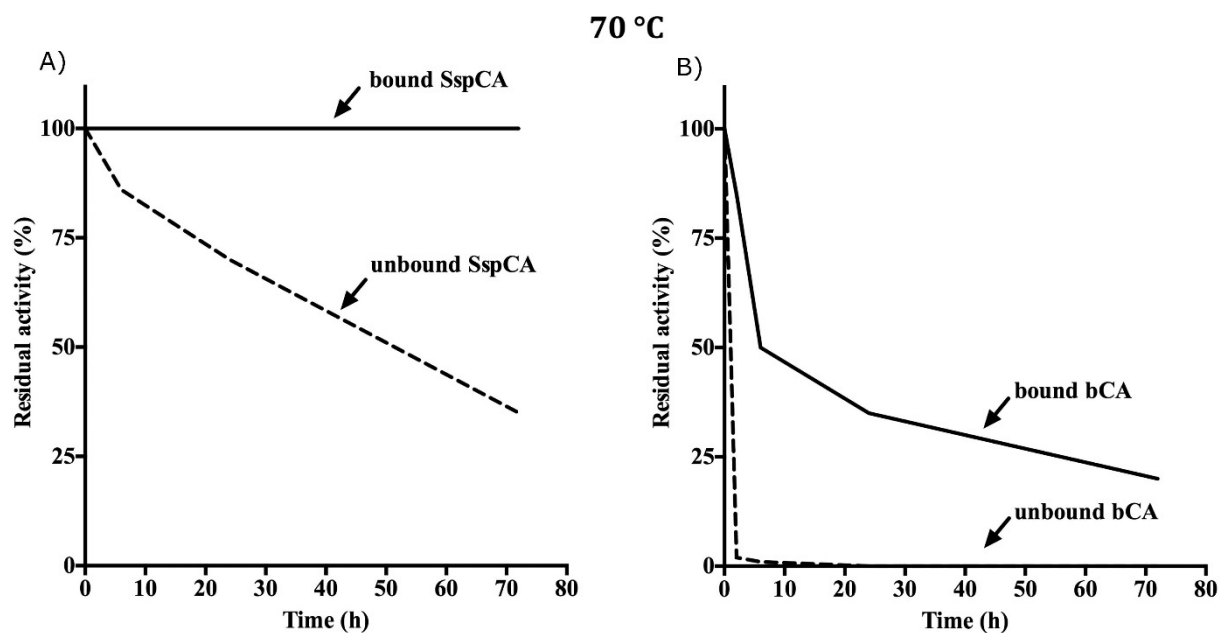
Figure 3.7: CO_2-hydration activity of SspCA and bCA bound and unbound to magnetic Fe_3O_4-Nanoparticles. Adapted from Ref.[134].

Heat stable CAs from thermophilic microorganism present a promising approach in order to circumvent the inadequate thermostability of natural CAs. However, partial drawbacks of all naturally occurring CA types is said to be their high cost and lack of stability in aqueous media containing relevant concentrations (ca. 50% v/v) of amine-based solutions that are considered as benign alternatives to MEA, such as Methyldiethanolamin (MDEA).[138] Nevertheless, amine solvents are not a prerequisite for PCCC methods as aqueous K_2CO_3 solutions are also under consideration. So far, no relevant application using naturally occurring thermophilic CAs has been reported.

The second approach towards the application of CA in PCCC involves the use of protein engineering. In particular, directed evolution introduced a powerful tool to evolve a potential CA variant towards resistance to environmental stresses that are present under industrial conditions. A great example of using directed evolution to enable CAs for PCCC methods is given by the company "CO_2 Solutions inc." of Québac, Canada in 2015, who were able to successfully commercialize their CA-mediated CO_2-capture process.[139] They targeted a CA from thermophilic bacteria that exhibited relevant initial thermostability for directed evolution using an in-house, screening procedure. Due to company secrets no detailed information on the screening procedure nor the initially used CA and its respective modifications are available. The evolved CA was implemented into a large-scale pilot system near Montreal, Canada in Salaberry-de-Valleyfield (short: Valleyfield) in 2015 (Fig. 3.8A).
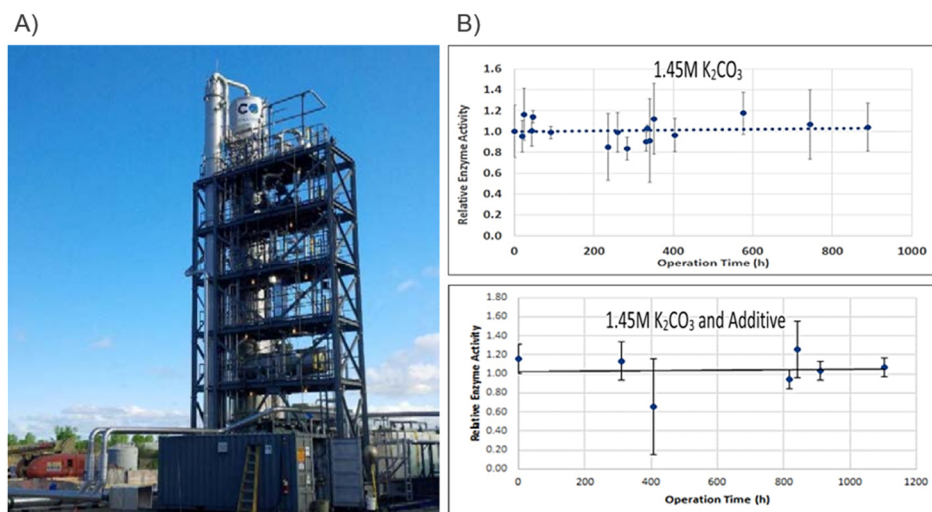
Figure 3.8: (A) Photo of the CA-mediated CO_2-capture demonstration unit of CO_2-Solutions inc. (B) Activity profile of modified CA employed during the demonstration of the plant over a period of approx. 45 days.[139]

The Valleyfield project was the largest enzyme-based CO_2-capture study ever performed and was used to sequester 10 tons CO_2/day (tpd) CO_2 from a natural gas fired steam generator over the period of 150 days. The process ran using 1.45 M aqueous K_2CO_3 as the primary solvent in which the enzyme is homogenously dissolved, without any immobilization. The evolved CA variant was demonstrated to be stable and active over more than 45 days under process conditions (Figure 3.8B). Adaptive CO_2 capture rates in the range of 65–95% were achieved and the purity of the isolated CO_2 was 99.95%. In fact, the obtained CO_2 has a level of purity for immediate usage as a C1-building block in chemical synthesis and only modest treatment is necessary to enable its use in food or beverage industry. Moreover, technoeconomical-analysis revealed a total cost of captured CO_2 of \$28.00/ton,[139] which is significantly lower compared to previous MEA-scrubber with capture costs of 51-82\$ per ton.[122] In addition, by using water as a non-corrosive solvent, no solvent degradation or formation of hazardous compounds was observed, no solvent treatment was necessary during the process and the relatively low amounts of produced wastewater were directed into the surrounding sewer systems.[139] Deployment of further demonstration system for the sequestration of CO_2 in larger scales of up to 30tpd and 300 tpd CO_2 for extended periods of 10 years has already been initiated in Saint-Félicien (Québec) and Alberta, respectively.

The application of CAs, together with joint efforts in biology, chemistry and engineering enabled the development of a CO_2-capture technology that is a superior and highly environmentally benign alternative to conventional PCCC based on amine solvents. However, a scale-up of the CA-based systems and the associated CA production is required to enable the implementation into medium and large power plants that emit at the least 150 000 – 500 000

tons CO_2 per year. Furthermore, the system needs to be tested over periods of years to sufficiently assess the enzymes long-term stability and life cycle/cost-efficiency.

The last approach used to overcome the limitations of CA (or enzymes in general) is a biomimetic approach. Instead of using CA as the active catalyst, it is used as a model for the design and manufacturing of new robust artificial enzymes. Scientists are continuously designing and developing novel artificial enzymes to obtain widely applicable, low-cost alternatives to enzymes, with high activity and selectivity that are readily synthesized and modified, also on a large scale. In the context of CO_2 capture, most of the mimics developed and studied are small molecules that mimic the active site of CA by using different macrocyclic or tripodal ligands for the coordination of metal ions, such as zinc, cobalt, copper and nickel.[140]

One of the most efficient and robust CA mimics is the cyclic polyamine 1,4,7,10-Tetraazacyclododecan (cyclen, Fig. 3.9A).[108,141] Cyclen is a small molecule that mimics the catalytic center of CA by acting as a multidentate ligand to form the corresponding chelate complex with a Zn(II)-ion. The resulting catalytically active Zn(II)-cyclen, shows great resemblance to the naturally occurring 3-His-Zn(II)-center found in natural CAs. Compared to the natural analogue, Zn(II)-cyclen shows greater robustness towards harsh experimental conditions, such as high temperatures up to 130 °C, high pH (>12) and nearly saturated salt-concentrations (45% w/w K_2CO_3) as determined by a laboratory scale CO_2-capture set-up.[108] Zn(II)-cyclen shows around one-third of the activity of a CA III isoform.[142] however, its activity is inhibited with increasing concentrations of formed hydrogen carbonate (product inhibition). To address the product inhibition, electron-donating ligand environments have been proposed to promote hydrogen carbonate dissociation from the metal center. Based on that, Lippert *et al.* reported a water-soluble, electron donating, imine containing salen-like ligand that coordinates Zn(II)-ions (Fig. 3.9B).[143] The Zn(II)-complex proved to be robust and exhibited rate constants larger by two orders of magnitude, compared to zinc cyclen.[143] An overall increase in CO_2-absorption of up to 34% was observed, which theoretically correlates to a reduction in absorber tower volume of approx. 30% and a significant reduction in capital cost of 15%. Nevertheless, a general disadvantage of this ligand scaffold are the potential hydrolysable imine groups.

In 2016 Kelsey *et al.* circumvented this problem, by using a bis(hydroxyphenyl) phenanthroline ligand (Fig. 3.9C).[13] The ligand shares similarities in coordination of the metal ion to the previous ligand but contains no hydrolyzable imine groups.[13] The respective Zn(II)-complexes were studied for CO_2 hydration in a post-combustion environment, using concentrated primary amine solutions. In comparison to the uncatalyzed reaction, the

phenanthroline complex showed a 25% increase in CO_2 absorption and a similar rate constant to the salen-based complex by Lippert *et al.*[143] Despite the advantages, solubility issues arose using the phenanthroline ligand. Therefore, undesired additions of acetonitrile or pyridine into the sorbent solvent were necessary to solubilize the catalyst.[13] Albeit, the progress in designing small molecule CA mimics, that can be used under industrial conditions, their structural complexity and the related catalytic efficiency cannot compete with natural CAs.
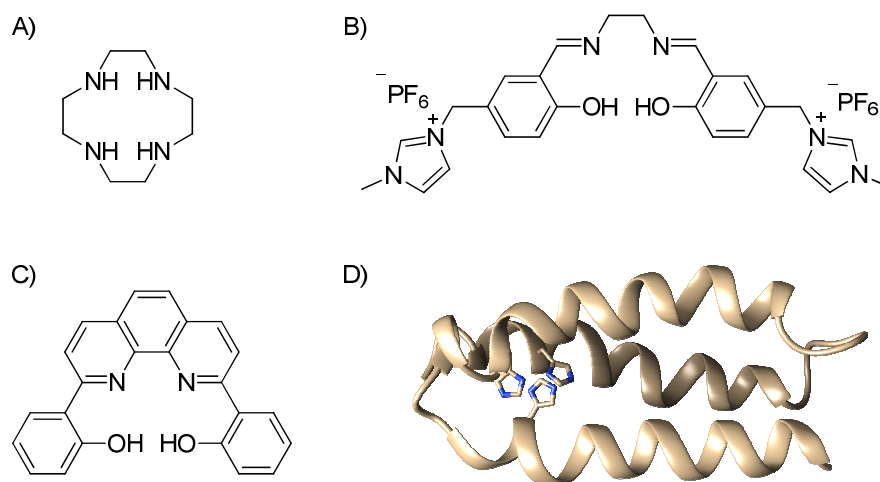
Figure 3.9: Scaffolds for the complexation of Zn(II) to mimic the catalytic center of CA: (A) cyclen; (B) imine-containing salen-ligand; (C) phenantroline-ligand; (D) α_3DH$_3$ three-helix bundle (PDB code: 2A3D).

In this context, Cangelosi *et al.* showed the advantages of using a more complex peptide scaffold as a CA mimic.[144] For that, a de novo designed peptide consisting of 73 amino acids (Fig. 3.9D) reported by DeGrado[145] that folds into a three-helix bundle was modified by incorporating three histidine residues into the primary structure. The modified peptide binds Zn(II) with high affinity through the three histidine imidazole rings. The resulting $Zn^{II}\alpha_3$DH$_3$ metalloenzyme catalyzed the hydration of CO_2 under physiological conditions better than any small molecule model of CA. The resulting metalloenzyme catalyzed the hydration of CO_2 under physiological conditions better than any small molecule model of CA to that date. The reason for the exceptionally good catalytic efficiency is said to be the more complex peptide architecture and developed secondary coordination sphere, in which hydrogen bond networks and cooperative effects are established. Nevertheless, the stability of $Zn^{II}\alpha_3$DH$_3$ is dictated by the frailty of the peptide backbone, which limits their application in industry, similar to natural CA. Hence, the design of artificial enzymes as CA mimics demands strategies that carefully combine both, a robust backbone and elaborate active sites structures in order to withstand harsh conditions, while maintaining reasonable catalytic activity.

3.2.2 Chemoenzymatic cascade reactions

The field of catalysis made tremendous progress over the last decades in developing novel catalysts for various industrial relevant processes. However, even to date, catalytic processes are designed to include only one chemical transformation at a time.[146] Since every single reaction step requires specific reaction conditions (solvents, additives, temperature etc.), methods of isolation and subsequent transfer of the product to the next reaction vessel, multistep syntheses are connected to considerable waste production and energy consumption.[147] In an attempt to minimize these ecological and economical drawbacks, the field of catalysis increasingly turned towards multistep processes in aqueous media, in which two or more catalysts are used in tandem to act on a given substrate, thus, enabling two or more reactions in one pot (Fig. 3.10).[148] As a result, no work-up steps of intermediates or transfer of chemicals is needed, which reduces the overall waste production, operating time and production cost.[149] Moreover, toxicity or instability of intermediates can be circumvented[150] and unfavorable reaction equilibria can be prevented by immediately converting the unfavored intermediate,[151] which results in an overall higher yield of the desired end-product.[152]
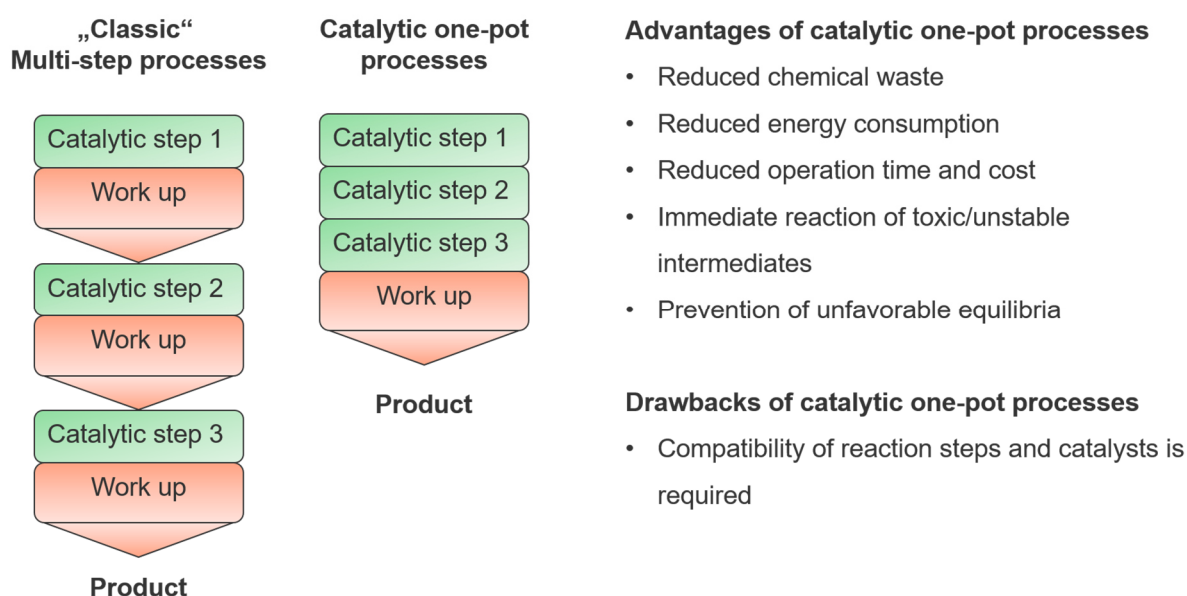
Figure 3.10: Comparison between the concepts of "Classic" multi-step processes and catalytic one-pot processes and a list summarizing the advantages and disadvantages of catalytic one-pot reactions. Drawn according to Gröger and Hummel.[149]

Despite the vast advantages, a major challenge in designing such reactions is associated with the compatibility of different catalysts or individual reaction steps under a single set of reaction conditions.[148,149] Therefore, several aspects need to be considered: pH, temperature and solvent

stability of all compounds; cross-inhibitions or poisoning of catalysts due to metal-cofactors;[153] cross-reactivity of substrates, intermediates and products.[154,155]

In literature, multistep one-pot reactions are frequently described with terms such as tandem,[156] domino[157] or cascade reactions.[158] The terms are either used synonymously or with a different meaning. In order to clarify the terms and introduce a coherent system, Rudroff *et al.* suggested in 2018 to classify all multistage one-pot syntheses, where two or more reactions take place, and the product of the first reaction serves as the substrate of the second reaction, as "cascade reactions".[148] Overall two modes of cascade reactions are possible: first, the "concurrent mode" in which reaction conditions remain unchanged throughout the whole synthesis; second, the "sequential mode", where catalysts or key components are added after the first reaction. Concurrent cascade reactions are further subdivided into domino, tandem and compartmentalized tandem reactions. Domino reactions apply only one catalyst that catalyzes the multistep synthesis, whereas tandem reactions apply two or more catalysts for the desired synthesis. In both cases, no temporal or spatial separation of the respective catalysts take place. In contrast, compartmentalized tandem reactions make use of spatial and temporal separation of different catalysts,[148] by encapsulating and protecting one of the catalytic units in, e.g., gels or polymers within the reaction mixture, thus preventing mutual inactivation or incompatibilities arising from solvents. Fig. 3.11 provides an overview over the suggested types of cascade reactions.
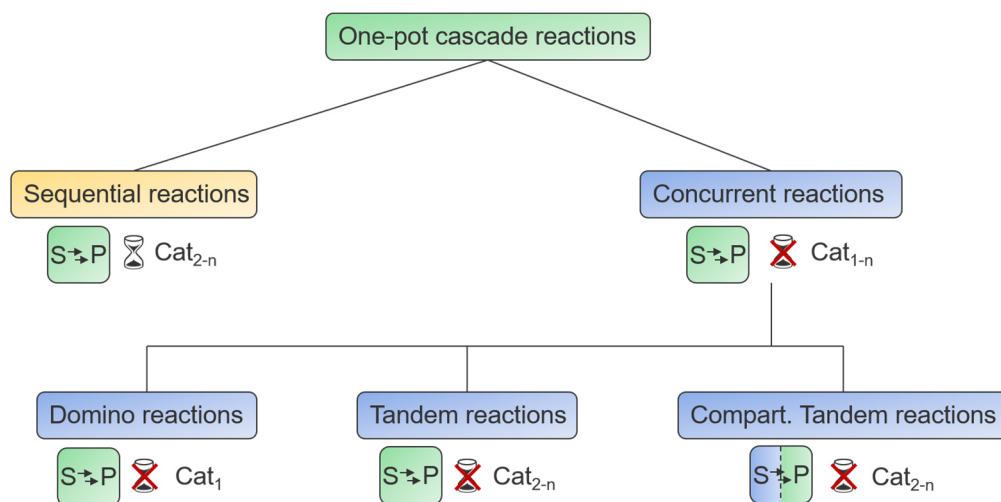

Figure 3.11: Different terms for one-pot cascade reactions defined by Rudroff *et al.* The number of catalysts is given from 1-n. The hourglass indicates temporal separation and a dashed line within the illustrated reaction vessel (green box) indicates also spatial separation in form of compartmentalization. Drawn according to Rudroff *et al.*[148]

Among various possibilities of different cascade systems, the combination of biocatalysis and chemocatalysis (metal- and organocatalysis) in aqueous media, so called chemoenzymatic

cascade reactions, emerged as an ecologically and economically appealing concept in organic synthesis.[148,149,153] Specifically, enzymes in conjunction with metal-catalysts complement their unique reaction scope.[148,149] While enzymes are typically used for asymmetric conversions of functional groups in a specific position of a molecule; metal-catalysts find frequent application in C-C-bond forming reactions including metathesis, cross-coupling (Suzuki, Heck etc.) and hydrogenation reactions. In combination, chemoenzymatic cascade reactions enable facile routes towards valuable products, without the necessity of protecting groups or harsh reaction conditions.

In the following, examples will be provided to give an overview over the field of chemoenzymatic cascade transformations and their potential in green synthesis. Although, some of the described reactions might not be directly relevant for the current thesis, they illustrate the concept of cascade transformations, which is utilized in one of the projects of this work (see section 7.1).

The first example is the successful combination of olefin metathesis and biocatalysis in water. This combination presents an attractive and environmentally friendly tool in organic synthesis as it provides a route towards asymmetric unsaturated compounds in one pot. Gröger and co-workers demonstrated a sequential cascade one-pot approach towards unsaturated cyclic acids, such as cyclic malonic acid monoesters, which can be transformed into non-natural amino acids having a quaternary carbon center (Scheme 3.2).[159]
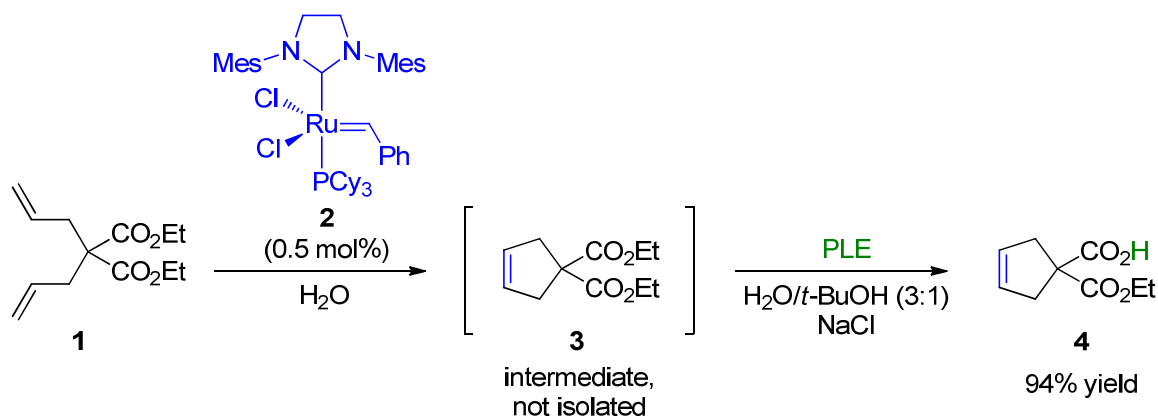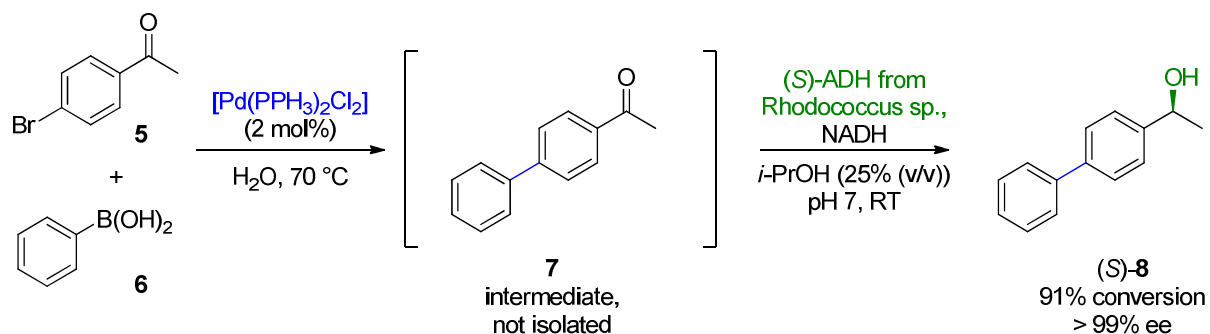

Scheme 3.2: Chemoenzymatic one-pot process combining olefin metathesis using Grubbs II catalyst (blue) with an enzymatic ester hydrolysis catalyzed by pig liver esterase (green). Drawn according to Tenbrink *et al.*[159]

The starting material diallyl malonate **1** was first converted into product **3** by a ring-closing metathesis using Grubbs II catalyst **2**. Interestingly, water turned out to be the preferred solvent for this reaction, enabling the reaction to proceed with high efficiency and excellent conversion, with only low catalyst loadings of 0.2–0.5 mol%. Immediate reaction of **3** with pig liver esterase (PLE) transformed the in-situ formed intermediate selectively into the monoester **4** with high

yield (94%) and high optical purity, without the formation of side-products. Further, studies showed that the two catalysts are highly compatible as PLE activity was not influenced by the chemocatalyst.

Next to olefin metathesis, cross-coupling reactions are an important type of organic transformations in industry. The joint effort of the Gröger and Hummels group led to the first example of an aqueous one-pot two-step process in which a Suzuki cross-coupling reaction was combined with an asymmetric biocatalytic transformation (Scheme 3.3).[160]

Scheme 3.3: Chemoenzymatic one-pot process combining a Suzuki cross-coupling reaction (blue) with an enzymatic (S)-alcohol dehydrogenase-reduction (green). Drawn according to Burda et al.[160]

In the first step, biaryl ketone **7** was obtained by Suzuki cross-coupling of aryl-ketone **5** and boronic acid **6** catalyzed by [Pd(PPh₃)₂Cl₂]. Then, after adjustment to neutral pH, **7** is converted to the corresponding biaryl alcohol (S)-**8** in a NADH-mediated biocatalytic step using alcohol dehydrogenase ((S)-ADH). Early attempts to perform the reaction were unsuccessful, however, after careful studies of the impact of individual components, boronic acid was found to be the key inhibitor of ADH. Thus, excess **6** needed to be avoided and the reactions has to be performed in a sequential mode. That is, after completed Suzuki cross-coupling and absence of boronic acid, (S)-ADH was added and (S)-**8** was obtained in high yield (91%), with >99 % ee.

Aside from metal complexes, Boffi *et al.* reported another interesting approach of a chemoenzymatic two-step one-pot synthesis by utilizing metal nanoparticles as the chemocatalytic component.[161] Perfluoro-tagged Pd-NPs with a diameter of 3.6 nm were immobilized on fluorous silica gel by fluorous interactions. The immobilized Pd-nanoparticles were then used as catalyst for the Heck reaction of, e.g., aryl iodide **10** with allylic alcohol **9** to the corresponding ketone **11** in water (Scheme 3.4). The formed product **11** was subsequently converted in an enantioselective (R)-ADH-catalyzed reaction to the corresponding chiral alcohol (R)-**12** with high yield (~90%) and excellent enantiomeric excess (>99% ee) without intermediate workup. The Pd-NPs were stable over eight rounds of recycling and did not leach into the reaction medium.
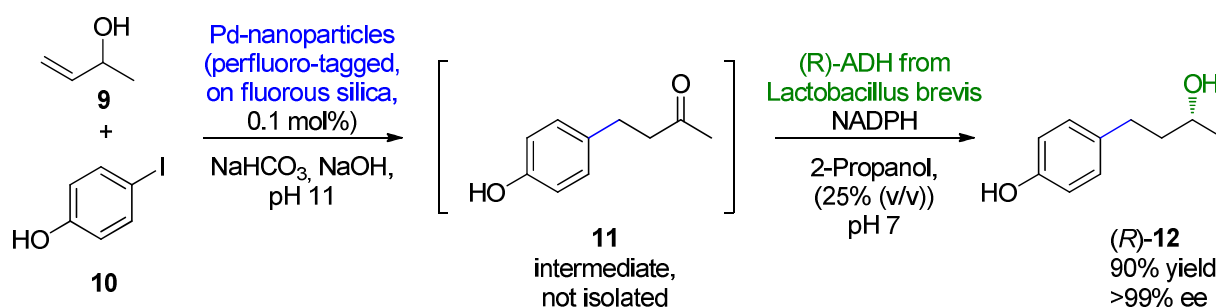
Scheme 3.4: Chemoenzymatic one-pot process combining a Heck reaction (blue) with a biocatalytic (*R*)-alcohol dehydrogenase-reduction (green). Drawn according to Boffi *et al.*[161]

A similar approach was reported by San *et al.* by creating a nanohybrid catalyst consisting of Pt-NPs conjugated to an oligomeric esterase (EST).[162] The EST-Pt-NP conjugate enabled hydrogenation reactions and ester hydrolysis in aqueous solutions in one pot. EST self-assembles into cube-like structures, in which channels for ester hydrolysis are established. Pt-nanoparticles with diameters in the range of 2-3 nm were directly grown onto the outside of the assembled EST architecture, thus, both catalysts were fully accessible to the substrate. Using the EST-Pt-NP conjugate, the multi-step synthesis of acetaminophen (paracetamol, **16**), a broadly used antipyretic, was readily accessible using cheap starting material 4-nitrophenylacetate (4-NPA, **13**) as staring material (Scheme 3.5).
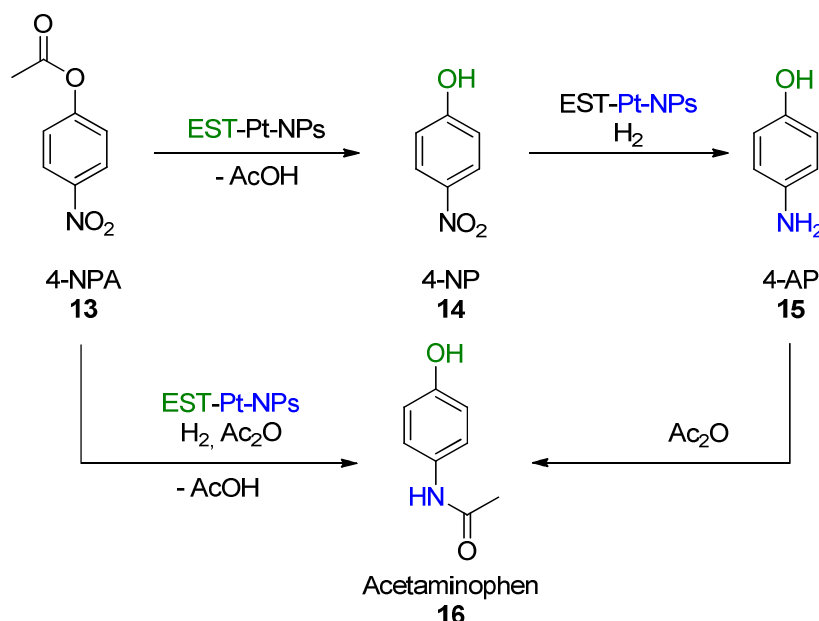

Scheme 3.5: Chemoenzymatic one-pot route towards acetaminophen **16** by pairing an enzymatic ester hydrolysis (green) with a Pt-NP-catalyzed reduction (blue). Drawn according to San *et al.*[162]

13 is first converted by an enzyme-catalyzed ester cleavage to 4-nitrophenol (4-NP, **14**) and acetic acid. Subsequently, in presence of $NaBH_4$ as a hydride donor, **14** is readily converted to 4-aminophenol (4-AP, **15**) by a Pt-NP-catalyzed hydrogenation reaction. After that, acetylation using acetic anhydride (Ac_2O) leads to the desired product **16**. An important part of the

multi-step reaction is the generation of acetic acid in the ester hydrolysis and the acidification of the reaction medium. Weakly acidic aqueous conditions are known to enable acetylation reactions by acetic anhydride, thus, avoiding the use of any organic solvents. The cascade reaction is also performable in a concurrent mode by simply mixing all the components in water, leading to an efficient conversion to **16** within 10 minutes and 96% yield. Furthermore, EST-Pt-NP conjugate was compared to the individual catalysts, i.e., assembled EST and citrate-stabilized Pt-NPs, respectively. Interestingly, the conjugated variant EST-Pt-NP was superior in both, ester hydrolysis and hydrogenation reaction, indicating synergistic effects between the enzyme and nanoparticles. For EST it was suggested that binding of the Pt-NPs to the surface induces slight conformational changes in the enzyme structure, which was indicated by small alterations in the respective CD-spectrum. It was proposed that the conformational changes of the protein result in more exposed and accessible substrate binding sites. Thus, binding and conversion of 4-NPA is facilitated, which in total leads to the observed increased rates of reaction, compared to the individual components.

Besides (transition) metal catalysts, organocatalysts present another powerful type of chemocatalysts. Recent advances in asymmetric organocatalysis led to the development of various catalytic methodologies towards enantiomerically enriched or pure products. Pairing these methods with biocatalysis enables the formation of complex stereoselective products.

Gröger and co-workers pioneered the field by showing the first example of a sequential organoenzymatic cascade reaction for the production of 1,3-diols with great diastereomeric ratios and enantioselectivity (Scheme 3.6).[163]
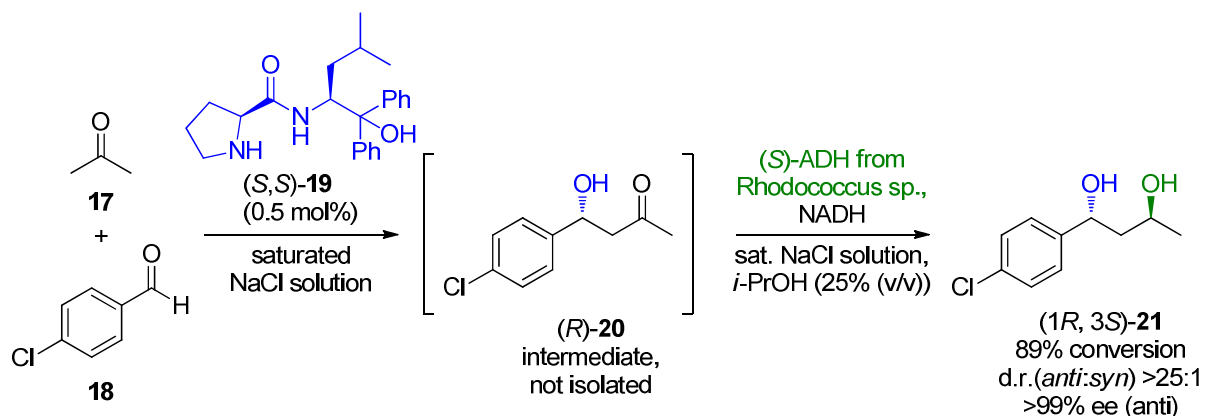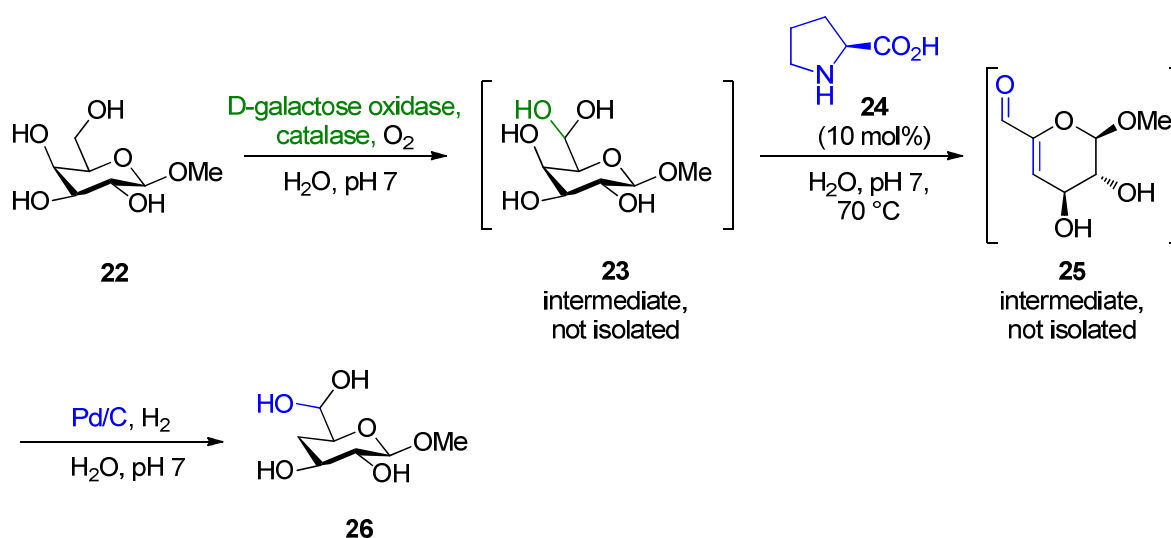

Scheme 3.6: Chemoenzymatic one-pot process combining an organocatalytic aldol reaction (blue) with an enzymatic (*R*)-alcohol dehydrogenase-reduction (green). Drawn according to Rulli *et al.*[163]

A peptidic Pro-Leu-based catalyst (*S, S*)-**19** was used as the organocatalytic component as it was shown to catalyze the enantioselective aldol reaction of **17** and **18** to give aldol product (*R*)-**20** also in water. This opened up the possibility for a subsequent enzymatic conversion as

(R)-**20** was reduced in a following step by addition of (S)-ADH to give the respective 1,3-diol (1R, 3S)-**21** with good conversion (89%) remarkable diastereoselectivity (>25:1 (anti/syn)) and enantioselectivity (>99% ee).

The supreme discipline in chemoenzymatic cascade reactions, which is considered to be a major long-term goal, is the successful combination of more than two catalysts in one-pot. Although very difficult to design, the Kieboom group combined metal-, organo- and biocatalysis into an aqueous one-pot process for the synthesis of 4-deoxy-D-glucose derivatives **26** from D-galactose **22** (Scheme 3.7).[164] In the first step, **22** is selectively oxidized by the enzyme D-galactose oxidase in conjunction with the enzyme catalase to the geminal diol intermediate **23**. A following dehydration catalyzed by L-proline (L-**24**) transforms **23** into the α,β-unsaturated aldehyde **25**. **25** then undergoes a Pd-catalyzed hydrogenation to be reduced to the final product **26**. This example illustrates the potential and power of cascade reactions as no stochiometric amounts of reagents or protecting groups are needed during the whole synthesis.

Scheme 3.7: Chemoenzymatic one-pot process combining a biocatalytic oxidation (green) with a L-Proline catalyzed reduction (blue) and a subsequent Pd/C-catalyzed hydrogenation (blue). Drawn according to Kieboom *et al.*[164]

In summary, chemoenzymatic cascade reactions in aqueous media has proven to be a promising approach for the design of efficient and environmental-friendly multistage syntheses. However, the compatibility of individual catalysts or reaction steps remains a major challenge and needs to be assessed and optimized for each catalyst composition. In addition, stability and recycling of (mostly) biocatalysts will play a major role in reaction engineering. Compartmentalization and immobilization of biocatalyst are expected to be a future trend.[149] Furthermore, an ultimate goal in catalyst design is the development of single multifunctional catalysts that combines, e.g., chemo- and biocatalysis in one unit, while being robust and easily recoverable from a reaction mixture.

4 Nanozymes: alternatives to natural enzymes

Catalysis is an integral part of sustainable and green chemistry, but it is considered that nanotechnology makes catalysis "greener".[165] The field of nanocatalysis rapidly advanced within the last decades, as the advantages of using nanometer sized heterogenous catalyst became increasingly evident. The advantages include high catalytic activities and selectivities, while the catalyst is robust and easily separable from a reaction mixture.[166] Owing to the combination of these aspects, nanocatalysis is frequently referred to as the bridging gap between homogenous and heterogenous catalysis.[167]

In particular, nanomaterials with enzyme-like activities have attracted considerable research attention as cost-efficient alternatives to natural enzymes. In this context, the collective term "nanozyme" is used to encompass and describe a large number of inorganic nanomaterials with enzyme-like activities.[168] Within the past decade, the field of nanozymes has rapidly grown, which is also reflected by the exponential number of publications in this field (Fig. 4.1).
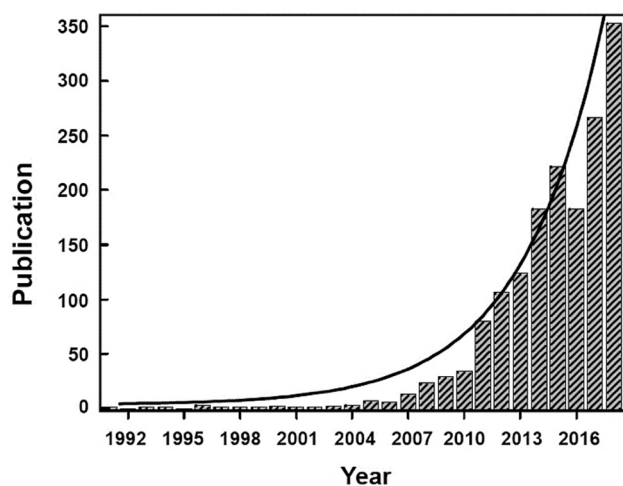

Figure 4.1: Number of publications in the field of nanozymes from 1992 until the end of 2018. Figure reproduced with permission from Ref.[169], which was initially adapted from Ref.[30].

Several hundred types of nanomaterials have been studied and were found to intrinsically mimic the activity of one or several natural enzymes, mostly oxidoreductases or hydrolases. To obtain these artificial nano-enzymes, various approaches have been reported, which include the application of carbon-based nanomaterials (fullerenes, carbon nanotubes, graphene oxide), metal-organic-frameworks, metal-oxide- (iron, cerium, vanadium, copper) and noble-metal-nanoparticle (Au, Pt), to name a few. A comprehensive summary over the different archetypes of nanozymes and their catalytic activities is shown in Table 4.1.

Due to the vast number of different nanomaterials and origin of their respective catalytic properties, the term "nanozyme" will be used to refer to metal nanoparticles (NP) with enzyme-like characteristics only, if not specified otherwise.

Table 4.1. Overview over archetypal nanozymes and their respective enzyme-like activities.

Type of Nanomaterial		Enzyme-like activities
Noble metal-based	(Functionalized) Gold nanoparticles	Catalase,[170] esterase,[45,46,171] glucose oxidase,[172–174] nuclease,[175] nitroreductase,[176] peroxidase,[177] silicatein,[178] superoxide dismutase[170]
	Platinum nanoparticles	Catalase,[179] peroxidase,[179] superoxide dismutase[180]
Metal-oxide-based	Iron oxide nanoparticles	Catalase,[181] peroxidase[181–184]
	Ceriumoxide nanoparticles	Catalase,[185] oxidase,[186,187] peroxidase,[188] phosphatase,[189] superoxide dismutase[190]
	Vanadium oxide	Peroxidase[191,192]
Carbon-based	Fullerenes	Superoxide dismutase,[193] nuclease[194,195]
	Graphene oxide	Peroxidase[196]
	Carbon nanotubes	Peroxidase[197,198]
	Carbon nanodots	Peroxidase[199]
Miscellaneous	Metal-organic frameworks	Peroxidase,[200] phosphotriesterase,[201] hydrogenase,[202] carbonic anhydrase[203]
	CdS-Pt nanoparticles	Alcohol dehydrogenase,[204] nitrate reductase,[205] nitroreductase[206]
	PtPd-Fe$_3$O$_4$	Peroxidase[207,208]

Nanozymes possess unique material/composition- and size-dependent physicochemical properties.[169] Thus, nanozymes possess the potential to overcome the limitations of natural enzymes (Tab. 4.2).[209] To be specific, the core structure of nanozymes mainly consists of clustered metal atoms, which form robust nanoparticles. They show high stability under harsh environmental conditions (high temperatures, pH changes) and durability for long-term storage. In contrast to natural enzymes, nanozymes can readily be separated from a reaction mixture by, e.g., filtration. Therefore, less purification steps are needed, and the catalyst can readily be recycled, hence, increased cost-effectiveness. Moreover, because of their nanometer size, nanozymes have a high surface-area-to-volume-ratio, thus, large number of exposed, high-energy surface atoms for efficient catalysis. Since the surface-area-to-volume-ratio depends on

the size and shape of the nanoparticles, catalytic activity can readily be tuned by changing those parameters.[210,211] In addition, the NP-surfaces can be functionalized with various ligands, which presents another aspect of affecting the chemical and physical properties of those particles.[212] Depending on the properties of the applied ligand molecules, the ligand-shell can bring about increased stability of individual particles,[213] biocompatibility[214] or additional catalytic activity[215] and molecular recognition.[216] Besides, nanozyme synthesis is considered to be straightforward and (depending on the material) accessible at low cost, in an environmentally benign manner,[217] also on a large scale.

Table 4.2: Comparison between natural enzymes and nanozymes.

	Advantages	**Challenges**
Enzymes	High activity	High cost
	High selectivity	Large-scale production
	Biocompatible	Long-term storage
	Broad spectrum of biocatalysis	Limited stability
	Broad range of applications	effortful separation and purification
	Protein engineering possible	Limited use under harsh conditions
		Recycling (immobilization needed)
Nanozymes	High activity (also tunable)	Limited substrate specificity
	Tunable reaction type	Inconclusive reaction mechanisms
	Multienzyme mimic	Control over size, shape, composition
	High stability and robustness	Missing reference materials
	long-term storage	Ambiguous nanotoxicity
	Low-cost	
	Mass-production	
	Recycling possible	
	Facile surface functionalization	
	Unique size-dependent properties (fluorescence, magnetic- and electric properties etc.)	

Due to these advantages, nanozymes have also proven to be superior over conventional artificial enzymes and contributed to various fields of (environmental) research,[169,218] including

biosensing,[219–222] therapeutics,[223–225] and pollutant removal.[226–228] Albeit, the tremendous progress in the young field of nanozymes and their implementation into valid processes, there are still challenges that need to be considered, which have been comprehensively summarized by Liang and Yan.[169] One of these challenges is the establishment of basic design principles. So far, there is no set of design rules in order to rationally design and predict the properties of nanozymes based on their material, size, shape and ligand layer. Moreover, characterization of nanozymes in terms of appropriate kinetic models needs to advance to include appropriate kinetic models that precisely describe the catalytic processes at their surface. However, this is not straightforward as the exact structure-function-relationship and mechanisms of nanozymes has only been partly unraveled. Liang and Yan pointed out, that a frequently used method to describe nanozyme kinetics originate from enzymology, like the Michaelis-Menten-Theory. But, nanozymes considerably differ from enzymes, as they are heterogenous catalysts, in which catalysis is mainly executed by surface atoms and adsorption mechanisms.

Another valid challenge concerns the effect of nanozymes on the environment or biological systems.[169] So far, the field lacks comprehensive, reliable, systematic investigations of cytotoxicity, uptake, biodistribution and immune responses, which generally limits their (*in vivo*) application. However, the field is rapidly advancing, and various research groups already address those challenges.

5   Gold nanozymes: prospecting for artificial enzymes

Gold, the shiny, bright yellow noble metal, was considered to be chemically inert for a long time. In fact, it is the only metal with an endothermic oxygen chemisorption energy, i.e., it does not bind oxygen on its surface, thus preventing it from participating in oxidation reactions.[229,230] However, in 1987, the pioneer work by Haruta *et al.* demonstrated that nanosized gold cluster are indeed capable of performing efficient catalysis, such as the oxidation of CO to CO_2 under mild conditions – at atmospheric pressure and ambient temperatures.[231] Up until today, this finding stimulates extensive research on gold nanoparticles (Au-NPs) and their potential to function as green catalysts for various transformations under mild conditions. However, what remains to be a matter of debate is the origin and nature of their distinct catalytic properties at the nanoscale.[230] In particular, the identification of occurring active species and valence states during catalysis are not entirely understood as numerous parameters influence Au-NP catalysis.[35] The consensus is that the size and shape of the particles, significantly dictate the catalytic activity, as an adequate number of low-coordination surface atoms is needed.[232] Additionally, quantum effects become more pronounced at the nanoscale. Specifically, the quantum size effect (quantum confinement effect) leads to discrete energy transition levels (Fig. 5.1A),[233] thus, Au-NPs possess various redox states, e.g., 15 in hexanethiol functionalized Au-NPs with a diameter of 1.6 nm.[234] The discrete energy levels are said to considerably affect the catalytic performance.[235]
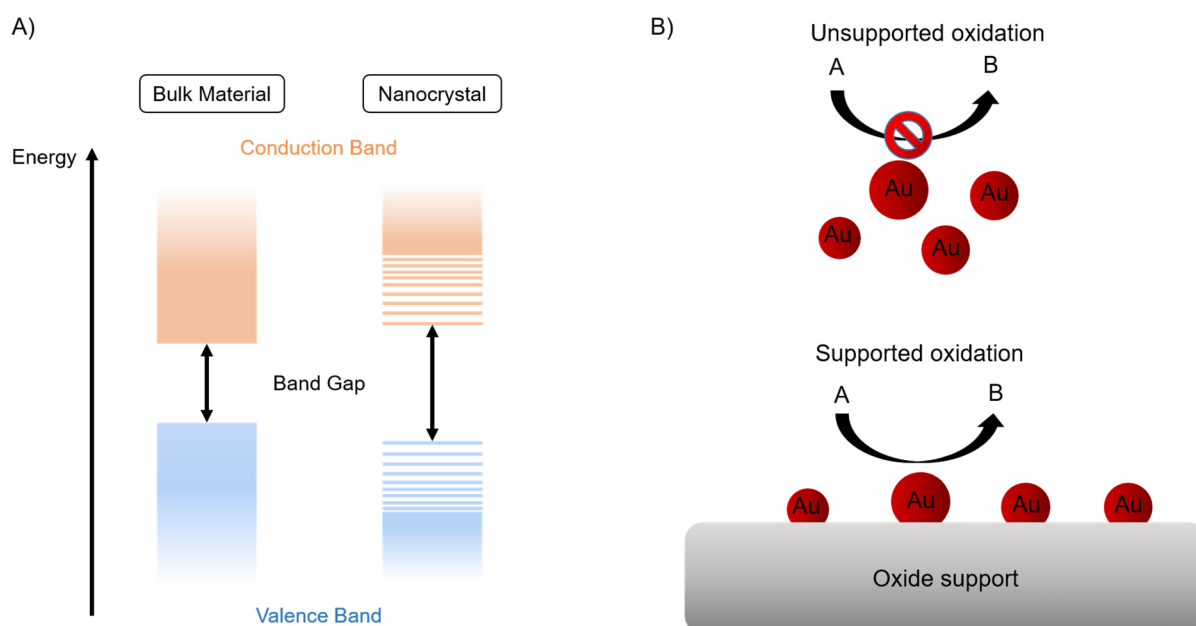

Figure 5.1: A) Energy levels of a bulk material semiconductor compared to a nanocrystal semiconductor. Splitting of conduction and valence bands into discrete energy levels due to the quantum confinement effect and semiconductor band gap increases with decreasing size. Modified and drawn according to Ref. [233] B) Comparison between unsupported Au-NPs and oxide-supported Au-NPs and the effect on catalysis. Drawn according to Ref.[236].

Furthermore, Au-NPs are frequently immobilized onto high-surface-area oxide supports,[237] such as TiO_2, ZrO_2, Fe_3O_4 or NiO. The nature of those supports is also considered to influence the electronic properties of Au-NPs, thus, catalytic activity (Fig. 5.1B).[35]

Over the years, the repertoire of Au-NP-catalyzed reactions has been extended to include also hydrogenation and other oxidation reactions. Au-NPs were found to intrinsically mimic the activities of natural oxidoreductases, including catalase, superoxide dismutases, nitroreductases, peroxidases or glucose oxidases (see Table 4.1). Specifically the latter two enable Au-NPs to be applied, e.g., in glucose meters for the detection of glucose in blood,[238,239] or in the control of water pollution, by efficiently oxidizing nonbiodegradable and carcinogenic dye pollutants, such as phenol,[240] bisphenol A,[241] methyl blue[242] and acid orange[243] from wastewater. Another enzyme-like activity of Au-NPs that bears great potential in pollution control and organic synthesis is the nitroreductase activity, which will be elaborated in detail Section 5.2.1.

Other than facilitating catalytic reactions at the metal surface, Au-NPs are also viable and robust templates for the conjugation and multivalent presentation of suitable catalytically active ligands on their surface. The anchoring of ligands onto Au-surfaces and the nature and strength of the interaction follows Pearson's hard-soft acid-base (HSAB) concept for a soft Au(I) surface.[244] Thus, amines and carboxylates as hard bases are able to reversibly adsorb to the surface by Van-der-Waals interactions resulting in a labile surface coating. By contrast, thiol-ligands as soft bases directly and irreversible react with the Au-surface. The application of thiols to functionalize Au-surfaces is widely applied and investigated. It involves chemisorption of the thiol to the Au-surface, subsequent deprotonation of the sulfhydryl-group[245] to yield a thiyl-radical (R-S·) and formation of a stable Au(I)-thiolate-bond (40 – 50 kcal/mol).[246,247] The resulting thiol-functionalized Au-NPs are commonly referred to as monolayer-protected gold clusters (Au-MPCs). These clusters possess a dense ligand-shell which have been shown to perform various catalytic processes by cooperative interactions between functional groups present within the appropriately designed ligand-layer. Thus, Au-MPCs were shown to mimic the activity of enzymes, such as nucleases,[248] silicateins[178] and esterases.[215] In particular, the usage of peptides as ligands to generate Pep-Au-NPs further broadened the spectrum of complex monolayers and concomitant intricate interactions achievable within these systems.[45,46,171] So far, Pep-Au-NPs have been shown to possess esterase activity and distinct catalytic properties, compared to other Au-MPC systems, which will be outlined in detail in section 5.2.2.

An important optical property of Au-NPs, which is not directly related to catalysis, however applied in conjunction with catalysis as a useful analytical tool, is the localized surface plasmon resonance (LSPR). The LSPR is a collective oscillation of conduction electrons localized across the Au-NP.[249,250] That is, when the diameter of an Au-NP is smaller than the wavelength of incoming light, conduction electrons are collectively excited by the electric field of incoming photons. The resonant excitation leads to a collective polarization and movement of the conduction electron cloud across the Au-NP relative to an equilibrium position (Fig. 5.2A). Due to Coulomb attraction, the electron cloud is pulled into the opposite direction, leading to an oscillating electron movement (surface plasmons). For Au-NPs, resonance conditions are satisfied by light in the visible spectrum,[251] for example 520 nm for Au-NPs with a diameter of 7 nm (Fig. 5.2B). Therefore, Au-NPs are usually observed to have an intense red color. However, the LSPR is influenced by various parameters that change the structure or electronic nature of the surface, like size and shape, interparticle distance or dielectric constant of the surrounding medium (solvents, ligand-shell).[249,251] To be precise, changes in size and shape of the particle, lead to alterations in surface geometries and associated electric field density, causing a shift in the resonance frequency.
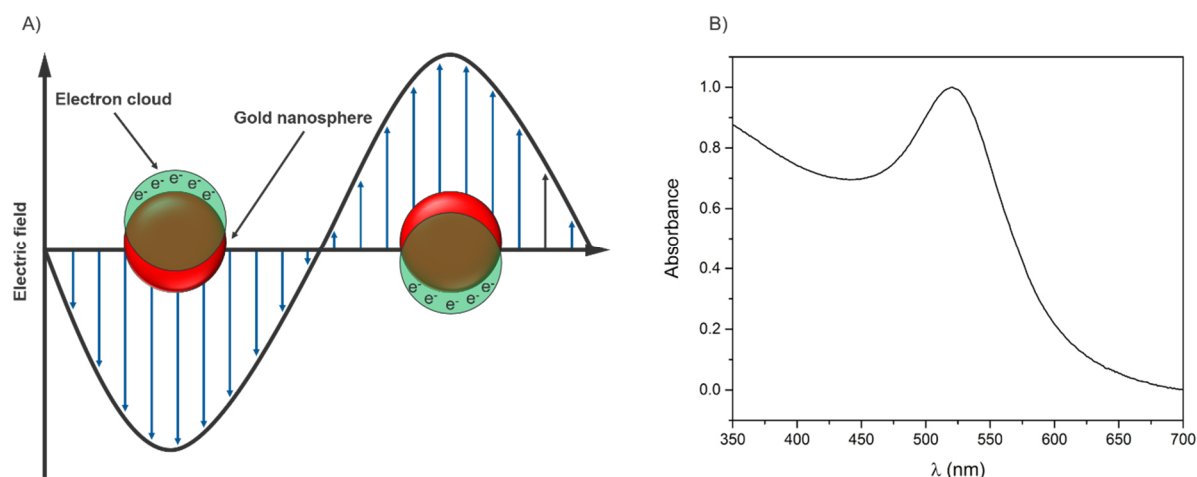
Figure 5.2: (A) Schematic illustration of surface plasmon resonance in plasmonic gold nanospheres. (B) UV/vis-absorption spectrum of a gold nanoparticle with a diameter of 7 nm showing the plasmon resonance maximum at 520 nm.

Moreover, surface plasmons of Au-NPs at close proximity are able to interact with each other. As a result, plasmon oscillations are coupling and lower energy is necessary in order to excite the plasmon assembly, which results in a significant shift of the excitation wavelength into the red.[252] Therefore, aggregation of Au-NPs can readily be observed by changes in color form red to blue.

Another important aspect is the influence of the surrounding medium on the plasmon frequency. Depending on the polarizability or dielectric constant of the surrounding medium,

the oscillating charge density on the metal surface is attenuated leading to a change in plasmon frequency. More significant is the effect of adsorbed or bound molecules onto the Au-surface that change the electronic density of the surface, thus, altering the plasmon frequency. Generally, the nature of the LSPR and the responses to external stimuli present the fundamental principles in using Au-NPs as sensitive (colorimetric) sensors.[249,251]

5.1 Synthesis and surface functionalization

Over the years, numerous synthetic strategies, including "top-down"- and "bottom-up"-protocols have been applied in order to understand and control the size and shape, as well as surface functionalization of gold nanozymes.[253] "Top-down"-strategies apply physical-chemical methods in order to degrade bulk material into small nanosized particles, whereas "bottom-up"-approaches are associated with wet chemical methods, such as the reduction of a gold precursor to elemental gold particles.[254] In the following, emphasize will be placed primarily on "bottom-up"-approaches using liquid phase synthesis for the generation of Au-NPs and Au-MPCs as they present the most prominent route.

The most applied methods towards the synthesis of Au-NPs are based on the reduction of an Au(III)-salt (usually $HAuCl_4$) to elemental Au^0 by a reducing agent, such as citric acid, ascorbic acid, sodium borohydride ($NaBH_4$) or others. In either case, the basic principle involves the reduction of Au(III)-ions to elemental Au-atoms. The Au-atoms cluster and pack in a face-centered cubic (fcc) structure and form the nuclei for the subsequent growth of Au-NPs.[255] The formed "naked" nanoparticles are not colloidal stable, due to their high surface energies originating from large surface area and correspondingly high number of surface atoms with unsaturated coordination. Thus, Au-NPs minimize their surface energy by forming undesired agglomerates/aggregates. In order to prevent the aggregation process and achieve colloidal stability, ligands are added to the reaction dispersion that bind to the high energy surface and stabilize the formed particles either sterically[256] or electrostatically (Fig. 5.3) .[257]

In case of steric stabilization, the bound ligand physically prevents the aggregation of individual particles by shielding the particle surface and acting as spacers. By contrast, electrostatic stabilization prevents aggregation of individual particles by Coulomb repulsion between similarly charged particles. For electrostatic stabilization to occur, sufficient charge density needs to be present at the ligand-solvent interface.
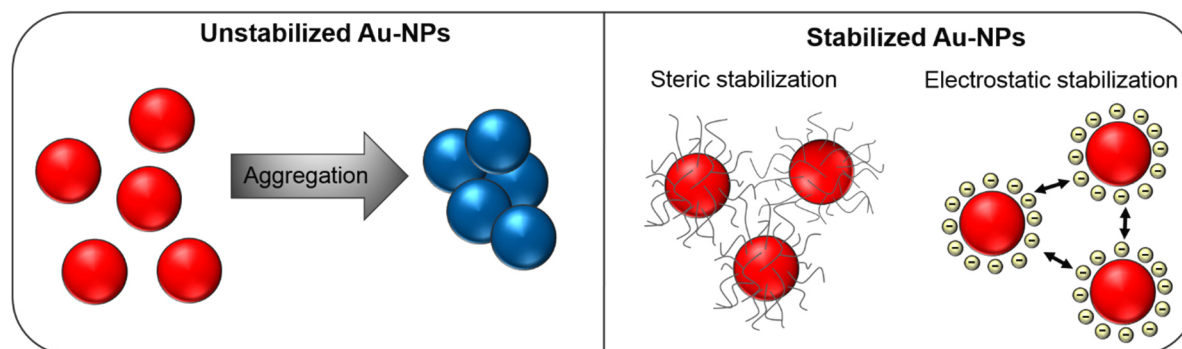
Figure 5.3: (left) Depiction of unstabilized Au-NPs and their aggregation in order to minimize the surface energy. (right) Au-NPs stabilized either by extended ligands that sterically hinder the clustering auf Au-NPs or by charged ligands that electrostatically stabilize Au-NPs by Coulomb repulsion.

The colloidal stability of electrostatically stabilized particles can be estimated by measuring the zeta potential of the functionalized particles. A zeta potential of ± 40 to 60 mV is usually associated with good colloidal stability.[258–260] Commonly applied stabilizing ligands are, e.g., thiols, such as dodecanethiol or cysteamine, polyvinylalcohol (PVA), polyvinylpyrrolidone (PVP), sodium citrate, polymers, including polyethylene glycol (PEG) of various length or quarternary ammonium surfactants like cetyltrimethylammoniumbromide (CTAB).[251]

To date, the most popular approach towards colloidal stable Au-NPs, due to its simplicity, is the Turkevich strategy,[261] also referred to as "citrate method". The method was first introduced in 1951 by Turkevich *et al.* and was refined by Frens in the following years.[262] In this synthesis, an aqueous solution of $HAuCl_4$ is mixed with sodium citrate at elevated temperatures (Fig. 5.4A). The citrate molecules act as a weak reducing agent and stabilizing ligand at the same time, resulting in stable spherical Au-NPs with a narrow size distribution and a sizes regime of around 10 - 20 nm.

The convenience of this method stems from the fact that the size of Au-NP is strongly dependent on the ratio of reducing agent to gold precursor and used temperature. Thus, size of the particles can readily be adjusted by changing those parameters. Since the synthesized particles are capped with citrate molecules, ligand-exchange reactions are required in order to obtain thiol-functionalized Au-MPCs. Numerous strategies have been reported to exchange citrate for various ligands like alkane-thiols, polymers, peptides etc. In particular, the direct one-step ligand-exchange presents a simple ligand displacement strategy. The citrate-capped Au-NPs are physically mixed with the desired thiol-ligand in one pot. Due to their high binding affinity for the Au-surface, thiols gradually displace the citrate molecules from the gold surface over time. The efficiency of the displacement is related to the reaction time and ratio of citrate to thiol ligand. However, incomplete ligand-exchange reactions have often been reported. Another possible downside of the direct ligand-exchange is the occurrence of unstable Au-NPs,

due to a decrease in surface potential owing to the fast exchange of highly charged citrate molecules for often less charged thiols.

In 1994, Brust and Schiffrin reported a direct route towards thiol-functionalized Au-NPs. The Brust-Schiffrin method utilizes a two-phase system of an aqueous solution of $HAuCl_4$ and toluene (Fig. 5.4B). The toluene phase contains dodecanethiol as stabilizing ligand and tetraoctylammonium bromide (TOAB) as a phase-transfer agent. TOAB transfers $AuCl_4^-$-ions into the toluene phase, which are subsequently reduced by a strong reducing agent ($NaBH_4$) to yield spherical Au-NPs. The formed particles are immediately stabilized by strongly bound dodecanethiol molecules. Due to the strong nature of the Au-thiol-bond, the synthesized Au-MPCs are stable in various organic solvents without significant aggregation, enabling the facile characterization and further functionalization of these conjugates. Using the Brust-Schiffrin method, particle size can readily be controlled by the thiol/gold ratio, temperature, concentration of $NaBH_4$ and rate of addition. Despite its groundbreaking success in the synthesis of Au-MPCs, the method is limited to non-polar thiols, as they need to solubilize in the toluene phase.

Given this background, various modified strategies of the Brust-Schiffrin methods have been developed in order to enable the facile synthesis of Au-MPCs functionalized by a wide spectrum of different thiols (Fig. 5.4C). The basic principles remain the same, i.e., Au(III)-salt being reduced by a strong reducing agent $NaBH_4$. However, instead of a two-phase system only one-phase (mostly aqueous media) containing the stabilizing thiol is present. In case of an aqueous reaction system, the pH needs to be considered as it affects the protonation/deprotonation of the thiol-groups, thus, binding kinetics and possible charges at ionizable groups and their stabilizing effects. The control over the size of formed Au-NPs follows the same rules as the Brust-Schiffrin method.

With this strategy, numerous Au-NPs of different sizes have been synthesized that are exclusively coated with water soluble polymers, DNA, antibodies, antigens, proteins, peptides and more. The composition of the monolayer is also readily diversified by applying two (or more) different thiol-ligands during Au-NP synthesis, which results in mixed-monolayer protected Au-NPs that feature properties of both ligands. Zheng and Huang for example synthesized an Au-MPCs with a mixed-monolayer of tiopronin modified with biotin as a capture component and tri(ethylene glycol) as a shielding component.[263]
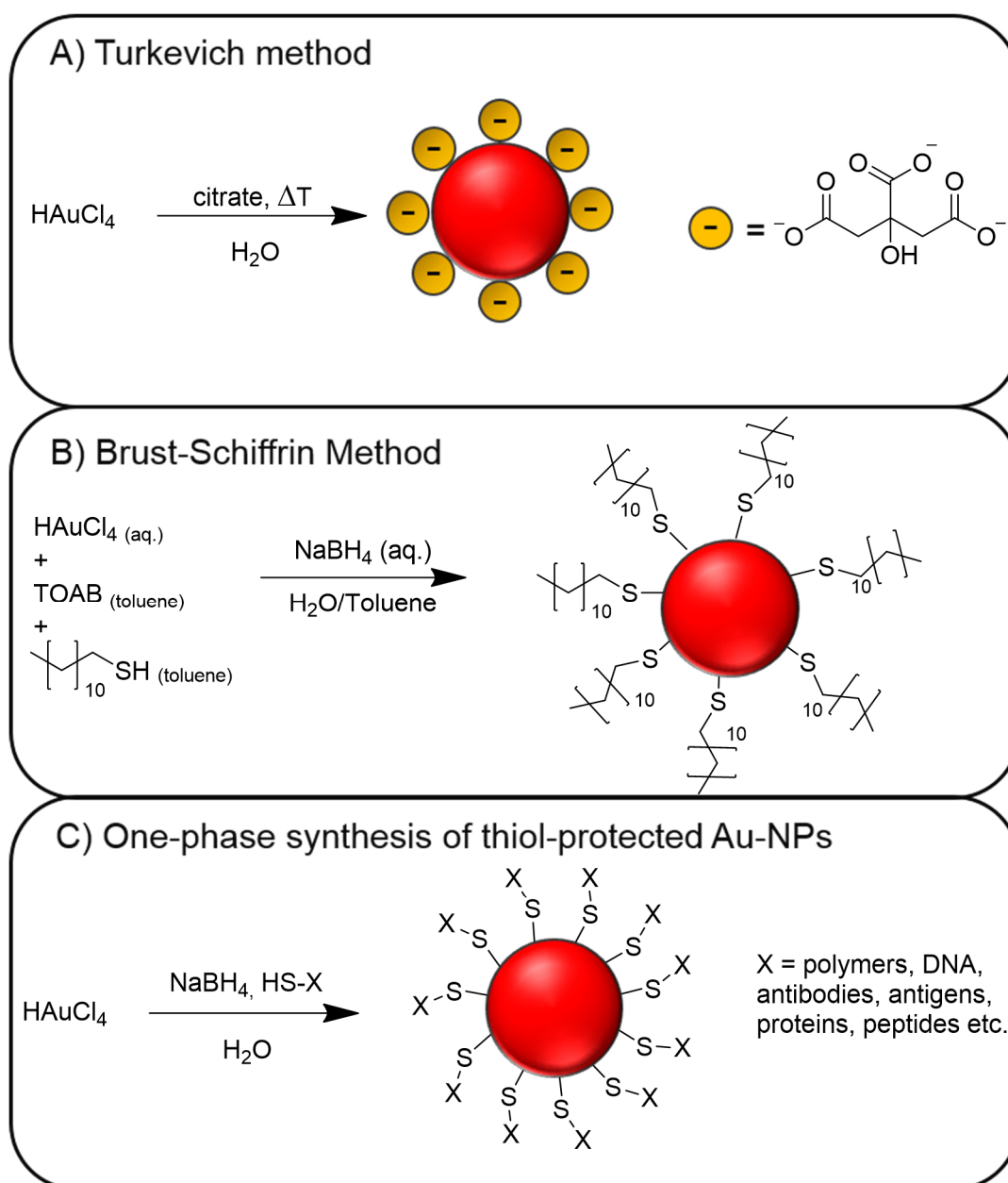
Figure 5.4: Summary of synthesis strategies to stable Au-NPs.

The mixed-monolayer was able to specifically bind to streptavidin, while the tri(ethylene glycol) efficiently prevented unspecific protein binding to the Au-surface.

In general, conjugated thiol-ligands are also replaceable by other thiols using a ligand-exchange protocol, analogous to citrate-capped Au-NPs. In order to efficiently displace an anchored thiol from the Au-surface, the free thiol needs to exhibit a higher binding affinity for the surface. This can be achieved, for example, by multivalent binding, applying di- or trithiols to replace a monothiol ligand. Otherwise an excess of free thiol is required to drive the displacement reaction.[251]

5.2 Enzyme mimics

5.2.1 Intrinsic nitroreductase activity

Nitroreductases (NR) belong to the class of oxidoreductases and catalyze the NADH-mediated sequential reduction of nitroaromatic compounds to the corresponding aromatic amines. NR have been extensively studied due to their broad substrate scope, which is an attractive property for potential applications in bioremediation[264–266] and in organic synthesis, since nitroaromatic compounds are readily available and their amine analogues are valuable synthons for the production of agrochemicals, pharmaceuticals and dyes.[267]

The NR-catalyzed biochemical transformation of nitro compounds to the respective amines proceeds through a series of two-electron reductions by a ping-pong mechanism (Scheme 5.1).[267] That is, NADH binds to NR and transfers two electrons to it. Then, NAD^+ dissociates from the enzyme and the nitro substrate binds to the reduced NR. The substrate is then reduced itself in a 2-e^--2-H^+ (solvent protons) transfer mechanism.[268] Subsequently, NADH again replaces the substrate and reduces the NR and the process iterates. The nitro-group of an aromatic ring is thereby sequentially converted into the corresponding nitroso, hydroxylamine and finally the amine compound.[267]
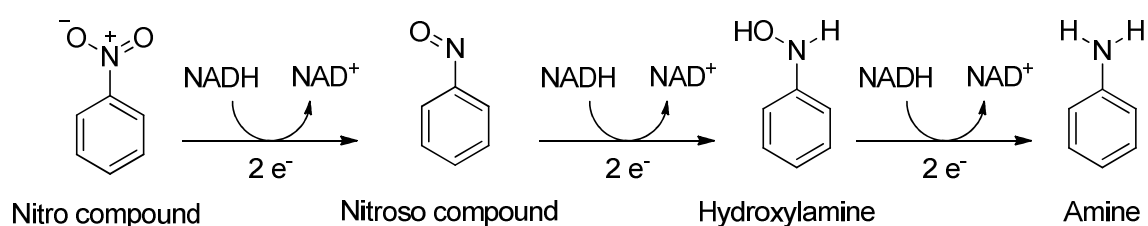
Scheme 5.1: Ping-Pong mechanism for the NR-catalyzed reduction of Nitro compounds to the corresponding amine.

So far, the most promising chemocatalytic approaches towards the selective hydrogenation of nitroaromatic compounds to the aromatic amines includes the usage of transition metal catalysts, such as Pt and/or Pd supported on active carbon or alumina, Raney nickel, Ru and Rh among others.[269] However, some of the studied catalysts often show low chemoselectivity, in particular, when other reducible groups, such as olefins are present.[270] In this regard, Au was studied as a potential metal for this type of reactions since it was shown that Au exhibits different adsorption properties for olefins and nitro-groups compared to Pd or Pt surfaces.[271,272] Thus, Au-NPs as a redox active catalyst were studied as potential NR mimics to enable the selective hydrogenation of nitro compounds into amines.
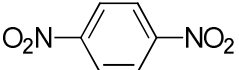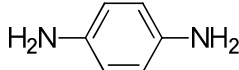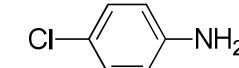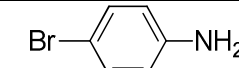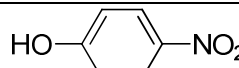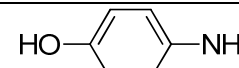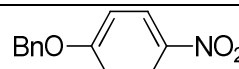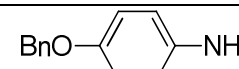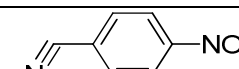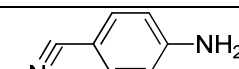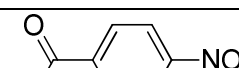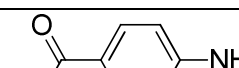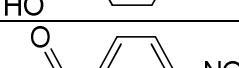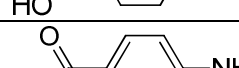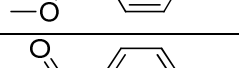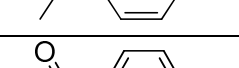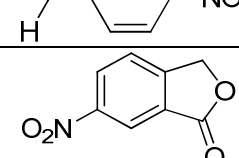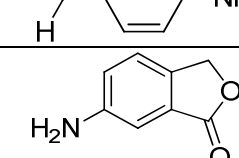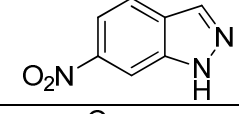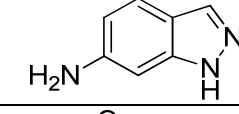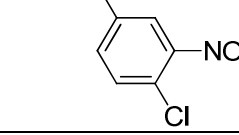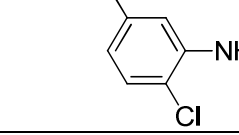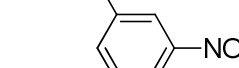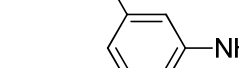
Au-NPs supported on solid oxide supports, such as AuNP/TiO_2 or AuNP/Fe_2O_3 were applied as catalysts for the H_2-mediated reduction of 3-nitrostyrene, 4-nitrobenzonitrile, 4-

nitrobenzaldehyde or 1-nitro-1-cyclohexene to the corresponding amines. The Au-NP catalysts showed exceptionally good chemoselectivities for the conversion of these substrates without modifying double-bonds, nitriles or carbonyls.[272] However, the process requires reaction conditions, such as H_2-pressures of 9 bar and temperatures of 120 °C. Thus, several other cheap and easily accessible reducing agents/hydrogen donors like $NaBH_4$, hydrosilanes or ammonium formate ($HCOONH_4$) were studied in order to perform the reduction under milder conditions.[273,274]

$NaBH_4$ has been thoroughly investigated as a potential hydrogen donor agent as Au-NPs are able to activate it for the selective reduction of aromatic nitro compounds to the respective amines under atmospheric pressure and ambient temperatures.

Fountoulaki *et al.* demonstrated the substrate scope of the $NaBH_4$-mediated transformation and selectively converted various nitroarenes into the respective amines (Tab. 5.1).[273] Mesoporous titania supported Au-NPs (Au-NP/MTA) were used as the catalyst in conjunction with $NaBH_4$ or hydrosilane 1,1,3,3-tetramethyl disiloxane (TMDS) as hydrogen donors. Since both reducing agents gave similar reaction outcomes, results of $NaBH_4$-assisted hydrogenation will be emphasized only. The studied nitro aromatic substrates contained various electron withdrawing (carbonyls, halogens, nitriles), donating (amines, alkoxy, hydroxy) or reducible functions (carbonyls, olefins). Au-NP/MTA showed high chemo- and regioselectivity for the transformation of the nitro group as no competing reductions or dehalogenations were observed. The high selectivity renders the use of protecting groups unnecessary, which further underlines the potential of Au-NPs for green syntheses.

Table 5.1: Nitro aromatic substrates studied by Fountoulaki et al.[273] that were converted into the corresponding amines using Au-NP/MTA as the active catalyst and NaBH4 as the reducing agent.

Nitro compound	Amine product	Time [h]	Yield [%]
O2N—⬡—NO2	H2N—⬡—NH2	1	94
Cl—⬡—NO2	Cl—⬡—NH2	1	97
Br—⬡—NO2	Br—⬡—NH2	1	92
HO—⬡—NO2	HO—⬡—NH2	3	90
BnO—⬡—NO2	BnO—⬡—NH2	3	95
N≡C—⬡—NO2	N≡C—⬡—NH2	1	92
HO(O)C—⬡—NO2	HO(O)C—⬡—NH2	3	95
—O(O)C—⬡—NO2	—O(O)C—⬡—NH2	1	94
CH3(O)C—⬡—NO2	CH3(O)C—⬡—NH2	1	97
H(O)C—⬡—NO2	H(O)C—⬡—NH2	1	98
O2N-isobenzofuranone	H2N-isobenzofuranone	6	94
O2N-indazole	H2N-indazole	8	90
—O / Cl / NO2 ring	—O / Cl / NH2 ring	3	93
vinyl—⬡—NO2	vinyl—⬡—NH2	0.3	98

Further studies have been directed towards understanding the reaction mechanism of the NR activity of Au-NPs. For that, model reaction of 4-nitrophenol (4-NP) to 4-aminophenol (4-AP) was chosen and studied.[275] The consensus is that the reduction by BH4- follows a Langmuir-Hinshelwood mechanism (Fig. 5.5). That is, BH4--ions reversible transfer hydrogen to the Au-

surface, generating surface-hydrogen-species accompanied by the adsorption of 4-NP. 4-NP is then reduced in two fast consecutive steps by bound hydrogen-species to the hydroxylamine intermediate and subsequently to 4-AP in a rate-determining step. Since the hydrogenation mechanism takes place exclusively at the Au-surface, hydrogenation activity can be tailored by particle size and bound ligands.
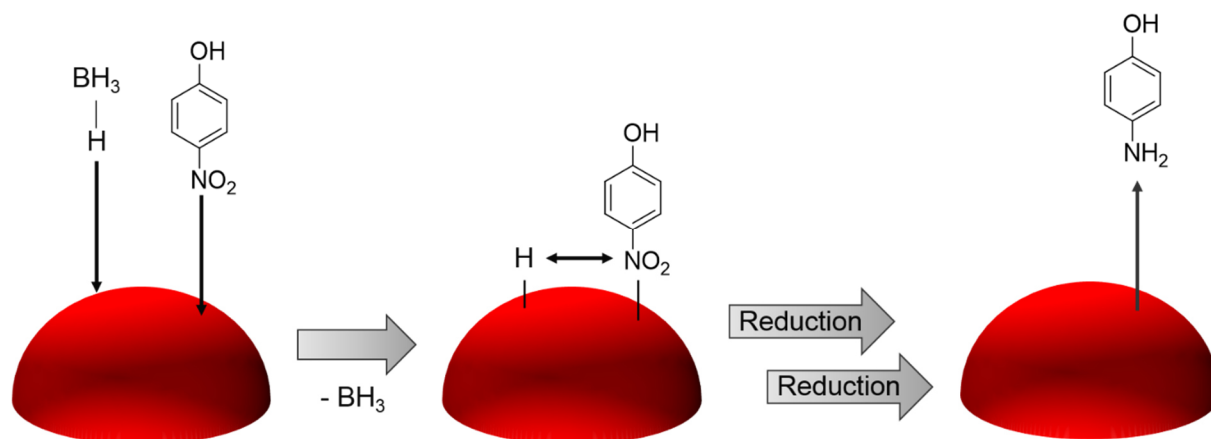
Figure 5.5: Langmuir-Hinshelwood mechanism for the NaBH4-mediated Au-NP-catalyzed reduction of 4-NP to 4-AP.

The impact of surface coatings on hydrogenation activity of Au-NPs was investigated by Satapathy et al.[276] Various Au-NPs with sizes ranging from 13 – 15 nm, stabilized by CTAB, PVP and citrate were synthesized and applied for the NaBH$_4$-mediated reduction of 4-NP to 4-AP. Hydrogenation kinetics of the respective Au-NPs significantly differed from another. That is, CTAB-capped Au-NPs showed highest rates of hydrogenation of 4-NP and followed both zero-order ($k_0 = 0.418$ M min^{-1}) and first-order reaction kinetics ($k_1 = 0.938$ min^{-1}). By contrast, citrate-capped Au-NPs only followed first-order reaction kinetics with a 4-fold lower activity ($k_1 = 0.243$ min^{-1}). By replacing citrate for CTAB ligands, zero-order kinetics ($k_0 = 0.345$ M min^{-1}) were obtained. Whereas replacement of citrate for PVP retained first-order reaction kinetics ($k_1 = 0.587$ min^{-1}) while catalysis improved by 2-fold.

In summary, the adsorbed ligand shell significantly influences the capability and reaction kinetics of Au-NPs to reduce aromatic nitro compounds to the respective amine. Therefore, hydrogenation activity can be tuned by changing the bound ligand. However, the impact of the ligand shell on the catalytic activity, especially the impact on the reaction order, is not yet understood and is subject of further studies.

An alternative reducing agent to NaBH$_4$ or TMDS is ammonium formate (HCOONH$_4$). Ammonium formate is a cheap, selective and ecofriendly hydrogen donor.[277] Lou et al. applied HCOONH$_4$ in combination with Au/TiO$_2$ in the selective hydrogenation of a wide range of different aromatic nitro compounds in ethanol.[274] Similar to the work by Fountoulaki et al.[273]

nitroarene substrates employed, contained various reducible groups (e.g., alkenes, aldehydes, ketones, esters, nitriles, *O*-benzyl units) that did not undergo any modifications or transformations during the catalytic process. Again, the Au/TiO$_2$ was highly chemo- and regioselective for the conversion of the nitro group without observable side-reactions. Further studies were directed to unravel the reaction mechanism using ammonium formate as the reducing agent. It was then proposed that HCOONH$_4$ performs a transfer hydrogenation to generate surface bound hydrogens (Au-H) as the active species, identical to the mechanism proposed for NaBH$_4$. The hydrogen species then reduces the co-adsorbed nitro-compound to the hydroxylamine intermediate and subsequently to the amine.

In additional experiments, Lou *et al.* exploited the fact that HCOONH$_4$ in aprotic solvents like acetonitrile functions as a formylation agent.[274] As a result, a one-pot cascade reaction was designed as a green approach towards the reductive *N*-formylation of aryl nitro compounds in acetonitrile (Scheme 5.2).
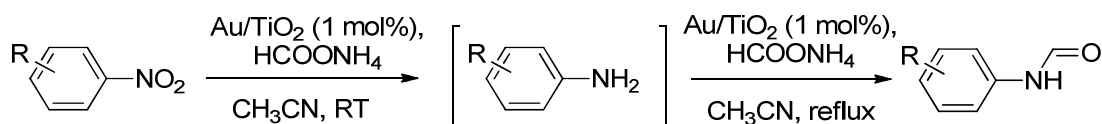
Scheme 5.2: One-pot process by combining Au-NP-catalyzed reduction of aromatic nitro compounds with HCOONH$_4$-mediated formylation of the *in-situ* formed amines.[274]

The aromatic nitro compounds are converted into the corresponding amines in an Au-NP-catalyzed, HCOONH$_4$-mediated step. The resulting amines are then immediately converted into the *N*-formylated derivatives without work-up in one pot. On the one hand, this study shows the high regio- and chemoselectivity achievable by using Au-NPs as hydrogenation catalysts; on the other hand, it represents a clever and highly atom efficient reaction design for the production of *N*-formanilides from aromatic nitro compounds.

5.2.2   Peptide-gold nanozymes as esterase mimics

The following section contains elements (figures and text passages) published in a review article entitled "Catalytically Active Peptide-Gold Nanoparticle Conjugates: Prospecting for Artificial Enzymes" written by Dorian J. Mikolajczak, Allison A. Berger and Beate Koksch.[278] *These elements were partly adapted, however, rewritten and modified in order to maintain a consistent style in the present work.*

The immobilization of peptides, with their sequence dependent specific recognition and catalytic properties onto Au-NPs, with their robustness and high stability, as well as other outstanding size-dependent physicochemical properties,[279] presents a promising field for the design of artificial enzymes. The conjugation of peptides onto Au-NPs (Pep-Au-NPs, Fig.5.6), and the resulting high peptide density induces close interactions between individual functional groups. Therefore, new hydrogen bond and/or charge-relay networks are established, which in total lead to distinct properties in catalysis, with the most prominent being the enhancement of catalytic activities. Furthermore, peptides are readily accessible at low-cost by solid-phase-peptide-synthesis (SPPS) and their structure can be easily modified by the choice and incorporation of (un)natural amino acids. Thus, reactivity and substrate interactions of the ligand shell can be easily fine-tuned.[44]
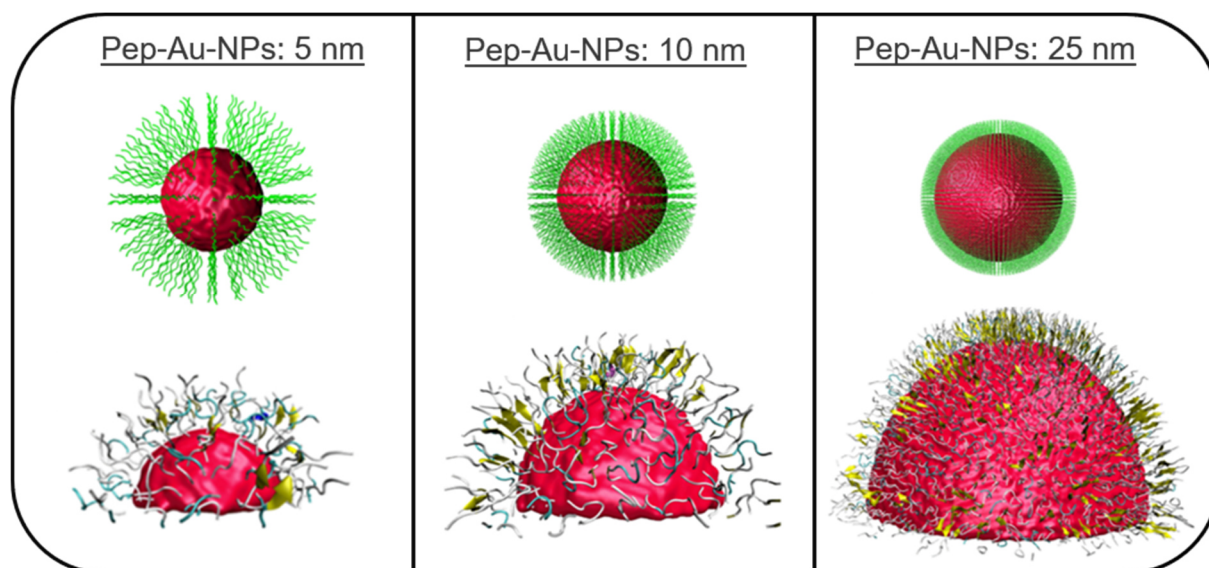

Figure 5.6: Snapshots of Au-NPs with diameters of 5, 10 and 25 nm functionalized with peptide CFGAILSS. Snapshots below show the simulated peptide arrangements and β-sheet formation (yellow arrows). Adapted from Colangelo *et al.*[280]

The field of catalytically active Pep-Au-NPs was pioneered by Scrimin and co-workers in 2005,[46] by reporting an esterolytically active Pep-Au-NP system consisting of a mixed-monolayer of undecanethiol-modified His-Phe-OH dipeptide **1**, immobilized onto Spherical Au-NPs functionalized by a monolayer of a water soluble *N*-(3,6,9-trioxadecyl)-8-sulfanyloctanamide (HS-C8-TEG) (Figure 5.7, left). The resulting Pep-Au-NPs are referred to as Au@**1**. The minimalistic His-Phe-OH sequence was chosen as the catalytic component as His presents an important amino acid present in the active sites of numerous esterases. His having a side chain pK_a around 6 is able to perform covalent, as well as efficient general acid/base catalysis together with other functional groups, such as carboxylic acids.[281,282] Therefore, **1** fulfils the most rudimentary requirements to function as an esterase mimic and presents a model system to study cooperativity effects between functional groups within the peptide-monolayer.[46]

Au@**1** and its peptidic *N*-acetylated control variant (Ac-**1**, Fig. 5.7, left) were studied in their ability to hydrolyse ester substrate 2,4-dinitrophenyl butyrate (DNPB, Fig. 5.7, left). At identical reaction conditions (including peptide concentration), Au@**1** shows rate improvements more than one order of magnitude greater compared to the Ac-**1**-catalyzed DNPB hydrolysis at elevated pH >7, and rate improvements greater by two orders of magnitude at pH <7.

After further investigation of the catalytic process by generating an activity versus pH profiles for Ac-**1** and Au@**1** (Fig.5.7, right), pK_a values of nucleophilic species involved in the catalytic processes were determined. The rate profile of Ac-**1** indicates the presence of a single nucleophile with a pK_a of 6.6, which was assigned to the His-imidazole, as expected.
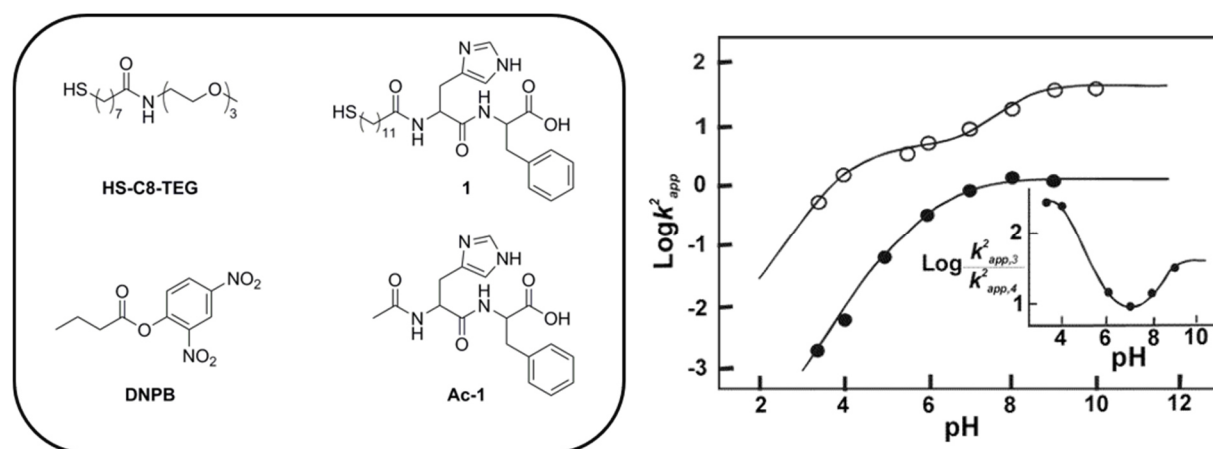

Figure 5.7: (Left) Peptides, peptidic ligands and substrates used by Scrimin and co-workers.[46] (Right) Dependence of Log of second-order rate constant k^2 on pH for the Ac-**1** (○) and Au@**1** (●) catalyzed hydrolysis of DNPB. Inset showing the ratio of the second order rate constants on pH. Adapted with permission from Ref.[46]. Copyright 2005, American Chemical Society.

Whereas, the pH profile of Au@**1** indicates the generation of two nucleophiles one having a pK_a of 4.2 and the other 8.1. The first pK_a was assigned to the *C*-terminal carboxylate of the phenylalanine whereas the second was assigned to the His-imidazole, which is 1.5 units higher than in control variant Ac-**1**.[46] Since the anchoring of **1** to the gold surface took place in a directed manner through S-Au bonds, the outer most layer of Au@**1** consists for the most part of *C*-terminal carboxylate anions. The resulting high local negative charge density favours the protonation of the proximal imidazole by electrostatic interactions, thus, increasing its pK_a. As a result, ester cleavage of DNPB by usual His-imidazole catalysis was ruled out and an alternative cooperative carboxylate-imidazole mechanism for the ester hydrolysis was proposed. In this cooperative mechanism, a *C*-terminal carboxylate acts as a general base, deprotonating a surrounding water molecule, thus generating a nucleophilic hydroxide ion that initiates the ester cleavage. The newly present imidazolium ion (His with increased pK_a) of the peptide-monolayer assists in the catalytic process by stabilizing the generated negatively charged intermediate of the ester hydrolysis by strong hydrogen bonding, leading to the observed rate enhancements of Au@**1** at pH >7.[46] Rate accelerations in the pH regimes <7 are attributed to the carboxylate anion that contributes to DNPB ester hydrolysis as an active nucleophile. Both the proposed cooperative carboxylate-imidazolium and nucleophilic-carboxylate mechanisms are said to be absent in unconjugated peptides.[46]

In 2007, Scrimin and co-workers extended the field of Pep-Au-NP catalysts by substituting **1** of the previously reported system, with a rationally designed, more complex peptide **2** (Fig. 5.8, left).[171] **2** consists of 12 amino acids and its peptide design was rationalized as follows: His again functions as the central catalytic moiety by enabling imidazole catalysis and is present at an intermediate position within the peptide sequence. Thus, after immobilization onto the Au-NPs, His is buried inside the resulting monolayer, in a less solvated region, analogous to the active sites of natural enzymes. Moreover, positively charged amino acids Lys and two Arg were incorporated for two reasons: first, to contribute to the stabilization of the negatively charged transition state of the ester hydrolysis and, together with His, to enable nucleophilic and/or general acid/base catalysis; second, to further stabilize the individual Pep-Au-NPs due to electrostatic repulsion between the terminal Arg residues. Hydrophobic residues such as Phe and Ala were incorporated in proximity to the His in order to enhance substrate binding and bring about proximity effects by hydrophobic interactions.[171] **2** was immobilized onto the surface of HS-C8-TEG functionalized Au-NPs, analogous to aforementioned Au@**1** resulting in Au@**2** with a ligand ratio of HS-C8-TEG to **2** of 3:1 as determined by ^{1}H-NMR.[171]

Catalysts Au@**2** and the S-acetylated control variant Ac-**2** were studied in the ester hydrolysis of DNPB. The results were compared to dipeptidic Au@**1**. At low pH regimes, Au@**1** and Au@**2** behaved similarly, due to the carboxylate being an active nucleophile in both Pep-Au-NP systems. However, up to pH 5, Au@**2** exceeds the catalytic efficiency of Au@**1** by almost one order of magnitude. This corresponds to 3000- and 500-fold rate accelerations compared to the unconjugated control variants Ac-**1** and Ac-**2**, respectively. At pH 10, rate improvements of Au@**2**-catalyzed ester hydrolysis was up to 40-fold higher, compared to Ac-**2**. The aforementioned cooperative carboxylate-imidazolium mechanism evoked by the high peptide density of the peptide-monolayer was suggested to be the most likely explanation for the rate improvements.[171]
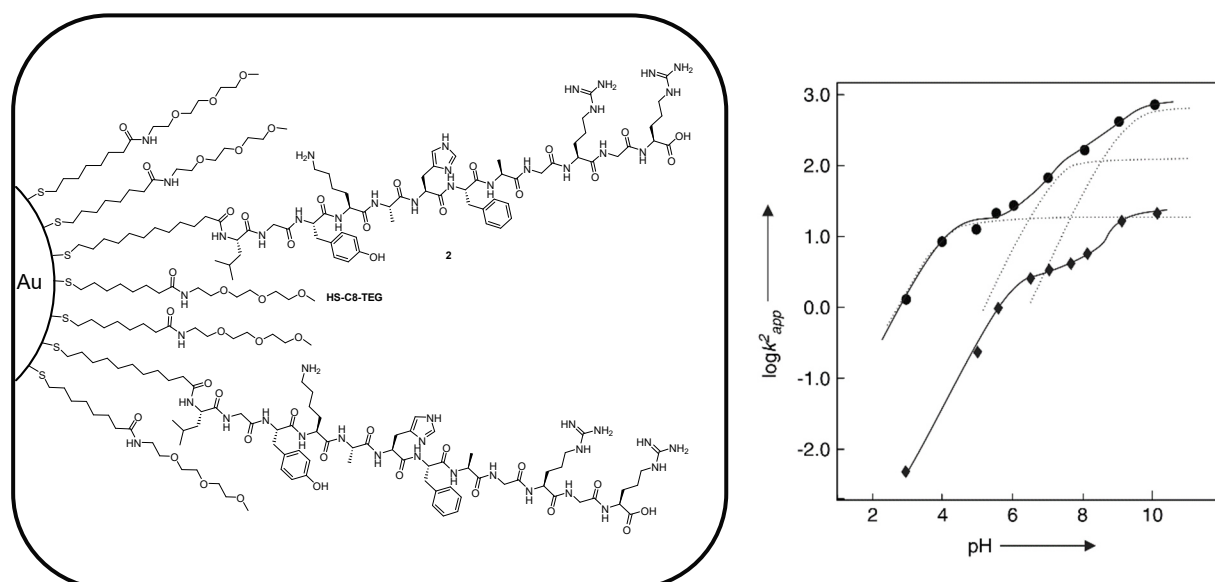
Figure 5.8: (Left) Schematic depiction of Au@**2** studied by Scrimin and co-workers.[171] (Right) Dependence of logarithm of second-order rate constant on pH for the Ac-**2** (♦) and Au@**2** (●) catalyzed DNPB hydrolysis. Adapted with permission from Ref.[171] Copyright 2007, WILEY-VCH Verlag GmbH & Co. KGaA.

Further, activity versus pH plots of Ac-**2** and Au@**2** were generated and compared (Fig. 5.8, right).[171,283] A rather complex rate profile was obtained for Pep-Au-NP Au@**2**, indicating three pK_a of 4.2, 7.1 and 9.9. Those were assigned to the *C*-terminal carboxylate, the His imidazole and the phenol group of Tyr, respectively. The overall higher rate improvements of Au@**2** at elevated pH was explained by the presence of the contributing nucleophile with a pK_a of 9.9. Despite His being buried inside the peptide-monolayer, it still shows a 1.1 unit higher pK_a than unconjugated Ac-**2**. Hence, it was still suggested that the carboxylate and the His residues are spatially in close proximity.[171]

Since, the His is buried inside the monolayer and is flanked by hydrophobic amino acids Ala and Phe, further studies of Au@**2** were directed to investigate the accommodation and

hydrolysis of ester substrates that differ in their hydrophobicity. Thus, more complex 4-nitrophenyl esters of Z-protected amino acids leucine (Z-Leu-ONp) and glycine (Z-Gly-ONp) were applied as substrates. The results indicated that Au@2 shows indeed different kinetics for the more hydrophobic Z-Leu-ONp compared to Z-Gly-ONp and DNPB. Up to a certain concentration threshold, the hydrolysis of Z-Gly-ONp and Z-Leu-ONp catalyzed by Au@2 was shown to proceed with similar efficiency.[171] Above that concentration threshold, the nucleophilic attack of the His imidazole becomes more efficient for hydrophobic Z-Leu-ONp. The increased nucleophilicity of the imidazole is explained by the accommodation of Z-Leu-ONp within the peptide-monolayer. Z-Leu-ONp penetrates into and resides within the peptide-monolayer, which leads to the exclusion of water. This in turn increases the hydrophobic and nucleophilic character of the region around the catalytic His. In addition, the formation of an intermediate, most likely the acetylated imidazole, was observed. Despite these changes in catalysis, the overall catalytic process did not proceed faster, since the breakdown of the acetylated imidazole is said to be rate limiting.[171]

These two examples by Scrimin and co-workers demonstrated that the conjugation of peptides onto the surface of Au-NPs leads to distinct properties that resemble properties of natural enzymes. Pep-Au-NPs are able to evoke effects, such as the perturbation of pK_a of functional groups due to confinement effects, modulation of catalysis according to the hydrophobic nature of the substrate and the execution of new catalytic mechanisms that greatly increase the catalytic efficiency of a peptide over a broad range of pH.

An advantage of applying peptides as ligands for the functionalization of Au-NPs is their ability to adopt sequence dependent, defined secondary and tertiary structures or to assemble into highly ordered structures. Given this background, the Koksch group studied the structure-function relationships of Pep-Au-NPs by disrupting the self-assembled peptide arrangement surrounding the nanoparticles by induced coiled-coil formation (Fig. 5.9).[45]

For that, two peptides that originate from the parallel, heterodimeric IAAL-E3/IAAL-K3 coiled-coil system[284] were chosen, designed accordingly and synthesized (Fig. 5.10A).[45] The IAAL-E3 derived peptide, namely E3H15, features a His in a central position of the Glu-rich peptide sequence (E3H15) to generate esterolytic activity and promote previously mentioned carboxylate-imidazole interactions when conjugated to Au-NPs. The catalytically inactive complementary peptide K3 remained unmodified. Both peptides are specifically designed in a way that one peptide alone does not display a defined secondary structure or conformation.
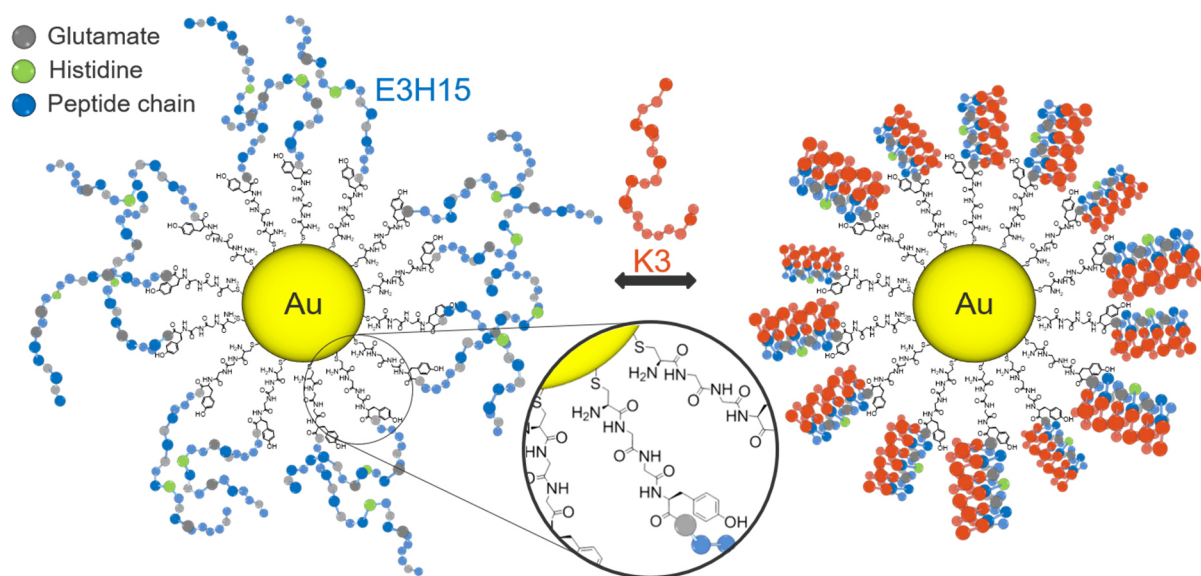
Figure 5.9: Concept of disrupting the multivalent peptide arrangements of the peptide-monolayer by coiled-coil formation as reported by Koksch and co-workers.[45] Copyright © 2017, American Chemical Society.

However, mixing of the two specifically designed peptides in aqueous media induces hydrophobic and electrostatic interactions between the two peptide chains, which lead to the formation of α-helices that wrap around each other to form an α-helical coiled-coil bundle (Fig. 5.10B).[285] α-helix formation was verified by CD-spectroscopy (Fig. 5.11A) showing two new ellipticity minima at 222 and 202 nm.

E3H15 was conjugated to Au-NPs by performing a one-phase synthesis as described in section 5.1, to give spherical Au@E3H15 exclusively covered with E3H15.
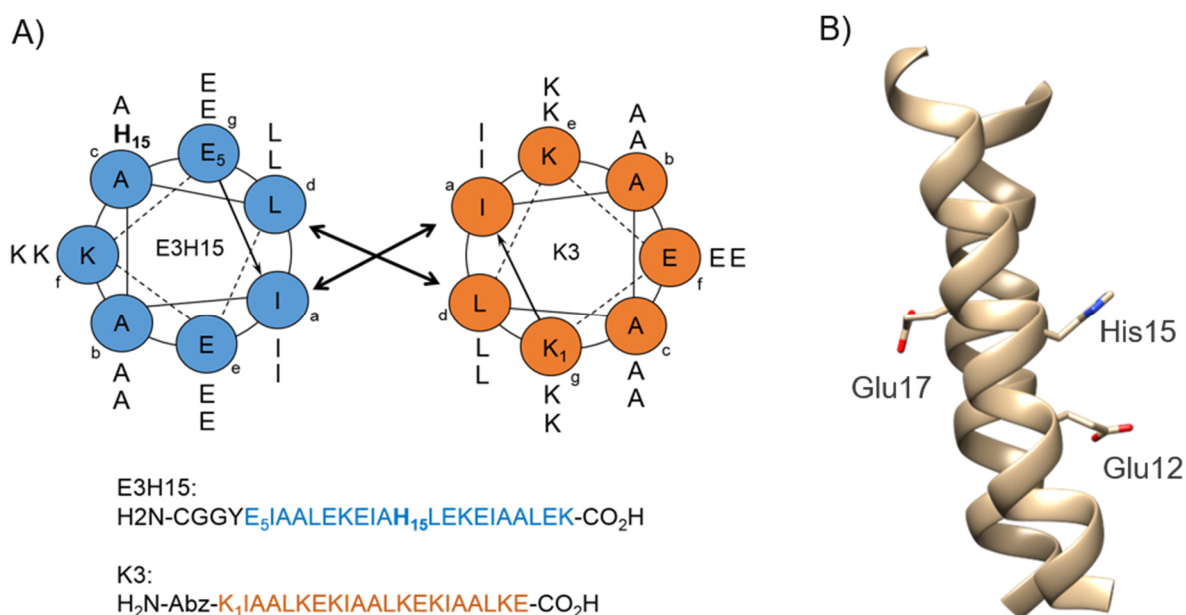
Figure 5.10: (A) Peptide sequence of E3H15 and K3 and the respective helical wheel representation. (B) Coiled-coil structure of E3H15/K3 and the positions of catalytically competent His and Glu residues (PDB code: 1U0I). Copyright © 2017, American Chemical Society.

Saturation kinetic experiments were performed using model ester substrate 4-NPA to study the effect of immobilization on catalytic activity. The results were analyzed according to the Michaelis-Menten theory (Fig. 5.11B). Immobilization of E3H15 leads to an increase in catalytic efficiency (k_{cat}/K_M) of more than one order of magnitude compared to the unconjugated variant. The increase in k_{cat}/K_M can be attributed to changes in the catalytic mechanism for the ester hydrolysis, as mentioned for Au@**1** and Au@**2**.[46]

Further experiments were conducted to probe the effect of changing peptide conformation on the esterolytic activity of Au@E3H15 and E3H15, when mixed with equimolar K3. CD-spectroscopy revealed no defined secondary structure for the individual peptides of Au@E3H15, E3H15 and K3 by themselves (Fig. 5.11A). However, the addition of K3 to Au@E3H15 and E3H15, respectively, results in the formation of α-helical coiled-coil structures.[45] Saturation kinetic experiments were conducted with coiled-coils comprised of Au@E3H15 in the presence of K3. An overall 85% decrease in k_{cat}/K_M was observed for Au@E3H15/K3, whereas only a slight decrease in k_{cat}/K_M was observed for the unconjugated coiled-coil variant of E3H15 in the presence of K3 (Fig 5.11B).[45]
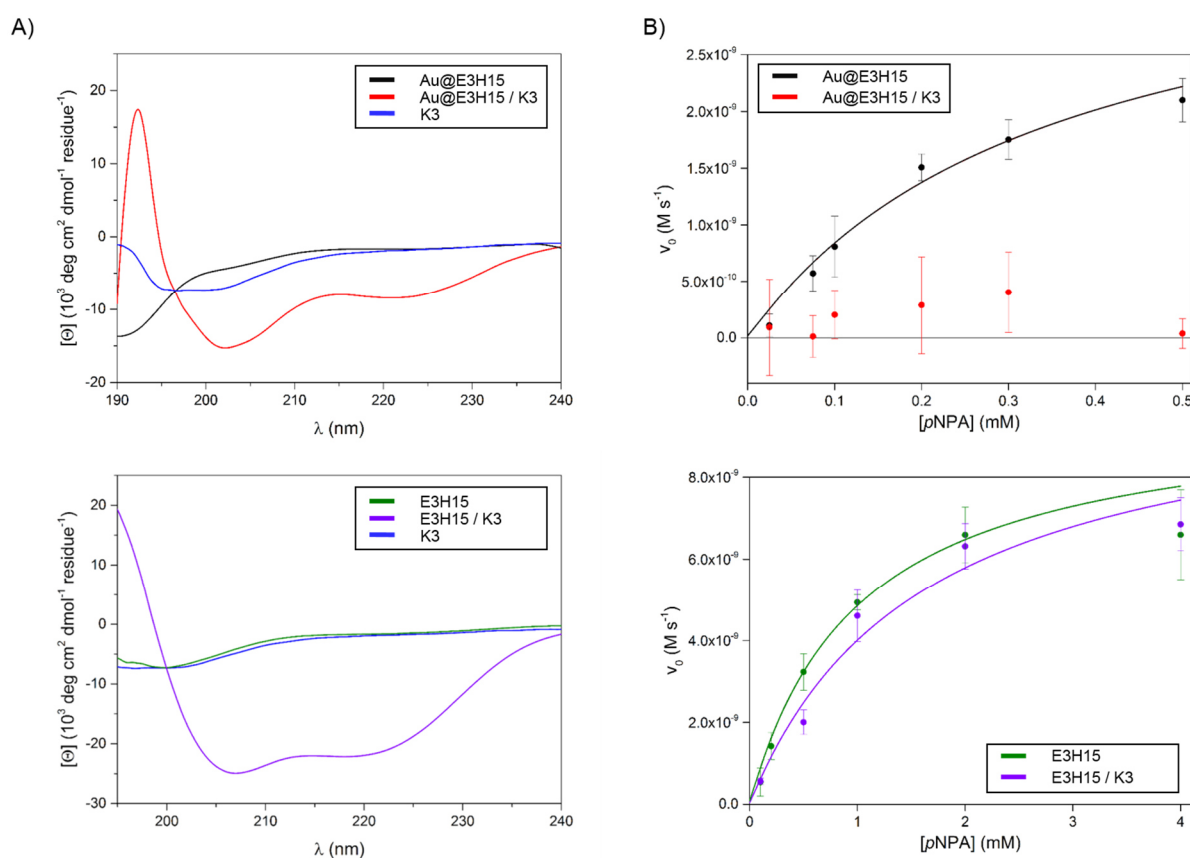
Figure 5.11: (A) Normalized CD-spectra of E3H15 and Au@E3H15 in the absence or presence of K3. B) Saturation curve of 4-NPA hydrolysis catalyzed by E3H15 and Au@E3H15 in the absence or presence of K3. Adapted with permission from Ref.[45]. Copyright 2018, WILEY-VCH Verlag GmbH & Co. KGaA.

The significant decrease in catalytic efficiency upon addition of K3 to Au@E3H15 were attributed to a combination of effects within the monolayer. The presence of Lys-rich K3 within the Glu-rich E3H15-monolayer might lead to changes in pK_a values, as the positive charge of the Lys counteract any pK_a effects evoked by negatively charged Glu of E3H15. Consequently, the proposed cooperative imidazolium-carboxylate mechanism is diminished, and rate improvements are decreased. Moreover, after coiled-coil formation, the peptides are involved in defined, more rigid α-helical coiled-coil architectures. Thus, flexibility of residues/functional groups to form intermolecular binding grooves or access beneficial orientations for substrate interactions are decreased or hindered. In addition, within coiled-coil structures, position and orientation of individual amino acids and residues is predefined. Possible intramolecular interactions of particular residues necessary for catalysis to occur (e.g., histidine and glutamate) is decreased. In any case, the formation of α-helical coiled-coil structures on the surface of Au-NPs results in lower rate improvements.[45]

In conclusion, the results of the Koksch group highlight the importance that peptide topology has on the catalytic activity of Pep-Au-NPs. Although, not directly apparent from the CD-spectroscopic experiments, peptides do possess an internal organization within the assembled monolayer, the perturbation of which results in notable losses in catalytic efficiency.

The field of peptide-gold nanozymes, where catalysis is performed by the peptide-monolayer, is largely undiscovered, which is also reflected by the number of publications in this field (three publications, excluding the publications of this thesis). Despite that, the results indicate a promising field of research for the design of new artificial enzymes as there is much to be learned and applied.

6   Aim of this work

The current work focuses on a strategy that combines peptides and gold nanoparticles (Au-NPs) as a new approach to create robust and recyclable nano-enzyme mimics (nanozymes) for the application in green technologies, specifically, post combustion CO_2-capture systems. For that, novel histidine containing peptides will be designed that mimic the active site of naturally occurring zinc metalloenzyme carbonic anhydrase (CA). By confining these peptides to the surface of robust Au-NPs a dense peptide-monolayer is generated and multiple, primary Zn(II) coordination sites per single nanoparticle are created. The high density of peptides on the nanoparticle surface will generate an additional secondary coordination sphere that potentially assists in the catalytic process by favorable binding interactions with the substrate. The generated peptide-gold nanoparticles conjugates (Pep-Au-NPs) are to be studied in their ability to convert CO_2 to HCO_3^- in aqueous media and alternative amine solvents and their thermostability as well as solvent compatibility is to be assessed.

All peptides will be synthesized by means of solid-phase-peptide-synthesis (SPPS). Conjugation of peptides onto Au-NPs will be performed by applying peptides as ligands for the stabilization of *in situ* formed Au-NPs during the reduction of gold salt $HAuCl_4$ by reducing agent $NaBH_4$. The successful conjugation of peptides onto Au-NPs will be verified by IR-spectroscopy and size and shape of the resulting Pep-Au-NPs will be determined by transmission electron microscopy (TEM) and UV/vis-spectroscopy. The average peptide loading per nanoparticle will be assessed by supernatant analysis *via* UV/vis-spectroscopy. Saturation kinetic measurements using 4-nitrophenylacetate (4-NPA) will be performed to validate the successful functionality of the coordinated Zn(II) centers. Lastly, CO_2-hydration will be investigated using the delta pH-method.

7 Published work

Overview of peer-reviewed publications involved in this thesis:

- D. J. Mikolajczak, B. Koksch, Peptide-Gold Nanoparticle Conjugates as Sequential Cascade Catalysts. *ChemCatChem* **2018**, *10*, 4324–4328.
- D. J. Mikolajczak, J. Scholz, B. Koksch, Tuning the Catalytic Activity and Substrate Specificity of Peptide-Nanoparticle Conjugates. *ChemCatChem* **2018**, *10*, 5665–5668
- D. J. Mikolajczak, B. Koksch, Peptide-Gold Nanoparticle Conjugates as Artificial Carbonic Anhydrase Mimics. *Catalysts* **2019,** *9(11)*, 903, 1-11.

7.1 Peptide-Gold Nanoparticle Conjugates as Sequential Cascade Catalysts

D. J. Mikolajczak, B. Koksch, *ChemCatChem* **2018**, *10*, 4324–4328.

7.1.1 Contributions of Authors

Beate Koksch and I developed the general concept of this project. Beate Koksch supervised the project. I wrote and Beate Koksch revised the manuscript. I performed the syntheses of the studied compounds and carried out all experiments and analysis.

7.1.2 Rationale and summary of the project

As described in section 3.2.2, the combination of bio- and chemocatalysis has proven to be a powerful tool for the development of efficient and ecological one-pot processes in water. However, a main challenge remains to be the compatibility of the individual catalytic components for individual reaction steps. Therefore, the development of a single multifunctional catalyst that performs two consecutive reactions on one substrate under a given set of aqueous reaction conditions presents a highly attractive approach. Previous works addressed this challenge by, for example, combining polymers[287] or enzymes[288] together with noble metal nanoparticles to generate hybrid cascade catalysts. In this project, we approached

the design of a multifunctional catalyst by creating an artificial nano-enzyme that combines both, peptide catalysis (esterase activity) and gold nanoparticle catalysis (hydrogenation).[286] The advantage of this approach is that the developed peptide-monolayer dictates important properties of Au-NPs such as solubility and stability, thus, compatibility of both catalysts in a given medium (here: aqueous solution) is ensured.

The peptide component was designed to possess esterase activity while being able to sufficiently stabilize Au-NPs after conjugation. Truncation of our previously established esterolytically active E3H15 peptide led to peptide E1H8 that only comprises important amino acids required for ester hydrolysis and Au-NP conjugation and stabilization (Fig. 7.1).

E1H8: NH$_2$-Cys-Gly-Gly-Tyr-Glu-Ile-Thr-His-Leu-Glu-Lys-OH
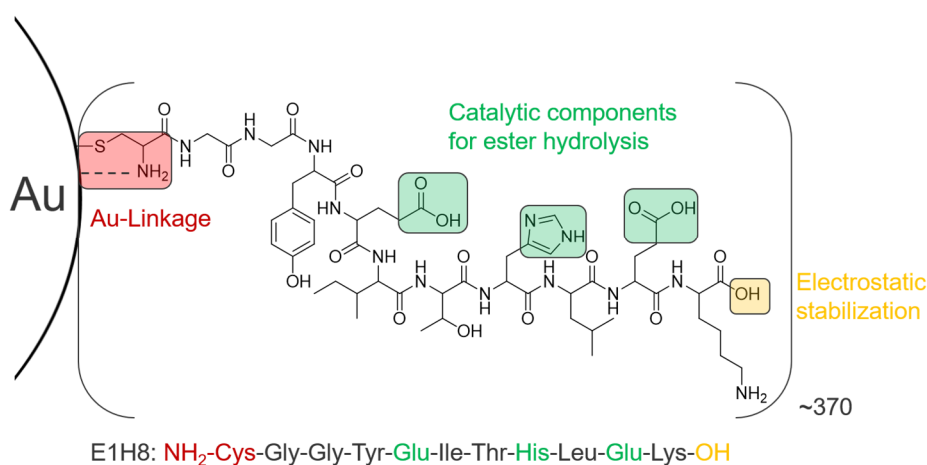
Figure 7.1: Schematic illustration of studied peptide E1H8 conjugated to a Au-NP and its primary structure. Amino acids and moieties competent for Au-conjugation (red), ester hydrolysis (green) and electrostatic stabilization (yellow) are highlighted in colored boxes.

The synthesis of Au-NPs and simultaneous conjugation of E1H8 to the nanoparticles was achieved by the NaBH$_4$-mediated reduction of gold salt HAuCl$_4$ in presence of E1H8 as the stabilizing ligand. Spherical Au-NPs coated exclusively with E1H8, referred to as Au@E1H8, were obtained with a mean diameter of 6.8 ± 1.7 nm (determined by TEM) and an average peptide density of 2.44 peptides/nm^2 (determined by supernatant analysis), which is comparable to literature values.[45,280,289]

Au@E1H8 was studied for its potential to function as a cascade catalyst. For that, model substrate 4-NPA was chosen to undergo two transformations: a peptide-catalyzed ester hydrolysis of 4-NPA to 4-NP; a Au-NP-mediated hydrogenation in the presence of NaBH$_4$ to reduce 4-NP to 4-AP (Fig. 7.2). Formation of the respective products was monitored by UV/vis-spectroscopy utilizing the different absorption maxima of 4-NP ($\lambda_{max} = 405$ nm) and 4-AP ($\lambda_{max} = 300$ nm).

Saturation kinetics were performed for (Au@)E1H8-catalyzed ester hydrolysis in order to determine kinetic parameters k$_{cat}$ and K$_M$. In summary, no catalytic activity was observed for

the unconjugated E1H8, whereas Au@E1H8 showed a sigmoidal saturation profile and significant activity for the hydrolysis of 4-NPA with a catalytic efficiency k_{cat}/K_M of 58.74 ± 4.17 M^{-1} s^{-1}. Furthermore, the sigmoidal behavior for the dependence of 4-NPA hydrolysis on increasing substrate concentrations, indicates positive cooperativity in substrate binding. Further studies are necessary to elucidate the mechanism behind this behavior.
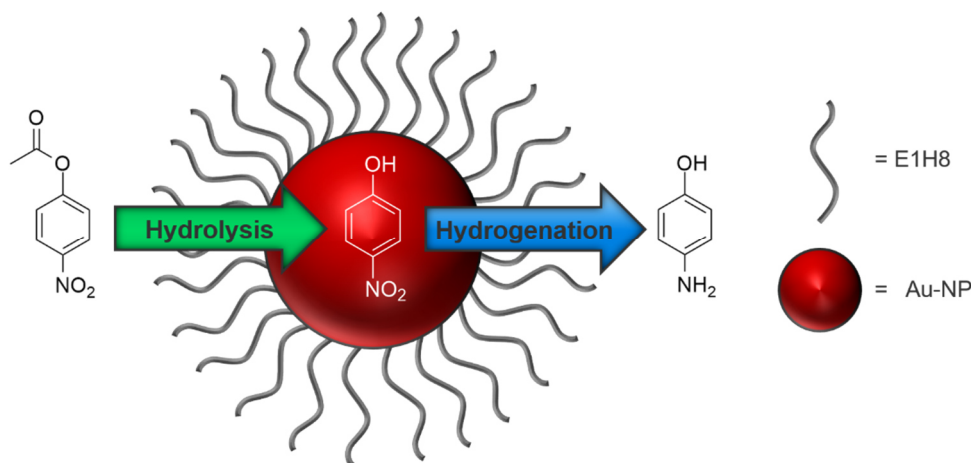
Figure 7.2: Concept of studied catalyzed cascade reaction performed by Au@E1H8 on 4-NPA.

Upon completion of 4-NPA hydrolysis, addition of $NaBH_4$ to the reaction mixture initiated the Au-NP-catalyzed conversion of 4-NP to 4-AP. A quantitative reduction of 4-NP to 4-AP occurred with first-order rate constants k_1 of 3.01 min^{-1} and 0.83 min^{-1} for Au-NP concentrations of 1 nM and 0.1 nM, respectively. Control experiments using citrate-capped Au-NPs mixed with E1H8 revealed Au@E1H8 to be the superior hydrogenation catalyst. Comparison to literature values suggested that the established peptide-monolayer contributes to the rates of hydrogenation at the Au-surface. We proposed, that the peptide-monolayer interacts with 4-NP molecules by hydrogen bonding and/or electrostatic interactions, which increases the residence time of 4-NP near the Au-surface. Upon initiation of the surface-catalyzed hydrogenation reaction, 4-NP molecules are already in proximity to the activated surface-hydrogen species, which in total increases the rate of conversion.

Recycling of the catalyst was only possible after ester hydrolysis, whereas immediate work-up was required after the hydrogenation reaction in order to prevent aggregation and precipitation of Au@E1H8.

Au@E1H8 presents the first example of a Pep-Au-NP that functions as a multifunctional catalyst for sequential cascade reactions in water in one pot. The conjugation of E1H8 to Au-NPs did not just combine both components, but evoked synergistic effects that greatly increased the catalytic activity of each individual catalyst, respectively.

7.2 Tuning the Catalytic Activity and Substrate Specificity of Peptide-Nanoparticle Conjugates

7.2.1 Contributions of Authors

Beate Koksch and I developed the general concept of this project. Beate Koksch supervised the project. I wrote the manuscript and Beate Koksch revised it. Jonas Scholz synthesized the peptides. I synthesized the peptide-gold nanoparticle conjugates and carried out all experiments and analysis.

7.2.2 Rationale and summary of the project

So far, the design of peptide-gold nanozymes, in which catalysis is executed by the peptide-monolayer, is performed based on rational design and trial-and-error experiments. However, designing an appropriate peptide-monolayer that also shows the desired catalytic properties is hard to predict. The assembly and orientation of individual peptides at the nanoparticle surface is not fully understood and less so are the intrinsic properties and interactions that are evoked due to the dense packing of peptides. There is no set of design rules, which can be applied to anticipate the catalytic properties or extent of catalytic activity of Pep-Au-NPs.

In this context, we performed the first systematic study on Pep-Au-NPs as we investigated the effect the location of the catalytic center relative to the Au-surface has on the catalytic activity of these conjugates. The rationale behind this study was that the flexibility of individual peptide chains, within a densely packed peptide-monolayer, varies as they are highly constraint proximal to the Au-surface and more flexible at the end of the monolayer. This feature consequently affects the local peptide-density and potential cooperative effects between peptides and substrate. Moreover, it was shown that the dense packing of ligands near the Au-NP surface leads to the exclusion of water. Thus, a solvation gradient exists that gradually

increases with distance from the Au-surface. Given this background, we wanted to utilize these intrinsic properties of the self-assembled peptide-monolayer in order to find the optimal position for catalysis and tune the substrate specificity of these conjugates, based on the differences in solvation of individual regions.

For that, three peptides were designed, namely E3H8, E3H15 and E3H22 (Fig. 7.3). Each peptide sequence consists of three repetitions of seven amino acids (heptad repeat 1-3) and is identical except for the location of the catalytic residues. In total, three different esterolytically active peptides were generated that only differ in the position of the catalytic histidine center and region in which catalysis takes place when conjugated to Au-NPs. The regions are defined as surface proximal, intermediate and surface distal for E3H8, E3H15 and E3H22, respectively.
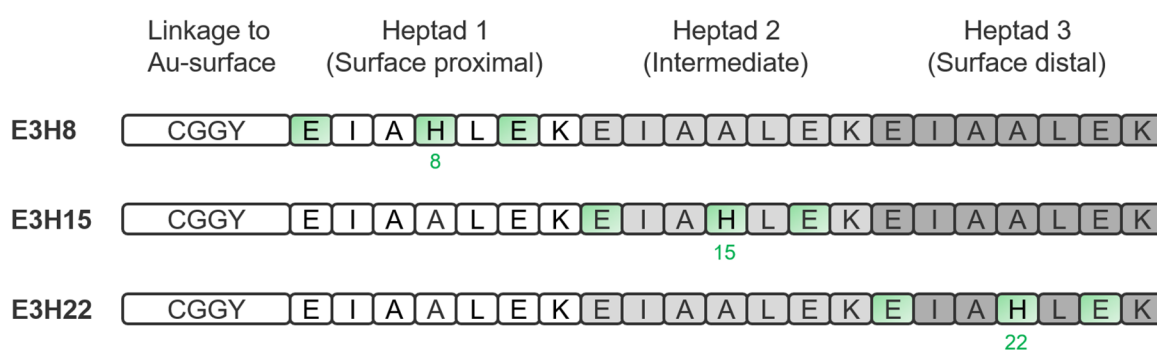
Figure 7.3: Peptide sequence of E3H8, E3H15 and E3H22 showing the position of the catalytic histidine and the respective catalytic components for ester hydrolysis (green).

Owing to the peptide design, the only parameters that potentially influence the catalytic activity of the peptide-monolayer are size of the Au-NPs, peptide loading and region in which catalysis takes place.

The first two parameters are related to the synthesis of Pep-Au-NPs and the batch-to-batch variation was kept as small as possible. E3H8, E3H15 and E3H22 were conjugated to *in situ* formed Au-NPs, synthesized by the reduction of $HAuCl_4$ using $NaBH_4$. The resulting spherical Pep-Au-NPs are referred to as Au@E3H8, Au@E3H15 and Au@E3H22. All three Pep-Au-NPs were similar in size (6.6 ± 1.5 nm, 6.3 ± 1.1 nm and 6.5 ± 1.4 nm) and had a similar peptide density (1.48 pep/nm^2, 1.41 pep/nm^2 and 1.44 pep/nm^2), as determined by TEM and supernatant analysis, respectively. Therefore, significant differences in catalytic efficiency can be attributed primarily to the location in which catalysis takes place.

Kinetic experiments were conducted by applying five substrates of different polarity/hydrophobicity, namely 4-NPA and Z-protected nitrophenyl esters (Z-L-X-ONp) of amino acids Gln, Ala, Phe and Leu. Saturation kinetics were performed only with highly soluble

4-NPA, whereas kinetic studies were conducted under pseudo-first-order reaction conditions for Z-L-X-ONp amino acids.

The results revealed that highly hydrophobic substrates Z-L-Leu-ONp and Z-L-Phe-ONp are most efficiently cleaved in the least solvated surface proximal region of Au@E3H8. Considering, that His is flanked by aliphatic amino acids Ala, Leu and Ile, we explained the superior activity of Au@E3H8 by the increased hydrophobic character of the surface proximal region, due to the exclusion of water. Z-L-Leu-ONp and Z-L-Phe-ONp penetrate the peptide-monolayer and have a greater affinity for the surface proximal region to engage in favorable, stabilizing hydrophobic interactions. The stabilized substrates are kept in place for the subsequent conversion.
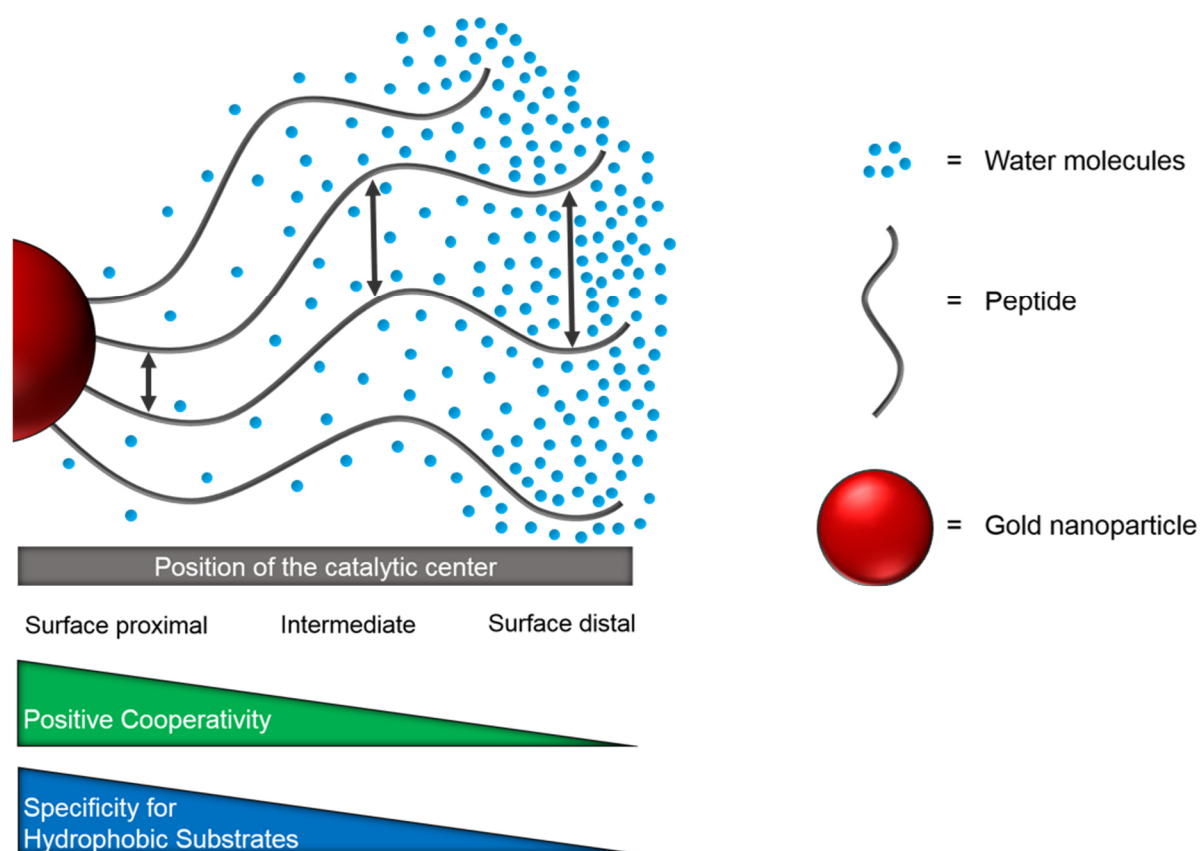
Figure 7.4: Schematic illustration of solvation differences (water molecules, blue) and spatial interactions between peptide chains (black arrow) and their effect on positive cooperativity (green, trendline) and substrate specificity (blue trendline), when catalysis is performed in that region.

In contrast, less hydrophobic 4-NPA, Z-L-Gln-ONp and Z-L-Ala-ONp were most efficiently cleaved by Au@E3H15 in the intermediate region of the monolayer. We explained this finding by comparing the three regions in terms of two parameter. First, constraint of peptide chains, which is associated with the effective peptide-density and cooperativity effects and is gradually decreasing from surface proximal to surface distal. Second, the amount of water present in each region, which is required for the ester hydrolysis and is increasing from surface

proximal to surface distal. In brief, the surface proximal and distal region both present extremes regarding those parameters. Whereas, constraint of peptides and solvation of residues is seemingly more balanced within the intermediate region of the monolayer as it is not highly solvent exposed, nor deeply buried. We drew an analogy to the active site of natural enzymes, which is usually located in a pocket or groove of the folded protein architecture. Within this sheltered pocket, rigidity of the protein scaffold as well as orientation and solvation of functional groups is optimal for substrate accommodation and conversion.

In conclusion, we found that rates of Pep-Au-NP-catalyzed ester hydrolysis correlate with the region at which catalysis takes place and polarity of the chosen ester substrate. Highly hydrophobic ester substrates were found to be more efficiently hydrolyzed in the surface proximal region, whereas less hydrophobic substrates are most efficiently hydrolyzed in the intermediate region of the peptide-monolayer. This finding is of importance, as it shows that the construction of Pep-Au-NP catalysts does not solely need to focus on the design and features of the peptide chain, but as importantly needs to consider effects and properties evoked by developed peptide-monolayer. Moreover, it offers the possibility for fine-tuning specificity of such catalysts.

7.3 Peptide-Gold Nanoparticle Conjugates as Artificial Carbonic Anhydrase Mimics

7.3.1 Contributions of Authors

I developed the general concept of this project. Beate Koksch supervised the project and refined it. I wrote the manuscript and Beate Koksch revised the manuscript. I performed the syntheses of the studied compounds and carried out all experiments and the related analysis.

7.3.2 Rationale and summary of the project

As described in section 3.2.1, the enzyme carbonic anhydrase has been extensively studied due to its potential application in PCCC systems. However, the natural enzyme structure does not possess the required stability to withstand the applied conditions of a CO_2 capture system, thus, preventing its application therein. In order to circumvent the frailty of the protein scaffold, artificial CAs have been developed, based on small molecules that mimic the catalytic center of CA and catalyze the hydration of CO_2 to HCO_3^-, while showing greater robustness towards harsh reaction conditions. Albeit, the progress in designing such CA mimics, their structural complexity and catalytic efficiency cannot compete with their natural analogue. To address the low complexity of small molecule CA mimics, this project focuses on a new strategy that combines peptides and Au-NPs as an approach to create a complex and robust artificial CA. Specifically, Au-NPs will function as a durable substitute for the protein scaffold, while tailored peptides are confined to the Au-surface generating a complex self-assembled peptide monolayer (see section 5.2.2) that executes the hydration of CO_2 to HCO_3^-.

Considering the results of the previously described project (section 7.2) and the structure of the active site cleft of natural CA (section 3.1), a peptide was designed that not only mimics the catalytic metal center but the active site as a whole. We utilized the brush-like nature of the

peptide-monolayer and designed peptide IHQ-NP (Figure 7.5). IHQ-NP evolved around the IHIHIQI (IHQ) peptide sequence reported by Rufo et al.,[292] which contains alternating hydrophobic residues and His in positions i and $i+2$ and assembles into parallel β-sheet structures. Within the parallel β-sheet structure, three His-imidazole bind a Zn(II)-ion to form a catalytically active interstrand 3-His-Zn(II)-center that is embedded into a hydrophobic environment, analogous to the active site of CA. In addition, a hydrophilic region was incorporated adjacent to the hydrophobic region in the solvent exposed region of the monolayer to facilitate solvent recruitment and proton shuttle.

The formation of β-sheet structures and concomitant development of 3-His-Zn(II)-center of IHQ-NP in solution or when conjugated to Au-NPs (Au@IHQ-NP) is a prerequisite for catalysis and was verified by CD-spectroscopy. Subsequently, kinetic experiments were performed by studying the esterase and CA activity of IHQ-NP and Au@IHQ-NP in presence and absence of Zn(II). The background reaction was always accounted for.
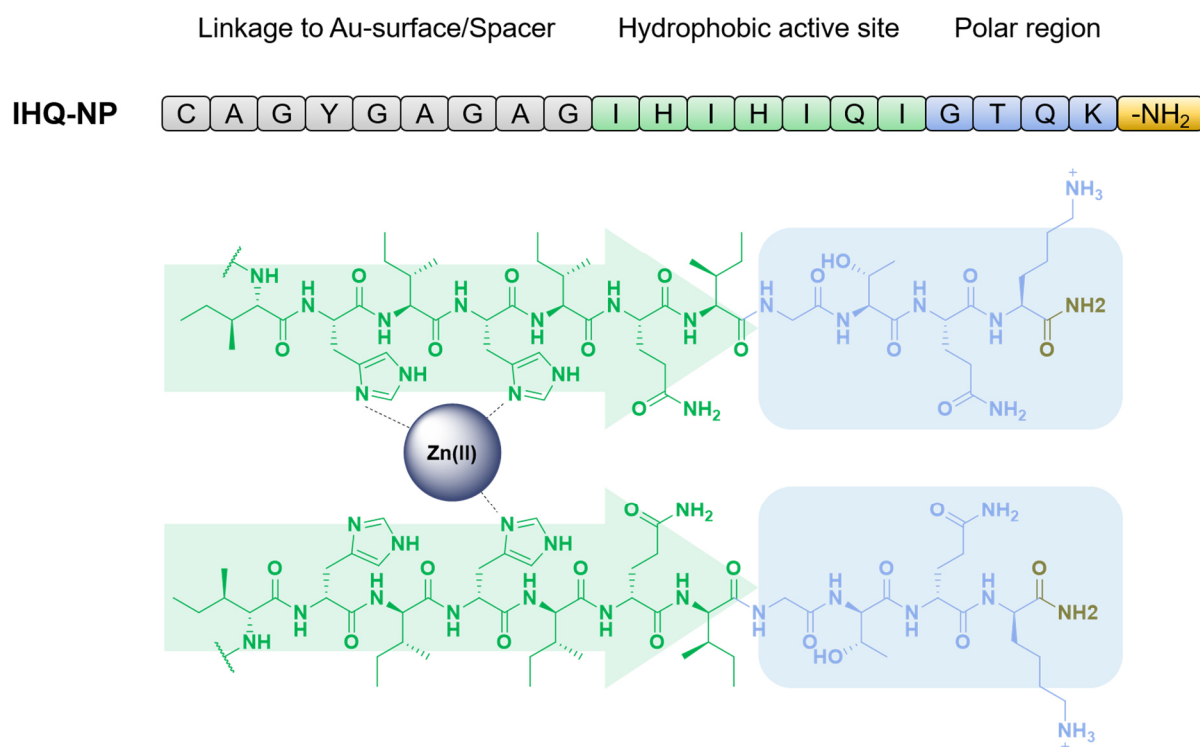
Figure 7.5: (Top) Peptide sequence of IHQ-NP. (Bottom) Structure of IHQ-NP and its designed hydrophobic (green) and hydrophilic (blue) region, as well as the formed 3-His-Zn(II)-center after formation of the parallel β-sheet.

IHQ-NP and Au@IHQ-NP both showed increased k_{cat}/K_M of ester hydrolysis of model substrate 4-NPA in presence of Zn(II). The increased k_{cat}/K_M primarily results from a 2- and 3-fold increase in turnover number k_{cat}, respectively, strongly indicating a change in catalytic mechanism to the more rapid Zn(II)-bound hydroxide mechanism.[292]

IHQ-NP and Au@IHQ-NP were studied as catalysts for the hydration of CO_2 using the delta pH method. While in absence of Zn(II) only marginal CO_2-hydration activity was observed for IHQ-NP and Au@IHQ-NP, the presence of Zn(II) led to significant improvements in rates of CO_2-hydration of approx. 21% and 55%, respectively, compared to the Zn(II) containing Tris buffer control. Intriguingly, Zn(II)-Au@IHQ-NP showed a considerably greater rate of CO_2 hydration compared to unconjugated Zn(II)-IHQ-NP. So far, rate accelerations evoked by the peptide-monolayer have only been observed for ester hydrolysis reactions. This example shows that such rate improvements are also applicable to reactions performed by metal centers and might be a general effect of the peptide-monolayer. However, IHQ-NP was designed to fully unfold its catalytic potential after conjugation to Au-NPs, by developing specific regions (hydrophobic and hydrophilic region) within the peptide-monolayer that assist the catalytic process. Thus, dissection of the observed rate improvements in ester hydrolysis and CO_2 hydration into individual contributions is not straightforward.

Further reusability studies revealed Zn(II)-Au@IHQ-NP to maintain 94% of its CO_2-hydration efficiency over at least five rounds of recycling. In order to reset the pH to the initial value of 8.9, Zn(II)-Au@IHQ-NP was treated at least 1 hour at 60 °C. Thus, Zn(II)-Au@IHQ-NP is thermostable at least up to this temperature.

In conclusion, we herein presented the proof-of-principle that Pep-Au-NPs can be designed to function as recyclable metalloenzyme mimics and execute the hydration of CO_2 in aqueous solution. These results are of significance, since metalloenzymes constitute a large class of natural enzymes that perform a variety of reactions, including phosphodiester and amide bond hydrolysis or alcohol (de)hydrogenation reactions and more. The inclusion of the reaction spectrum of metalloenzymes opens up new possibilities to study Pep-Au-NPs, e.g., in further cascade reactions.

8   Summary and Outlook

The covalent conjugation of peptides onto the surface of gold nanoparticles presents a promising approach towards complex self-assembled systems that function as artificial enzymes with distinct properties in catalysis and substrate binding. The current work dealt with the extension of fundamental design principles of Pep-Au-NPs and the evaluation of their potential to be applied as catalysts in cascade reactions and CO_2-capture systems.

The following sections summarize the individual projects included in this thesis and provide an outlook on future studies.

Peptide-Gold Nanoparticle Conjugates as Sequential Cascade Catalysts

Summary: Pep-Au-NPs are organic-inorganic hybrid nanomaterials in which catalytically active peptides are conjugated to the surface of inorganic Au-NPs, which serve as robust templates. However, Au-NPs have been demonstrated to catalyze a variety of hydrogenation or oxidation reactions at their Au-surface. Given this background, we utilized the hybridity of Pep-Au-NPs to generate a multifunctional cascade catalyst for one-pot syntheses in water.

A truncated variant of our previously established esterolytically active E3H15 peptide, referred to as E1H8, was chosen as the peptide component. The developed E1H8-monolayer surrounding the Au-NP (Au@E1H8) possessed esterase activity and was used to catalyze the hydrolysis of model ester 4-NPA to 4-NP. In a subsequent step, without work-up, $NaBH_4$ was added to the same reaction dispersion, initiating the Au-NP-mediated hydrogenation of 4-NP to 4-AP. Au@E1H8, showed greater rates of reaction for both, the ester hydrolysis and 4-NP hydrogenation, compared to either unconjugated E1H8 or unconjugated E1H8 physically mixed with citrate-capped Au-NPs. Thus, immobilization of E1H8 to Au-NPs evoked synergistic effects that even accelerate catalytic mechanisms executed by the Au-surface. It is suggested that the peptide-monolayer engages in hydrogen-bonding and/or electrostatic interactions with the diffusing 4-NP molecules. Therefore, 4-NP molecules are kept in proximity to the Pep-Au-NP and residence time of 4-NP around the Au-surface is increased, which results in overall improved rates of hydrogenation.

Recycling of Au@E1H8 was possible only after 4-NPA hydrolysis; whereas, after addition of $NaBH_4$ and complete hydrogenation, immediate work-up is required to prevent aggregation and precipitation of Au@E1H8.

Outlook: Future studies should focus on expanding the repertoire of potential one-pot cascade reactions. Peptide catalysis offers a broad reaction spectrum to choose from, including Friedel-

Crafts-alkylation, asymmetric aldol reactions, Michael additions or Baylis-Hillman reaction, to name a few. Coupling these with, e.g., selective oxidation or hydrogenation reactions catalyzed by metal NPs could introduce synthetic routes towards valuable products, while avoiding the necessity of protecting groups and excessive work-up steps.

Furthermore, molecular dynamic simulations should be performed in order to elucidate the factors that lead to the observed rate improvements of Au@E1H8. So far, all catalytic effects evoked by the conjugation of peptide onto Au-NPs have only been hypothesized based on results of kinetic experiments.

Tuning the Catalytic Activity and Substrate Specificity of Peptide-Nanoparticle Conjugates

Summary: Within the scope of this project, we systematically investigated the effect the location of the catalytic center relative to the Au-surface has on the catalytic properties of Pep-Au-NPs. For that, three esterolytically active peptides, namely E3H8, E3H15 and E3H22 have been designed and synthesized, that only differ in their position of the catalytic His residue. Consequently, after conjugation to Au-NPs catalysis is executed in three different regions, referred to as surface proximal, intermediate and surface distal, for Au@E3H8, Au@E3H15 and Au@E3H22, respectively. The three Pep-Au-NPs have been studied in their ability to cleave five ester substrates (4-NPA, Z-L-Gln-ONp, Z-L-Ala-ONp, Z-L-Phe-ONp and Z-L-Leu-ONp) that differ in their hydrophobic nature. In conclusion, rates of Pep-Au-NP-catalyzed ester hydrolysis were found to correlate with the region in which catalysis takes place and the hydrophobicity of the chosen substrates. That is, hydrophobic substrates Z-L-Phe-ONp and Z-L-Leu-ONp were found to be most efficiently cleaved by the surface proximal region of Au@E3H8, while more hydrophilic substrates 4-NPA, Z-L-Gln-ONp and Z-L-Ala-ONp were hydrolyzed most effectively at the intermediate region of Au@E3H15. This correlation was explained by comparing the different regions in terms of solvation, peptide-peptide and peptide-substrate interactions. Briefly, aliphatic amino acids flanking the catalytic His in the surface proximal region are in a less solvated states. Thus, highly hydrophobic substrates increasingly accumulate in the surface proximal region to engage in favorable hydrophobic interactions, which results in overall higher rates of hydrolysis, compared to the intermediate or surface distal region. On the other hand, the intermediate region is seemingly more balanced in terms of solvation of functional groups, rigidity of the peptide scaffold and cooperative effects between peptides, which leads to superior rates of hydrolysis for less hydrophobic substrates. Altogether,

the results point towards the importance of intrinsic effects within the peptide-monolayer that needs to be taken into consideration when designing Pep-Au-NP catalysts.

Outlook: Further systematic studies should be directed to elucidate the effects of the peptide length and loading on the catalytic properties of Pep-Au-NPs. These parameters dictate the overall peptide topology, in terms of rigidity or flexibility of the monolayer and spatial proximity of peptide chains, thus, potential interaction networks. Furthermore, size-dependency of Pep-Au-NP catalysis should be systematically examined as it dictates the total amount of peptide able to bind to the surface. Also, in case of spherical NPs, the size also influences the curvature of the sphere and affects the formation and extent of peptides to adopt secondary structures, e.g., β-sheets.[280]

Peptide-Gold Nanoparticle Conjugates as Artificial Carbonic Anhydrase Mimics

Summary: So far, Pep-Au-NPs have only been designed and applied as esterase mimics to cleave organic ester bonds of model ester substrates. However, to consider Pep-Au-NPs as catalysts for (green) applications, for example, in CO_2-capture systems, their reaction scope needs to be extended. Therefore, this work dealt with the design and synthesis of a stable Pep-Au-NP that mimics the catalytic activity of zinc metalloenzyme carbonic anhydrase (CA).

For that, a modified variant of reported Zn(II)-binding IHIHIQI (IHQ) peptide was designed and used, referred to as IHQ-NP. IHQ-NP comprises three regions that were designed for Au-NP conjugation and mimicry of the active site cleft of natural CA when densely conjugated to Au-NPs. Unconjugated IHQ-NP, as well as the conjugated variant (Au@IHQ-NP) assembles into parallel β-sheet structures as determined by CD-spectroscopy and by virtue of the IHQ design, an interstrand 3-His-Zn-binding site is developed, analogous to the catalytic center of CA.

Kinetic assays were performed by applying IHQ-NP and Au@IHQ-NP in presence and absence of Zn(II) as catalysts for the hydrolysis of model substrate 4-NPA monitored by UV/vis-spectroscopy, and for the hydration of CO_2 followed by the delta pH method. For both reactions a significant increase in catalytic activity was observed in presence of Zn(II), indicating the successful development and function of the 3-His-Zn(II)-center within the β-sheet structures of IHQ-NP and Au@IHQ-NP, respectively. Compared to unconjugated IHQ-NP, Au@IHQ-NP showed a 2-fold higher catalytic efficiency k_{cat}/K_M for the hydrolysis of 4-NPA, and increased rates of CO_2-hydration by more than 2-fold. Thus, conjugation of

IHQ-NP to Au-NPs not only established CA activity within a Pep-Au-NP but significantly accelerated the catalytic process, compared to the unconjugated variant.

Furthermore, Au@IHQ-NP was applied and recycled five times for the hydration of CO_2 and maintained at least 94% of its catalytic activity, even after treatment at 60 °C over at least 1 h. The results provide a proof-of-concept that Pep-Au-NPs can be designed to also mimic metalloenzyme activity within their peptide-monolayer, while being robust and recyclable.

Outlook: Kinetic experiments under stopped-flow conditions should be performed in order to obtain quantitative kinetic parameters of CO_2-hydration and to enable comparison to literature reported systems.

The peptide design should also be refined, since the formation of extended β-sheet fibrils of the IHQ-NP sequence was observed at neutral to basic pH during the synthesis of Au@IHQ-NP, which made the determination of exact peptide loading by supernatant analysis inaccurate. Careful adjustment of the pH was required in order to prevent aggregation and precipitation of IHQ-NP. In order to avoid daunting handling of the peptide, the design should either include a Zn(II)-binding domain, which is not based on amyloidogenic peptide sequences, or fibril formation should be suppressed or limited by, e.g., destabilization of β-sheets due to electrostatic repulsion by flanking amino acids bearing charged functional groups.

Moreover, to lower the production costs of Pep-Au-NPs and enable large-scale production, the Au-NP should be substituted for low-cost alternatives, such as silica- or magnetic Fe_3O_4-NPs. However, these strategies require different chemistries for peptide-NP-conjugation.

9 References

[1]   J. C. Védrine, *Catalysts* **2017**, *7*, DOI 10.3390/catal7110341.

[2]   A. Fortuny, C. Bengoa, J. Font, F. Castells, A. Fabregat, *Catal. Today* **1999**, *53*, 107–114.

[3]   M. Iwamoto, *Stud. Surf. Sci. Catal.* **2000**, *130*, 23–47.

[4]   Y. I. Matatov-Meytal, M. Sheintuch, *Ind. Eng. Chem. Res.* **1998**, *37*, 309–326.

[5]   M. O'Connell, M. . Morris, *Catal. Today* **2000**, *59*, 387–393.

[6]   P. . Thassitou, I. . Arvanitoyannis, *Trends Food Sci. Technol.* **2001**, *12*, 185–196.

[7]   M. Megharaj, B. Ramakrishnan, K. Venkateswarlu, N. Sethunathan, R. Naidu, *Environ. Int.* **2011**, *37*, 1362–1375.

[8]   D. Stanners, P. Bourdeau, *Europe's Environment: The Dobris Assessment*, European Environment Agency Copenhagen, **1995**.

[9]   G. M. Bond, J. Stringer, D. K. Brandvold, F. A. Simsek, G. Egeland, *Energy & fuels* **1999**, *20*, 713–717.

[10]   R. R. Yadav, K. Krishnamurthi, S. N. Mudliar, S. S. Devi, P. K. Naoghare, A. Bafana, T. Chakrabarti, *J. Basic Microbiol.* **2014**, *54*, 472–481.

[11]   X.-L. YUE, Q.-X. GAO, *Adv. Clim. Chang. Res.* **2018**, *9*, 243–252.

[12]   T. Kuc, K. Rozanski, M. Zimnoch, J. . Necki, A. Korus, *Appl. Energy* **2003**, *75*, 193–203.

[13]   R. A. Kelsey, D. A. Miller, S. R. Parkin, K. Liu, J. E. Remias, Y. Yang, F. C. Lightstone, K. Liu, C. A. Lippert, S. A. Odom, *Dalt. Trans.* **2016**, 324–333.

[14]   W. Cai, A. Santoso, G. Wang, S.-W. Yeh, S.-I. An, K. M. Cobb, M. Collins, E. Guilyardi, F.-F. Jin, J.-S. Kug, et al., *Nat. Clim. Chang.* **2015**, *5*, 849.

[15]   S. C. Doney, V. J. Fabry, R. A. Feely, J. A. Kleypas, *Ann. Rev. Mar. Sci.* **2009**, *1*, 169–192.

[16]   C. Turley, M. Eby, A. J. Ridgwell, D. N. Schmidt, H. S. Findlay, C. Brownlee, U. Riebesell, V. J. Fabry, R. A. Feely, J.-P. Gattuso, *Mar. Pollut. Bull.* **2010**, *60*, 787–792.

[17]   H. Kurihara, *Mar. Ecol. Prog. Ser.* **2008**, *373*, 275–284.

[18]   A. Ipcc, S. Report, *IPCC Report Global Warming of 1.5 C: Summary for Policymakers*, **2018**.

[19]   E. M. Fischer, R. Knutti, *Nat. Clim. Chang.* **2015**, *5*, 560.

[20]   A. D. King, D. J. Karoly, B. J. Henley, *Nat. Clim. Chang.* **2017**, *7*, 412.

[21]   G. Naumann, L. Alfieri, K. Wyser, L. Mentaschi, R. A. Betts, H. Carrao, J. Spinoni, J. Vogt, L. Feyen, *Geophys. Res. Lett.* **2018**, *45*, 3285–3296.

[22]   N. S. Diffenbaugh, D. L. Swain, D. Touma, *Proc. Natl. Acad. Sci.* **2015**, *112*, 3931 LP – 3936.

[23]   C.-E. Park, S.-J. Jeong, M. Joshi, T. J. Osborn, C.-H. Ho, S. Piao, D. Chen, J. Liu, H. Yang, H. Park, et al., *Nat. Clim. Chang.* **2018**, *8*, 70–74.

[24]   P. Marion, B. Bernela, A. Piccirilli, B. Estrine, N. Patouillard, J. Guilbot, F. Jérôme, *Green Chem.* **2017**, *19*, 4973–4989.

[25]   C. M. Clouthier, J. N. Pelletier, *Chem. Soc. Rev.* **2012**, *41*, 1585–1605.

[26]   J. L. Heier, De Novo Self-Assembing Peptides Possessing Esterase Properties, Freie Universität Berlin, **2015**.

[27]   H. Renata, Z. J. Wang, F. H. Arnold, *Angew. Chemie Int. Ed.* **2015**, *54*, 3351–3367.

[28]   S. C. Hammer, A. M. Knight, F. H. Arnold, *Curr. Opin. Green Sustain. Chem.* **2017**, *7*, 23–30.

[29]   X. Zhang, D. Wu, X. Zhou, Y. Yu, J. Liu, N. Hu, H. Wang, G. Li, Y. Wu, *TrAC Trends Anal. Chem.* **2019**, *121*, 115668.

[30]   J. Wu, X. Wang, Q. Wang, Z. Lou, S. Li, Y. Zhu, L. Qin, H. Wei, *Chem. Soc. Rev.* **2019**, *48*, 1004.

[31]   S. Singh, *Front. Chem.* **2019**, *7*, 46.

[32]   C. Pezzato, S. Maiti, J. L. Chen, A. Cazzolaro, C. Gobbo, L. J. Prins, *Chem. Commun.* **2015**, *51*, 9922–9931.

[33]   M. C. Daniel, D. Astruc, *Chem. Rev.* **2004**, *104*, 293–346.

[34]   Y. Lin, J. Ren, X. Qu, *Adv. Mater.* **2014**, *26*, 4200–4217.

[35] N. Lopez, T. V. W. Janssens, B. S. Clausen, Y. Xu, M. Mavrikakis, T. Bligaard, J. K. Nørskov, *J. Catal.* **2004**, *223*, 232–235.

[36] P. Ghosh, G. Han, M. De, C. K. Kim, V. M. Rotello, *Adv. Drug Deliv. Rev.* **2008**, *60*, 1307–1315.

[37] R. Shukla, V. Bansal, M. Chaudhary, A. Basu, R. R. Bhonde, M. Sastry, *Langmuir* **2005**, *21*, 10644–10654.

[38] S. K. Nune, N. Chanda, R. Shukla, K. Katti, R. R. Kulkarni, S. Thilakavathy, S. Mekapothula, R. Kannan, K. V. Katti, *J. Mater. Chem.* **2009**, *19*, 2912.

[39] E. Pensa, E. Cortés, G. Corthey, P. Carro, C. Vericat, M. H. Fonticelli, G. Benítez, A. A. Rubert, R. C. Salvarezza, *Acc. Chem. Res.* **2012**, *45*, 1183–1192.

[40] T. Taguchi, K. Isozaki, K. Miki, *Adv. Mater.* **2012**, *24*, 6462–6467.

[41] L. Pasquato, P. Pengo, P. Scrimin, *J. Mater. Chem.* **2004**, *14*, 3481–3487.

[42] L. Riccardi, L. Gabrielli, X. Sun, F. De Biasi, F. Rastrelli, F. Mancin, M. De Vivo, *Chem* **2017**, *3*, 92–109.

[43] L. Gao, M. Liu, G. Ma, Y. Wang, L. Zhao, Q. Yuan, F. Gao, R. Liu, J. Zhai, Z. Chai, et al., *ACS Nano* **2015**, *9*, 10979–10990.

[44] M. I. Stodulski, T. Gulder, *Angew. Chemie - Int. Ed.* **2012**, *51*, 11202–11204.

[45] D. J. Mikolajczak, J. L. Heier, B. Schade, B. Koksch, *Biomacromolecules* **2017**, *18*, 3557–3562.

[46] P. Pengo, S. Polizzi, L. Pasquato, P. Scrimin, *J. Am. Chem. Soc.* **2005**, *127*, 1616–1617.

[47] P. T. Anastas, **1998**.

[48] P. Anastas, N. Eghbali, *Chem. Soc. Rev.* **2010**, *39*, 301–312.

[49] P. T. Anastas, *Chem. Rev.* **2007**, *107*, 2167–2168.

[50] B. A. de Marco, B. S. Rechelo, E. G. Tótoli, A. C. Kogawa, H. R. N. Salgado, *Saudi Pharm. J.* **2019**, *27*, 1–8.

[51] R. A. Sheldon, *ACS Sustain. Chem. Eng.* **2018**, *6*, 32–48.

[52] S. W. Chaikin, W. G. Brown, *J. Am. Chem. Soc.* **1949**, *71*, 122–125.

[53]   S. Werkmeister, K. Junge, M. Beller, *Org. Process Res. Dev.* **2014**, *18*, 289–302.

[54]   R. H. Grubbs, *Tetrahedron* **2004**, *60*, 7117–7140.

[55]   V. Sabatino, T. R. Ward, *Beilstein J. Org. Chem.* **2019**, *15*, 445–468.

[56]   D. J. C. Constable, A. D. Curzons, V. L. Cunningham, *Green Chem.* **2002**, *4*, 521–527.

[57]   A. D. Curzons, D. J. C. Constable, D. N. Mortimer, V. L. Cunningham, *Green Chem.* **2001**, *3*, 1–6.

[58]   F. M. Kerton, R. Marriott, *Alternative Solvents for Green Chemistry*, Royal Society Of Chemistry, **2013**.

[59]   S. V More, M. N. V Sastry, C.-F. Yao, *Green Chem.* **2006**, *8*, 91–95.

[60]   V. D. Dhakane, S. S. Gholap, U. P. Deshmukh, H. V. Chavan, B. P. Bandgar, *Comptes Rendus Chim.* **2014**, *17*, 431–436.

[61]   Q. Li, Y. Yan, X. Wang, B. Gong, X. Tang, J. Shi, H. E. Xu, W. Yi, *RSC Adv.* **2013**, *3*, 23402–23408.

[62]   D. C. Rideout, R. Breslow, *J. Am. Chem. Soc.* **1980**, *102*, 7816–7817.

[63]   M. T. De Martino, L. K. E. A. Abdelmohsen, F. P. J. T. Rutjes, J. C. M. Van Hest, *Beilstein J. Org. Chem.* **2018**, *14*, 716–733.

[64]   S. Wenda, S. Illner, A. Mell, U. Kragl, *Green Chem.* **2011**, *13*, 3007–3047.

[65]   J. Lu, M. J. Lazzaroni, J. P. Hallett, A. S. Bommarius, C. L. Liotta, C. A. Eckert, *Ind. Eng. Chem. Res.* **2004**, *43*, 1586–1590.

[66]   B. H. Lipshutz, S. Ghorai, W. W. Y. Leong, B. R. Taft, D. V Krogstad, *J. Org. Chem.* **2011**, *76*, 5061–5073.

[67]   B. Volesky, J. H. T. Luong, K. Aunstrup, *Crit. Rev. Biotechnol.* **1984**, *2*, 119–146.

[68]   S. Kobayashi, H. Uyama, S. Kimura, *Chem. Rev.* **2001**, *101*, 3793–3818.

[69]   S. I. Shoda, H. Uyama, J. I. Kadokawa, S. Kimura, S. Kobayashi, *Chem. Rev.* **2016**, *116*, 2307–2413.

[70]   S. Shoda, S. Kobayashi, *Trends Polym. Sci.* **1997**, *5*, 109–115.

[71]   I. Nakamura, A. Makino, M. Ohmae, S. Kimura, *Chem. Lett.* **2011**, *41*, 37–38.

[72] Y. Omagari, S. Matsuda, Y. Kaneko, J. Kadokawa, *Macromol. Biosci.* **2009**, *9*, 450–455.

[73] S. Kobayashi, H. Morii, R. Itoh, S. Kimura, M. Ohmae, *J. Am. Chem. Soc.* **2001**, *123*, 11825–11826.

[74] R. Di Cosimo, J. Mc Auliffe, A. J. Poulose, G. Bohlmann, *Chem. Soc. Rev.* **2013**, *42*, 6437–6474.

[75] P. K. Robinson, *Essays Biochem.* **2015**, *59*, 1–41.

[76] L. J. Kingsley, M. A. Lill, *Proteins Struct. Funct. Bioinforma.* **2015**, *83*, 599–611.

[77] R. A. Copeland, *Enzymes: A Practical Introduction to Structure, Mechanism, and Data Analysis*, John Wiley & Sons, **2001**.

[78] G. Zhou, T. Somasundaram, E. Blanc, G. Parthasarathy, W. R. Ellington, M. S. Chapman, *Proc. Natl. Acad. Sci. U. S. A.* **1998**, *95*, 8449–8454.

[79] T. C. Bruice, a Brown, D. O. Harris, *Proc. Natl. Acad. Sci. U. S. A.* **1971**, *68*, 658–61.

[80] S. Borman, *Chem. Eng. news* **2004**, *82*, 35.

[81] G. Dodson, A. Wlodawer, *Trends Biochem. Sci.* **1998**, *23*, 347–352.

[82] Y. Shimazaki, M. Takani, O. Yamauchi, *Dalt. Trans.* **2009**, 7854–7869.

[83] D. E. Benson, M. S. Wisz, H. W. Hellinga, *Proc. Natl. Acad. Sci.* **2000**, *97*, 6292 LP – 6297.

[84] M. L. Zastrow, V. L. Pecoraro, *Biochemistry* **2014**, *53*, 957–978.

[85] J. Steinreiber, T. R. Ward, *Coord. Chem. Rev.* **2008**, *252*, 751–766.

[86] R. L. Mikulski, D. N. Silverman, *Biochim. Biophys. Acta - Proteins Proteomics* **2010**, *1804*, 422–426.

[87] A. Angeli, L. Di Cesare Mannelli, C. Ghelardini, T. S. Peat, G. Bartolucci, M. Menicatti, F. Carta, C. T. Supuran, *Eur.J.Med.Chem.* **2019**, *177*, 188–197.

[88] D. W. Christianson, C. A. Fierke, *Acc. Chem. Res.* **1996**, *29*, 331–339.

[89] C. U. Kim, H. Song, B. S. Avvaru, S. M. Gruner, S. Park, R. McKenna, *Proc. Natl. Acad. Sci.* **2016**, *113*, 5257 LP – 5262.

[90] D. Duda, C. Tu, M. Qian, P. Laipis, M. Agbandje-McKenna, D. N. Silverman, R.

McKenna, *Biochemistry* **2001**, *40*, 1741–1748.

[91]   D. West, C. U. Kim, C. Tu, A. H. Robbins, S. M. Gruner, D. N. Silverman, R. McKenna, *Biochemistry* **2012**, *51*, 9156–9163.

[92]   J. Y. Liang, W. N. Lipscomb, *Proc. Natl. Acad. Sci. U. S. A.* **1990**, *87*, 3675–3679.

[93]   C. D. Boone, A. Habibzadegan, S. Gill, R. Mckenna, *Biomolecules* **2013**, *3*, 553–562.

[94]   D. N. Silverman, R. McKenna, *Acc. Chem. Res.* **2007**, *40*, 669–675.

[95]   S. Z. Fisher, C. Tu, D. Bhatt, L. Govindasamy, M. Agbandje-McKenna, R. McKenna, D. N. Silverman, *Biochemistry* **2007**, *46*, 3803–3813.

[96]   S. Z. Fisher, C. M. Maupin, M. Budayova-Spano, L. Govindasamy, C. Tu, M. Agbandje-McKenna, D. N. Silverman, G. A. Voth, R. McKenna, *Biochemistry* **2007**, *46*, 2930–2937.

[97]   B. S. Avvaru, C. U. Kim, K. H. Sippel, S. M. Gruner, M. Agbandje-McKenna, D. N. Silverman, R. McKenna, *Biochemistry* **2010**, *49*, 249–251.

[98]   Z. Fisher, J. A. Hernandez Prada, C. Tu, D. Duda, C. Yoshioka, H. An, L. Govindasamy, D. N. Silverman, R. McKenna, *Biochemistry* **2005**, *44*, 1097–1105.

[99]   A. Bottoni, C. Z. Lanza, G. Pietro Miscione, D. Spinelli, *J. Am. Chem. Soc.* **2004**, *126*, 1542–1550.

[100] J.-Y. Liang, W. N. Lipscomb, *Int. J. Quantum Chem.* **1989**, *36*, 299–312.

[101] S. K. Nair, D. W. Christianson, *Biochemistry* **1993**, *32*, 4506–4514.

[102] C. A. Fierke, T. L. Calderone, J. F. Krebs, *Biochemistry* **1991**, *30*, 11054–11063.

[103] L. L. Kiefer, S. A. Paterno, C. A. Fierke, *J. Am. Chem. Soc.* **1995**, *117*, 6831–6837.

[104] H. STEINER, B. -H JONSSON, S. LINDSKOG, *Eur. J. Biochem.* **1975**, *59*, 253–259.

[105] U. Carlsson, L. E. Henderson, S. Lindskog, *Biochim. Biophys. Acta - Protein Struct.* **1973**, *310*, 376–387.

[106] A. M. Klibanov, *Trends Biotechnol.* **1997**, *15*, 97–101.

[107] B. Kanbar, E. Ozdemir, *Biotechnol. Prog.* **2010**, *26*, 1474–1480.

[108] W. C. Floyd, S. E. Baker, C. A. Valdez, J. K. Stolaroff, J. P. Bearinger, J. H. Satcher, R.

D. Aines, *Environ. Sci. Technol.* **2013**, *47*, 10049–10055.

[109] Z. Fisher, C. D. Boone, S. M. Biswas, B. Venkatakrishnan, M. Aggarwal, C. Tu, M. Agbandje-McKenna, D. Silverman, R. McKenna, *Protein Eng. Des. Sel.* **2012**, *25*, 347–355.

[110] A. Sanna, M. Uibu, G. Caramanna, R. Kuusik, M. M. Maroto-Valer, *Chem. Soc. Rev.* **2014**, *43*, 8049–8080.

[111] H. M. Becker, M. Klier, J. W. Deitmer, *Carbonic Anhydrase: Mechanism, Regulation, Links to Disease, and Industrial Applications*, Springer Netherlands, Dordrecht, **2014**.

[112] G. M. Bond, J. Stringer, D. K. Brandvold, F. A. Simsek, M.-G. Medina, G. Egeland, *Energy & Fuels* **2001**, *15*, 309–316.

[113] A. C. Pierre, *Carbon Capture Storage CO2 Manag. Technol.* **2014**, *2012*, 122–176.

[114] M. Wahba, M. Mizutani, S. Katayama, *J. Mater. Process. Technol.* **2015**, *221*, 146–153.

[115] C. Aprea, A. Maiorino, *Int. J. Refrig.* **2008**, *31*, 1006–1011.

[116] S. Kattel, P. J. Ramírez, J. G. Chen, J. A. Rodriguez, P. Liu, *Science (80-.).* **2017**, *355*, 1296–1299.

[117] W. H. Wang, Y. Himeda, J. T. Muckerman, G. F. Manbeck, E. Fujita, *Chem. Rev.* **2015**, *115*, 12936–12973.

[118] E. Alper, O. Yuksel Orhan, *Petroleum* **2017**, *3*, 109–126.

[119] J. K. J. Yong, G. W. Stevens, F. Caruso, S. E. Kentish, *J. Chem. Technol. Biotechnol.* **2015**, *90*, 3–10.

[120] M. Stec, A. Tatarczuk, L. Więcław-Solny, A. Krótki, M. Ściążko, S. Tokarski, *Fuel* **2015**, *151*, 50–56.

[121] J. T. Yeh, H. W. Pennline, K. P. Resnik, *Energy & Fuels* **2001**, *15*, 274–278.

[122] G. T. Rochelle, *Science (80-.).* **2009**, *325*, 1652 LP – 1654.

[123] B. A. Oyenekan, G. T. Rochelle, *Int. J. Greenh. Gas Control* **2009**, *3*, 121–132.

[124] A. K. Chakraborty, G. Astarita, K. B. Bischoff, *Chem. Eng. Sci.* **1986**, *41*, 997–1003.

[125] F. A. Chowdhury, H. Okabe, S. Shimizu, M. Onoda, Y. Fujioka, *Energy Procedia* **2009**, *1*, 1241–1248.

[126] Y. G. Ko, S. S. Shin, U. S. Choi, *J. Colloid Interface Sci.* **2011**, *361*, 594–602.

[127] V. Darde, K. Thomsen, W. J. M. van Well, E. H. Stenby, *Energy Procedia* **2009**, *1*, 1035–1042.

[128] T. N. G. Borhani, A. Azarpour, V. Akbari, S. R. Wan Alwi, Z. A. Manan, *Int. J. Greenh. Gas Control* **2015**, *41*, 142–162.

[129] G. M. Bond, G. Egeland, D. K. Brandvold, M. G. Medina, F. A. Simsek, J. Stringer, *World Resour. Rev.* **1999**, *11*, 603–619.

[130] L. Fradette, S. Lefebvre, J. Carley, *Energy Procedia* **2017**, *114*, 1100–1109.

[131] G. M. Bond, J. Stringer, D. K. Brandvold, F. A. Simsek, M. G. Medina, G. Egeland, *Energy and Fuels* **2001**, *15*, 309–316.

[132] Y. Lu, X. Ye, Z. Zhang, A. Khodayari, T. Djukadi, *Energy Procedia* **2011**, *4*, 1286–1293.

[133] M. E. Russo, G. Olivieri, C. Capasso, V. De Luca, A. Marzocchella, P. Salatino, M. Rossi, *Enzyme Microb. Technol.* **2013**, *53*, 271–277.

[134] R. Perfetto, S. Del Prete, D. Vullo, G. Sansone, C. M. A. Barone, M. Rossi, C. T. Supuran, C. Capasso, *J. Enzyme Inhib. Med. Chem.* **2017**, *32*, 759–766.

[135] C. Capasso, V. De Luca, V. Carginale, R. Cannio, M. Rossi, *J. Enzyme Inhib. Med. Chem.* **2012**, *27*, 892–897.

[136] F. Migliardini, V. De Luca, V. Carginale, M. Rossi, P. Corbo, C. T. Supuran, C. Capasso, *J. Enzyme Inhib. Med. Chem.* **2014**, *29*, 146–150.

[137] M. Borchert, P. Saunders, *Heat-Stable Carbonic Anhydrases and Their Use.*, **2011**, US Patent US7892814.

[138] C. K. Savile, J. J. Lalonde, *Curr. Opin. Biotechnol.* **2011**, *22*, 818–823.

[139] L. Fradette, S. Lefebvre, J. Carley, in *Energy Procedia*, **2017**.

[140] R. Davy, *Energy Procedia* **2009**, *1*, 885–892.

[141] E. Kimura, T. Shiota, T. Koike, M. Shiro, M. Kodama, *J. Am. Chem. Soc.* **1990**, *112*, 5805–5811.

[142] X. Zhang, R. van Eldik, *Inorg. Chem.* **1995**, *34*, 5606–5614.

[143] C. a. Lippert, K. Liu, M. Sarma, S. R. Parkin, J. E. Remias, C. M. Brandewie, S. a. Odom, K. Liu, *Catal. Sci. Technol.* **2014**, *4*, 3620–3625.

[144] V. M. Cangelosi, A. Deb, J. E. Penner-Hahn, V. L. Pecoraro, *Angew. Chemie - Int. Ed.* **2014**, *53*, 7900–7903.

[145] J. W. Bryson, J. R. Desjarlais, T. M. Handel, W. F. DeGrado, *Protein Sci.* **1998**, *7*, 1404–14.

[146] C. A. Denard, J. F. Hartwig, H. Zhao, *ACS Catal.* **2013**, *3*, 2856–2864.

[147] C. Simons, U. Hanefeld, I. W. C. E. Arends, T. Maschmeyer, R. A. Sheldon, *Top. Catal.* **2006**, *40*, 35–44.

[148] F. Rudroff, M. D. Mihovilovic, H. Gröger, R. Snajdrova, H. Iding, U. T. Bornscheuer, *Nat. Catal.* **2018**, *1*, 12–22.

[149] H. Gröger, W. Hummel, *Curr. Opin. Chem. Biol.* **2014**, *19*, 171–179.

[150] Á. Gómez Baraibar, D. Reichert, C. Mügge, S. Seger, H. Gröger, R. Kourist, *Angew. Chemie Int. Ed.* **2016**, *55*, 14823–14827.

[151] M. Höhne, S. Kühl, K. Robins, U. T. Bornscheuer, *ChemBioChem* **2008**, *9*, 363–365.

[152] S. Schmidt, K. Castiglione, R. Kourist, *Chem. - A Eur. J.* **2018**, *24*, 1755–1768.

[153] J. Enoki, J. Meisborn, A.-C. Müller, R. Kourist, *Front. Microbiol.* **2016**, *7*, 425.

[154] E. Busto, R. C. Simon, N. Richter, W. Kroutil, *ACS Catal.* **2016**, *6*, 2393–2397.

[155] L. Klermund, S. T. Poschenrieder, K. Castiglione, *ACS Catal.* **2017**, *7*, 3900–3904.

[156] T. L. Lohr, T. J. Marks, *Nat. Chem.* **2015**, *7*, 477.

[157] L. F. Tietze, *Chem. Rev.* **1996**, *96*, 115–136.

[158] C. Grondal, M. Jeanty, D. Enders, *Nat. Chem.* **2010**, *2*, 167–178.

[159] K. Tenbrink, M. Seßler, J. Schatz, H. Gröger, *Adv. Synth. Catal.* **2011**, *353*, 2363–2367.

[160] E. Burda, W. Hummel, H. Gröger, *Angew. Chemie - Int. Ed.* **2008**, *47*, 9551–9554.

[161] A. Boffi, S. Cacchi, P. Ceci, R. Cirilli, G. Fabrizi, A. Prastaro, S. Niembro, A. Shafir, A. Vallribera, *ChemCatChem* **2011**, *3*, 347–353.

[162] B. H. San, S. Ravichandran, K. S. Park, V. K. Subramani, K. K. Kim, *ACS Appl. Mater.*

Interfaces **2016**, *8*, 30058–30065.

[163] G. Rulli, N. Duangdee, K. Baer, W. Hummel, A. Berkessel, H. Gröger, *Angew. Chemie - Int. Ed.* **2011**, *50*, 7944–7947.

[164] R. Schoevaart, T. Kieboom, *Tetrahedron Lett.* **2002**, *43*, 3399–3400.

[165] V. Polshettiwar, J. M. Basset, D. Astruc, *ChemSusChem* **2012**, *5*, 6–8.

[166] S. B. Kalidindi, B. R. Jagirdar, *ChemSusChem* **2012**, *5*, 65–75.

[167] V. Polshettiwar, R. S. Varma, *Green Chem.* **2010**, *12*, 743–754.

[168] D. Jiang, D. Ni, Z. T. Rosenkrans, P. Huang, X. Yan, W. Cai, *Chem. Soc. Rev.* **2019**, *48*, 3683–3704.

[169] M. Liang, X. Yan, *Acc. Chem. Res.* **2019**, *52*, 2190–2200.

[170] W. He, Y. T. Zhou, W. G. Wamer, X. Hu, X. Wu, Z. Zheng, M. D. Boudreau, J. J. Yin, *Biomaterials* **2013**, *34*, 765–773.

[171] P. Pengo, L. Baltzer, L. Pasquato, P. Scrimin, *Angew. Chemie - Int. Ed.* **2007**, *46*, 400–404.

[172] M. Comotti, C. Della Pina, R. Matarrese, M. Rossi, *Angew. Chemie - Int. Ed.* **2004**, *43*, 5812–5815.

[173] M. Comotti, C. Della Pina, E. Falletta, M. Rossi, *Adv. Synth. Catal.* **2006**, *348*, 313–316.

[174] W. Luo, C. Zhu, S. Su, D. Li, Y. He, Q. Huang, C. Fan, *ACS Nano* **2010**, *4*, 7451–7458.

[175] D. Zaramella, P. Scrimin, L. J. Prins, *Int. J. Mol. Sci.* **2013**, *14*, 2011–2021.

[176] N. M. Bedford, Z. E. Hughes, Z. Tang, Y. Li, B. D. Briggs, Y. Ren, M. T. Swihart, V. G. Petkov, R. R. Naik, M. R. Knecht, et al., *J. Am. Chem. Soc.* **2016**, *138*, 540–548.

[177] Y. Jv, B. Li, R. Cao, *Chem. Commun.* **2010**, *46*, 8017.

[178] D. Kisailus, M. Najarian, J. C. Weaver, D. E. Morse, *Adv. Mater.* **2005**, *17*, 1234–1239.

[179] J. Fan, J.-J. Yin, B. Ning, X. Wu, Y. Hu, M. Ferrari, G. J. Anderson, J. Wei, Y. Zhao, G. Nie, *Biomaterials* **2011**, *32*, 1611–1618.

[180] L. Zhang, L. Laug, W. Münchgesang, E. Pippel, U. Gösele, M. Brandsch, M. Knez, *Nano Lett.* **2010**, *10*, 219–223.

[181] Z. Chen, J.-J. Yin, Y.-T. Zhou, Y. Zhang, L. Song, M. Song, S. Hu, N. Gu, *ACS Nano* **2012**, *6*, 4001–4012.

[182] L. Gao, J. Zhuang, L. Nie, J. Zhang, Y. Zhang, N. Gu, T. Wang, J. Feng, D. Yang, S. Perrett, et al., *Nat. Nanotechnol.* **2007**, *2*, 577–583.

[183] K. S. Park, M. Il Kim, D.-Y. Cho, H. G. Park, *Small* **2011**, *7*, 1521–1525.

[184] S. Liu, F. Lu, R. Xing, J. J. Zhu, *Chemistry* **2011**, *17*, 620–625.

[185] T. Pirmohamed, J. M. Dowding, S. Singh, B. Wasserman, E. Heckert, A. S. Karakoti, J. E. S. King, S. Seal, W. T. Self, *Chem. Commun.* **2010**, *46*, 2736–2738.

[186] A. Asati, C. Kaittanis, S. Santra, J. M. Perez, *Anal. Chem.* **2011**, *83*, 2547–2553.

[187] A. Asati, S. Santra, C. Kaittanis, S. Nath, J. M. Perez, *Angew. Chemie Int. Ed.* **2009**, *48*, 2308–2312.

[188] E. G. Heckert, S. Seal, W. T. Self, *Environ. Sci. Technol.* **2008**, *42*, 5014–5019.

[189] M. H. Kuchma, C. B. Komanski, J. Colon, A. Teblum, A. E. Masunov, B. Alvarado, S. Babu, S. Seal, J. Summy, C. H. Baker, *Nanomedicine Nanotechnology, Biol. Med.* **2010**, *6*, 738–744.

[190] C. Korsvik, S. Patil, S. Seal, W. T. Self, *Chem. Commun.* **2007**, 1056.

[191] R. André, F. Natálio, M. Humanes, J. Leppin, K. Heinze, R. Wever, H. C. Schröder, W. E. G. Müller, W. Tremel, *Adv. Funct. Mater.* **2011**, *21*, 501–509.

[192] F. Natalio, R. André, A. F. Hartog, B. Stoll, K. P. Jochum, R. Wever, W. Tremel, *Nat. Nanotechnol.* **2012**, *7*, 530–535.

[193] L. L. Dugan, D. M. Turetsky, C. Du, D. Lobner, M. Wheeler, C. R. Almli, C. K.-F. Shen, T.-Y. Luh, D. W. Choi, T.-S. Lin, *Proc. Natl. Acad. Sci.* **1997**, *94*, 9434 LP – 9439.

[194] Y. N. Yamakoshi, T. Yagami, S. Sueyoshi, N. Miyata, *J. Org. Chem.* **1996**, *61*, 7236–7237.

[195] Y. N. Yamakoshi, T. Yagami, S. Sueyoshi, N. Miyata, *J. Org. Chem.* **1997**, *62*, 4885.

[196] Y. Song, K. Qu, C. Zhao, J. Ren, X. Qu, *Adv. Mater.* **2010**, *22*, 2206–2210.

[197] R. Cui, Z. Han, J.-J. Zhu, *Chem. – A Eur. J.* **2011**, *17*, 9377–9384.

[198] Y. Song, X. Wang, C. Zhao, K. Qu, J. Ren, X. Qu, *Chem. - A Eur. J.* **2010**, *16*, 3617–

3621.

[199] W. Shi, Q. Wang, Y. Long, Z. Cheng, S. Chen, H. Zheng, Y. Huang, *Chem. Commun.* **2011**, *47*, 6695.

[200] W. Zhou, H. Li, B. Xia, W. Ji, S. Ji, W. Zhang, W. Huang, F. Huo, H. Xu, *Nano Res.* **2018**, *11*, 5761–5768.

[201] M. J. Katz, J. E. Mondloch, R. K. Totten, J. K. Park, S. T. Nguyen, O. K. Farha, J. T. Hupp, *Angew. Chemie Int. Ed.* **2014**, *53*, 497–501.

[202] A. Fateeva, P. A. Chater, C. P. Ireland, A. A. Tahir, Y. Z. Khimyak, P. V Wiper, J. R. Darwent, M. J. Rosseinsky, *Angew. Chemie Int. Ed.* **2012**, *51*, 7440–7444.

[203] A. M. Wright, Z. Wu, G. Zhang, J. L. Mancuso, R. J. Comito, R. W. Day, C. H. Hendon, J. T. Miller, M. Dincă, *Chem* **2018**, *4*, 2894–2901.

[204] B. Pal, T. Torimoto, K. Iwasaki, T. Shibayama, H. Takahashi, B. Ohtani, *J. Phys. Chem. B* **2004**, *108*, 18670–18674.

[205] J. M. Slocik, A. O. Govorov, R. R. Naik, *Angew. Chemie Int. Ed.* **2008**, *47*, 5335–5339.

[206] B. Pal, T. Torimoto, K. Okazaki, B. Ohtani, *Chem. Commun.* **2007**, 483–485.

[207] X. Sun, S. Guo, C.-S. Chung, W. Zhu, S. Sun, *Adv. Mater.* **2013**, *25*, 132–136.

[208] X. Sun, S. Guo, Y. Liu, S. Sun, *Nano Lett.* **2012**, *12*, 4859–4863.

[209] M. Liang, X. Yan, *Acc. Chem. Res.* **2019**, *52*, 2190–2200.

[210] S. Kim, D.-W. Lee, K.-Y. Lee, *J. Mol. Catal. A Chem.* **2014**, *391*, 48–54.

[211] R. Xu, D. Wang, J. Zhang, Y. Li, *Chem. Asian J.* **2006**, *1*, 888–893.

[212] R.-A. Sperling, W. J. Parak, *Philos. Trans. R. Soc. London A Math. Phys. Eng. Sci.* **2010**, *368*, 1333–1383.

[213] F. Schulz, G. T. Dahl, S. Besztejan, M. A. Schroer, F. Lehmkühler, G. Grübel, T. Vossmeyer, H. Lange, *Langmuir* **2016**, *32*, 7897–7907.

[214] K. Tamarov, S. Näkki, W. Xu, V.-P. Lehto, *J. Mater. Chem. B* **2018**, *6*, 3632–3649.

[215] L. Pasquato, F. Rancan, P. Scrimin, F. Mancin, C. Frigeri, *Chem. Commun.* **2000**, *2*, 2253–2254.

[216] D. Wang, B. Liu, Y. Ma, C. Wu, Q. Mou, H. Deng, R. Wang, D. Yan, C. Zhang, X. Zhu, *J. Am. Chem. Soc.* **2017**, *139*, 14021–14024.

[217] J. Singh, T. Dutta, K.-H. Kim, M. Rawat, P. Samddar, P. Kumar, *J. Nanobiotechnology* **2018**, *16*, 84.

[218] X. Wang, Y. Hu, H. Wei, *Inorg. Chem. Front.* **2016**, *3*, 41–60.

[219] Z. Gao, M. Xu, L. Hou, G. Chen, D. Tang, *Anal. Chem.* **2013**, *85*, 6945–6952.

[220] Y. Song, K. Qu, C. Xu, J. Ren, X. Qu, *Chem. Commun.* **2010**, *46*, 6572–6574.

[221] Y. Guo, L. Deng, J. Li, S. Guo, E. Wang, S. Dong, *ACS Nano* **2011**, *5*, 1282–1290.

[222] Y. Xiong, S. Chen, F. Ye, L. Su, C. Zhang, S. Shen, S. Zhao, *Chem. Commun.* **2015**, *51*, 4635–4638.

[223] S. S. Ali, J. I. Hardt, L. L. Dugan, *Nanomedicine Nanotechnology, Biol. Med.* **2008**, *4*, 283–294.

[224] D.-M. Huang, J.-K. Hsiao, Y.-C. Chen, L.-Y. Chien, M. Yao, Y.-K. Chen, B.-S. Ko, S.-C. Hsu, L.-A. Tai, H.-Y. Cheng, et al., *Biomaterials* **2009**, *30*, 3645–3651.

[225] K. L. Quick, S. S. Ali, R. Arch, C. Xiong, D. Wozniak, L. L. Dugan, *Neurobiol. Aging* **2008**, *29*, 117–128.

[226] J. Zhang, J. Zhuang, L. Gao, D. Yang, J. Zhu, X. Yan, *Chemosphere* **2008**, *73*, 1524.

[227] Q. Cai, S. Lu, F. Liao, Y. Li, S. Ma, M. Shao, *Nanoscale* **2014**, *6*, 8117–8123.

[228] X. Wu, Y. Zhang, T. Han, H. Wu, S. Guo, J. Zhang, *RSC Adv.* **2014**, *4*, 3299–3305.

[229] B. Hvolbæk, T. V. W. Janssens, B. S. Clausen, H. Falsig, C. H. Christensen, J. K. Nørskov, *Nano Today* **2007**, *2*, 14–18.

[230] T. Fujita, P. Guan, K. McKenna, X. Lang, A. Hirata, L. Zhang, T. Tokunaga, S. Arai, Y. Yamamoto, N. Tanaka, et al., *Nat. Mater.* **2012**, *11*, 775–780.

[231] M. Haruta, T. Kobayashi, H. Sano, N. Yamada, *Chem. Lett.* **1987**, *16*, 405–408.

[232] G. C. Bond, D. T. Thompson, G. C. Bond, *Catal. Rev.* **2016**, *4940*, 319–388.

[233] J. Mckittrick, L. Shea-Rohwer, *J. Am. Ceram. Soc.* **2014**, *97*, DOI 10.1111/jace.12943.

[234] B. M. Quinn, P. Liljeroth, V. Ruiz, T. Laaksonen, K. Kontturi, *J. Am. Chem. Soc.* **2003**,

125, 6644–6645.

[235] Y. Zhu, H. Qian, R. Jin, *J. Mater. Chem.* **2011**, *21*, 6793–6799.

[236] E. Rombi, M. G. Cutrufello, R. Monaci, C. Cannas, D. Gazzoli, B. Onida, M. Pavani, I. Ferino, *J. Mol. Catal. A Chem.* **2015**, *404–405*, 83–91.

[237] J.-D. Grunwaldt, C. Kiener, C. Wögerbauer, A. Baiker, *J. Catal.* **1999**, *181*, 223–232.

[238] Y. Jv, B. Li, R. Cao, *Chem. Commun.* **2010**, *46*, 8017–8019.

[239] D. Zeng, W. Luo, J. Li, H. Liu, H. Ma, Q. Huang, C. Fan, *Analyst* **2012**, *137*, 4435–4439.

[240] M. Ferentz, M. V. Landau, R. Vidruk, M. Herskowitz, *Catal. Today* **2015**, *241*, 63–72.

[241] X. Yang, P.-F. Tian, C. Zhang, Y. Deng, J. Xu, J. Gong, Y.-F. Han, *Appl. Catal. B Environ.* **2013**, *134–135*, 145–152.

[242] E. Lorençon, D. C. Ferreira, R. R. Resende, K. Krambrock, *Appl. Catal. A Gen.* **2015**, *505*, 566–574.

[243] L. Ge, T. Chen, Z. Liu, F. Chen, *Catal. Today* **2014**, *224*, 209–215.

[244] E. C. Dreaden, A. M. Alkilany, X. Huang, C. J. Murphy, M. A. El-Sayed, *Chem. Soc. Rev.* **2012**, *41*, 2740–2779.

[245] H. Häkkinen, *Nat. Chem.* **2012**, *4*, 443–455.

[246] Y. Xue, X. Li, H. Li, W. Zhang, *Nat. Commun.* **2014**, *5*, DOI 10.1038/ncomms5348.

[247] H. Hinterwirth, S. Kappel, T. Waitz, T. Prohaska, W. Lindner, M. Lämmerhofer, *ACS Nano* **2013**, *7*, 1129–1136.

[248] L. Pasquato, P. Pengo, P. Scrimin, *Supramol. Chem.* **2005**, *17*, 163–171.

[249] S. Eustis, M. A. El-Sayed, *Chem. Soc. Rev.* **2006**, *35*, 209–217.

[250] V. Amendola, R. Pilot, M. Frasconi, O. M. Maragò, M. A. Iatì, *J. Phys. Condens. Matter* **2017**, *29*, 203002.

[251] K. Saha, S. S. Agasti, C. Kim, X. Li, V. M. Rotello, *Chem. Rev.* **2012**, *112*, 2739–2779.

[252] P. K. Jain, M. A. El-Sayed, *Chem. Phys. Lett.* **2010**, *487*, 153–164.

[253] V. Pareek, A. Bhargava, R. Gupta, N. Jain, J. Panwar, *Adv. Sci. Eng. Med.* **2017**, *9*, 527–544.

[254] L. Freitas de Freitas, G. H. C. Varca, J. G. Dos Santos Batista, A. Benévolo Lugão, *Nanomater. (Basel, Switzerland)* **2018**, *8*, 939.

[255] L. Guojun, X. Yang, Y. Li, Z. Yang, W. Hong, J. Liu, *Adv. Mater. Sci. Eng.* **2015**, *2015*, 1–11.

[256] H. Kang, J. T. Buchman, R. S. Rodriguez, H. L. Ring, J. He, K. C. Bantz, C. L. Haynes, *Chem. Rev.* **2019**, *119*, 664–699.

[257] J. Hierrezuelo, A. Sadeghpour, I. Szilagyi, A. Vaccaro, M. Borkovec, *Langmuir* **2010**, *26*, 15109–15111.

[258] M. R. Ivanov, H. R. Bednar, A. J. Haes, *ACS Nano* **2009**, *3*, 386–394.

[259] R. Greenwood, K. Kendall, *J. Eur. Ceram. Soc.* **1999**, *19*, 479–488.

[260] A. Kumar, C. K. Dixit, in *Adv. Nanomedicine Deliv. Ther. Nucleic Acids* (Eds.: S. Nimesh, R. Chandra, N.B.T.-A. in N. for the D. of T.N.A. Gupta), Woodhead Publishing, **2017**, pp. 44–58.

[261] J. Turkevich, P. C. Stevenson, J. Hillier, *Discuss. Faraday Soc.* **1951**, *11*, 55.

[262] G. Frens, *Nat. Phys. Sci.* **1973**, *241*, 20–22.

[263] M. Zheng, X. Huang, *J. Am. Chem. Soc.* **2004**, *126*, 12047–12054.

[264] J. C. Spain, *Annu. Rev. Microbiol.* **1995**, *49*, 523–555.

[265] C.-M. Kao, B.-H. Lin, S.-C. Chen, S.-F. Wei, C.-C. Chen, C.-L. Yao, C.-C. Chien, *Bioremediat. J.* **2016**, *20*, 165–173.

[266] M. E. Honeycutt, A. S. Jarvis, V. A. McFarland, *Ecotoxicol. Environ. Saf.* **1996**, *35*, 282–287.

[267] W. Pitsawong, J. P. Hoben, A. F. Miller, *J. Biol. Chem.* **2014**, *289*, 15203–15214.

[268] A. Christofferson, J. Wilkie, *Biochem. Soc. Trans.* **2009**, *37*, 413–418.

[269] H. U. Blaser, H. Steiner, M. Studer, *ChemCatChem* **2009**, *1*, 210–221.

[270] S. Fountoulaki, V. Daikopoulou, P. L. Gkizis, I. Tamiolakis, G. S. Armatas, I. N. Lykakis, *ACS Catal.* **2014**, *4*, 3504–3511.

[271] I. Tamiolakis, S. Fountoulaki, N. Vordos, I. N. Lykakis, G. S. Armatas, *J. Mater. Chem. A* **2013**, *1*, 14311–14319.

9 References

[272] A. Corma, P. Serna, *Science (80-.).* **2006**, *313*, 332–334.

[273] S. Fountoulaki, V. Daikopoulou, P. L. Gkizis, I. Tamiolakis, G. S. Armatas, I. N. Lykakis, *ACS Catal.* **2014**, *4*, 3504–3511.

[274] X. B. Lou, L. He, Y. Qian, Y. M. Liu, Y. Cao, K. N. Fan, *Adv. Synth. Catal.* **2011**, *353*, 281–286.

[275] S. Wunder, F. Polzer, Y. Lu, Y. Mei, M. Ballauff, **2010**, 8814–8820.

[276] S. Satapathy, J. Mohanta, S. Si, *ChemistrySelect* **2016**, *1*, 4940–4948.

[277] R. Arora, *J. Microw. Power Electromagn. Energy* **2011**, *45*, 94–102.

[278] D. J. Mikolajczak, A. A. Berger, B. Koksch, *Angew. Chemie Int. Ed.* **2020**, DOI 10.1002/anie.201908625.

[279] X. Wang, Y. Hu, H. Wei, *Inorg. Chem. Front.* **2016**, *3*, 41–60.

[280] E. Colangelo, Q. Chen, A. M. Davidson, D. Paramelle, M. B. Sullivan, M. Volk, R. Levy, *Langmuir* **2017**, *33*, 438–449.

[281] F. Schneider, *Angew. Chemie Int. Ed. English* **1978**, *17*, 583–592.

[282] G. L. Holliday, J. B. O. Mitchell, J. M. Thornton, *J. Mol. Biol.* **2009**, *390*, 560–577.

[283] C. Guarise, F. Manea, G. Zaupa, L. Pasquato, L. J. Prins, P. Scrimin, *J. Pept. Sci.* **2008**, *14*, 174–183.

[284] J. R. Litowski, R. S. Hodges, *J. Biol. Chem.* **2002**, *277*, 37272–37279.

[285] D. N. Woolfson, *Adv. Protein Chem.* **2005**, *70*, 79–112.

[286] D. J. Mikolajczak, B. Koksch, *ChemCatChem* **2018**, *10*, 4324–4328.

[287] S. Li, Y. Luo, M. J. Whitcombe, S. A. Piletsky, *J. Mater. Chem. A* **2013**, *1*, 15102–15109.

[288] B. H. San, S. Ravichandran, K. S. Park, V. K. Subramani, K. K. Kim, *ACS Appl. Mater. Interfaces* **2016**, *8*, 30058–30065.

[289] C. P. Shaw, D. A. Middleton, M. Volk, R. Lévy, *ACS Nano* **2012**, *6*, 1416–1426.

[290] D. J. Mikolajczak, J. Scholz, B. Koksch, *ChemCatChem* **2018**, *10*, 5665–5668.

[291] D. J. Mikolajczak, B. Koksch, *Catalysts* **2019**, *9*, 903.

[292] C. M. Rufo, Y. S. Moroz, O. V. Moroz, J. Stöhr, T. a. Smith, X. Hu, W. F. DeGrado, I. V. Korendovych, *Nat. Chem.* **2014**, *6*, 303–309.

10 Curriculum Vitae

Der Lebenslauf ist in der Online-Version aus Gründen des Datenschutzes nicht enthalten.